# PHYTOCHEMICAL INVESTIGATION OF *Walsura pinnata*

**MOHAMAD AZRUL BIN MAHDZIR**

**FACULTY OF SCIENCE**
**UNIVERSITY OF MALAYA**
**KUALA LUMPUR**

**2017**

# PHYTOCHEMICAL INVESTIGATION OF *Walsura pinnata*

**MOHAMAD AZRUL BIN MAHDZIR**

**THESIS SUBMITTED IN FULFILMENT OF THE REQUIREMENTS FOR THE DEGREE OF MASTER OF SCIENCE**

**DEPARTMENT OF CHEMISTRY**
**FACULTY OF SCIENCE**
**UNIVERSITY OF MALAYA**
**KUALA LUMPUR**

**2017**

**UNIVERSITY OF MALAYA**
**ORIGINAL LITERARY WORK DECLARATION**

Name of Candidate: MOHAMAD AZRUL BIN MAHDZIR

I.C/Passport No:

Matric No: SGR 140020

Name of Degree: MASTER OF SCIENCE

Title of Project Paper/Research Report/Dissertation/Thesis ("this Work"):

PHYTOCHEMICAL INVESTIGATION OF *Walsura pinnata*

Field of Study: ORGANIC CHEMISTRY

I do solemnly and sincerely declare that:

(1) I am the sole author/writer of this Work;
(2) This Work is original;
(3) Any use of any work in which copyright exists was done by way of fair dealing and for permitted purposes and any excerpt or extract from, or reference to or reproduction of any copyright work has been disclosed expressly and sufficiently and the title of the Work and its authorship have been acknowledged in this Work;
(4) I do not have any actual knowledge nor do I ought reasonably to know that the making of this work constitutes an infringement of any copyright work;
(5) I hereby assign all and every rights in the copyright to this Work to the University of Malaya ("UM"), who henceforth shall be owner of the copyright in this Work and that any reproduction or use in any form or by any means whatsoever is prohibited without the written consent of UM having been first had and obtained;
(6) I am fully aware that if in the course of making this Work I have infringed any copyright whether intentionally or otherwise, I may be subject to legal action or any other action as may be determined by UM.

Candidate's Signature Date:

Subscribed and solemnly declared before,

Witness's Signature Date:

Name:

Designation:

## ABSTRACT

Ten compounds were successfully isolated from the dichloromethane extract of bark of *Walsura pinnata* Hassk which was collected at 243 km, from Gua Musang, Kelantan to Kuala Lipis, Pahang. A new oleanane triterpenoids; 3-oxo-olean-9(11),12-dien-28-oic acid (**100**) was established along with nine known compounds, which are five terpenoids, 3-oxo-lup-20(29)-en-28-oic acid (**97**), 3*β*-hydroxy-5-glutinen-28-oic acid (**98**), 3-oxo-olean-11-en-28,13*β*-olide (**99**), 3-oxo-20(24)-epoxy-12*β*,25-dihydroxydammarane (**101**), 2(3),6(7)-diepoxy-9-humulene (**102**), two sterols compounds, stigmasterol (**103**), *β*-sitosterol glycoside (**104**) with two aromatic derivatives, which are 4-hydroxy-3-methoxybenzoic acid (**105**) and 4-hydroxy-4,8-dimethyl-1-tetralone (**106**) were analyzed and confirmed using various spectroscopic techniques. Compound **97** and **98** were tested *in vitro* for their cytotoxic activities against five type of cancer cell lines; human hepatocellular carcinoma (Hep3b and HepG2), human ovarian adenocarcinoma (SK-OV-3), human breast adenocarcinoma (MCF-7), and human acute myeloblastic leukemia (Kasumi-1). Compound **97** showed good cytotoxicity against leukemia, Kasumi-1 cell line with $IC_{50}$ value of 2.11 ± 0.48 µg/mL while compound **98** exhibit good cytotoxicity activities against both liver cancer cell lines, Hep3b ($IC_{50}$: 2.28 ± 0.00 µg/mL , SI = 8.81) and HepG2 ($IC_{50}$: 4.00 ± 0.63 µg/mL, SI = 5.02).

## ABSTRAK

Sepuluh juzuk kimia telah berjaya ditemui; daripada ekstark diklorometana kulit kayu *Walsura pinnata* Hassk yang dikumpul di 243 km, dari Gua Musang, Kelantan ke Kuala Lipis, Pahang. Stuktur satu sebatian triterpenoid oleanane baru; asid-3-oxo-olean-9(11),12-dien-28-oik (**100**) telah berjaya ditentukan bersama sembilan sebatian lain diantaranya lima terpenoid, asid-3-oxo-lup-20 (29) en-28-oik (**97**), asid-3*β*-hidroksida-5-glutinen-28-oik (**98**), 3-oxo-olean-11-en-28,13*β* -olide (**99**), 3-oxo-20(24)-epoksi-12*β*,25-dihidroksidadammarane (**101**), 2(3),6(7)-diepoksi-9-humulene (**102**), dua sebatian sterol, stigmasterol (**103**), *β*-sitosterol glikosida (**104**) dan dua sebatian aromatik, asid-4-hidroksida-3-methoksibenzoik (**105**) dan 4-hidroksida-4,8-dimetil-1-tetralone (**106**), melalui pelbagai teknik spektroskopi. Sebatian **97** dan **98** telah diuji secara *in vitro* bagi aktiviti sitotoksik terhadap lima jenis kanser sel; karsinoma hepatoselular manusia (Hep3b dan HepG2), adenokarsinoma ovari manusia (SK-OV-3), adenokarsinoma payudara manusia (MCF-7), dan leukemia myeloblastik akut manusia (Kasumi-1). Sebatian **97** menunjukkan aktiviti sitotoksik yang bagus terhadap sel kanser leukemia, Kasumi-1 dengan nilai $IC_{50}$ ialah 2.11 ± 0.48 μg/mL manakala sebatian **98** menunjukkan aktiviti sitotoksik yang bagus terhadap kedua-dua sel kanser hati, Hep3b (IC50: 2.28 ± 0.00 μg/mL, SI = 8.81) dan HepG2 (IC50: 4.00 ± 0.63 μg/mL, SI = 5.02).

**ACKNOWLEDGEMENTS**

It is a great pleasure to thank many people who have made this project a successful.

Firstly, I would like to thank Ministry of Eduation, Malaysia for awarding me the MyBrain15 scholarships which was used to pay the tuition fees.

I would like to express my deepest appreciation to my beloved supervisor, Prof. Dr. Khalijah Awang for her inspiration, motivation, constant guidance and advice.

To Prof. Dr. Jamil A. Shilpi, it is always to be my pleasure to have you helped me in lots of work. Your patience, wise advise and experience will always be remembered. A special thanks goes to Dr Leong, Dr Sujatha, Mrs. Norfaizah and Mr. Nurhisyam for running the cytotoxic activity of my compounds.

I am truly indebted to all the Phytolab members, past and present for sharing their experience and knowledge with most importantly, they gave me chance to be a part of this blessed family. To Mr. Nordin, a warmest thank for gave me chance to learnt a lot from your vast experience regarding the technical part of NMR machine.

My sincere thank goes to my beloved G426 housemate, 4$^{th}$ Legendz members and my college junior. For those that I did not mention their names, you are always in my heart. It is a wonderful gifts to have all of you.

Last and most importantly, I wish to thank my beloved family especially to my parents; En. Mahdzir bin Harun and Pn. Katyem bt. Sidal. They raised me, supported me, thought me and loved me. To my brother, Mohd. Nor Iman and both my sisters, Intan Nor Alia and Intan Nor Alisa, I hope that our family bonding will strengthen as time flies.

## TABLE OF CONTENTS

## LIST OF FIGURES

## LIST OF TABLES

## LIST OF SYMBOLS AND ABBREVIATIONS

| | | |
|---|---|---|
| µ | : | Micro |
| $^{13}$C NMR | : | Carbon Nuclear Magnetic Resonance |
| $^{1}$H NMR | : | Proton Nuclear Magnetic Resonance |
| *brs* | : | Broad Singlet |
| CC | : | Column Chromatography |
| $CH_2Cl_2$ | : | Dichloromethane |
| cm | : | Centimeter |
| $cm^{-1}$ | : | Per Centimeter |
| COSY | : | Correlation Spectroscopy |
| *d* | : | Doublet |
| *dd* | : | Doublet of doublets |
| *ddd* | : | Doublet of doublet of doublets |
| DEPT-135 | : | Distortionless Enhancement by Polarization Transfer at 135$^{o}$ |
| *dt* | : | Doublet of triplets |
| EtOAc | : | Ethyl Acetate |
| g | : | Gram |
| HMBC | : | Heteronuclear Multiple Bond Coherence |
| HSQC | : | Heteronuclear Single Quantum Coherence |
| Hz | : | Hertz |
| $IC_{50}$ | : | Concentration Needed for Inhibition of 50% Activity |
| IR | : | Infrared Spectroscopy |
| J | : | Coupling Constant |
| *m* | : | Multiplet |
| m/z | : | Mass to Charge Ratio |
| MeOH | : | Methanol |

| | | |
|---|---|---|
| mg | : | Milligram |
| MHz | : | Mega Hertz |
| mL | : | Milliliter |
| nd | : | Not Determined |
| nm | : | Nanometer |
| NMR | : | Nuclear Magnetic Resonance |
| NOE | : | Nuclear Overhouser Effect |
| ppm | : | Part per million |
| PTLC | : | Preparative Thin Layer Chromatography |
| *q* | : | Quartet |
| $R_f$ | : | Retention factor |
| *s* | : | Singlet |
| *sxt* | : | Sextet |
| *t* | : | Triplet |
| *td* | : | Triplet of doublets |
| TLC | : | Thin Layer Chromatography |
| UV | : | Ultraviolet Spectroscopy |
| α | : | Alpha |
| β | : | Beta |
| γ | : | Gamma |
| δ | : | Chemical Shifts |
| λ | : | Lambda |

# CHAPTER 1: INTRODUCTION

## 1.1 General

The art of using medicinal plants to treat illness has been recorded since the dawn of human civilizations. These activities were recorded in some of the oldest monographs such as 'Chakara-Samhita' of the Indian Subcontinent, 'Ebers Papyrus' of Egypt and 'Neijing Suwen' of China. During the middle ninth to late twelfth century, the Mediterranean's medicinal practitioners became pioneers on the compilation of knowledge on herbal practice from different parts of the world n. They also have standardized the art of drawing the medicinal plants for the identification purposes, procedures of establishing botanical gardens and preserving plant specimen.

In the late twentieth century, with the huge scientific achievements in chemistry and biology, the idea that plants contain some chemical agents that responsible for the observed pharmacological properties become stronger (Lehane, 1977). This was exemplified with the isolation of morphine (**1**) from the seed pods of opium poppy plants (*Papaver somniferum*) by young German pharmacist, Friedrich Sertüener (1783-1841) which became the first pure substance of natural origin to be commercialized as a drug (Goldstein et al., 1970). Other examples of some natural products isolated from plants and their therapeutic importance such as:-

- Paclitaxel (**2**), a natural taxane isolated by Monroe E. Wall and Mansukh C. Wani at Research Triangle Institute (Kinghorn & Powell, 2004) from the bark of Pacific yew tree, *Taxus brevifolia* and semisynthetic derivative, docetaxel (**3**) which was used for the treatment of breast, ovarian and lung cancer (Cragg & Newman, 2005).
- Vincristine (**4**) was founded by Dr. J. G. Armstrong while vinblastine (**5**) was purified by Robert Noble and Charles Thomas Beer from University

of Western Ontanio. Both drugs were isolated from Madagascar periwinkle plants, *Catharanthus roseus* and were commercially used in the treatment of most cancer disease (Pearce & Miller, 2005).

- Artemisinin (**6**), an anti-malarial drug that is used in chloroquine resistance was discovered in late 1960's by, Youyou Tu (Nobel Prize in Medicine, 2015) from wormwood of *Artemisia annua* L. (Meliaceae) (Ye et al., 2016)

Natural products based drugs can be isolated from various origin such as animals (Aramadhaka et al., 2013), microorganisms (Bringmann et al., 2009) and laboratories (Zhang et al., 2015), with most of the commercialized drugs originating from plants. Malaysia is one of the megadiverse countries that are blessed with almost 15,000 species of flowering plant, of which 23% are endemic. It was claimed that among those reported species, around 2,500 of it possess various medicinal values (Division, 2014). Therefore, in this study, *Walsura pinnata*, a plant from Meliaceae family will be the subject of chemical and biological activity investigation.

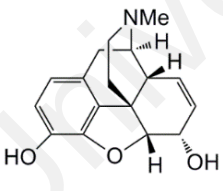


**1**

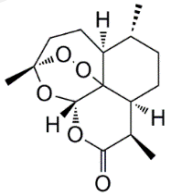


**6**

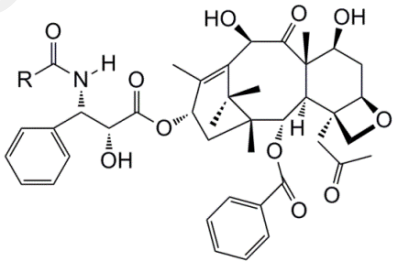


**2** Paclitaxel, R = $C_6H_5$
**3** Docetaxel, R = $OC(CH_3)_3$

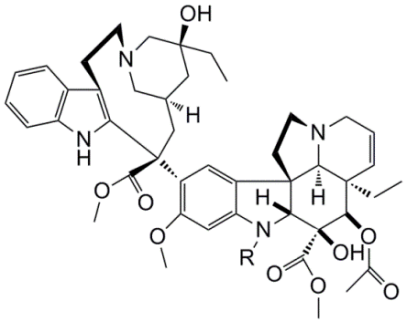


**4** Vincristine, R = CHO
**5** Vinblastine, R = Me

## 1.2 Family Meliaceae

### 1.2.1 Distributions

Meliaceae or the mahogany family, was so called because of the scented wood, is one of flowering plant type with most common type are trees, shrubs and few of it are mangroves and herbaceous plants. This family can usually be found in a variety of habitats occurring from rain forest and mangrove swamps to semi deserts around the tropical and subtropical region including Asia, Africa, Australia and South America which covers about 575 species in 50 genera (Pennington & Styles, 1975). In Malaysia, it is known as *Langsat* family with about 16 genera and 100 species, this family mostly can be found in the lowland forest, and some of it in the mountains.

### 1.2.2 Morphology

Morphology of a Meliaceae family can be divided into four categories which are tree, leave, flowers (petal, stamen, calyx/sepal and anther) and fruit (Ridley, 1952). It is medium sized tree about 20m tall and around 100 cm girths and appears with scant white latex. The leaves are spirally arranged in the form of either pinnate or trifoliate with the leaflets in opposite condition with absence of stipules. The Meliaceae flowers mostly appear in symmetrical and small size with white, yellow or greenish colour. It has four to five sepals joined in a small cup while the petals structures are narrow, separate and curved back with three to six pieces. Generally, the flowers have five to ten stamens joined in a tube surrounding the ovary and the anthers usually seated or separate on the rim of the tube. Lastly, the fruits are fleshy with large seeds or as capsules with flat winged seeds, often appeared coated with pulp.

### 1.2.3 Classifications

Meliaceae family can be classified into four subfamilies which comprises of Melioideae (7 tribes, 36 genera), Swietenioideae (3 tribes, 13 genera), and both

monogerenic of Quivisianthoideae and Capuronianthoideae. Figure 1.1 showed details about the botanical classification about the Meliaceae family.

Kingdom: Plantae (Plants)
Subkingdom: Tracheobionta (Vascular plants)
Superdivision: Spermatophyta (Seed plants)
Division: Magnoliophyta (Flowering plants)
Class: Magnoliopsida (Dicotyledons)
Subclass: Rosidae
Order: Sapindales
Family: Meliaceae (Mahogany family)

**Figure 1.1**: Botanical classification of Meliaceae family

## 1.3 The Genus *Walsura*

The genus *Walsura* (Meliaceae) belong to the Trichilieae tribe was comprised about 30-40 species and varieties is mainly distributed in Southern part of India, mainland of China and Southeast of Asia (Ridley, 1952). The *Walsura* genus usually appears as medium size tree between 12–37 m tall and 24–38 cm in diameter. Its bark is pale and smooth while its inner bark is pink-brown in color. The leaves are flattened adaxially with 50 cm long and 1–4 cm thick. The leaflets are subcoriaceous in structure with lower surface glabrous or glaucous (when fresh). It's has two or three leaflets on each side of rachis and the blades are usually narrowly oblanceolate and elliptical to oblong. *Walsura* genera flowers are small in size and appear in bisexual form with five petals and ovate oblong structure. The anthers either on terminal or inserted in a notch in the filament and appear in short five lobed calyxes that imbricate in bud while the stamens are united, and rarely can be seen free. Lastly, the fruits are seeded with baccate tomentose indehiscent with one or rarely two celled.

## 1.4 *Walsura pinnata*

*Walsura pinnata*, Figure 1.2 or locally known as *Lantupak mata kucing* can be found mainly in Northern and Southern part of Malaysia, Thailand, and Borneo island.

This species easily can be seen in lowland and hills up to 600 m above the sea level (Corner, 1940). This species can be seen as medium sized tree up to 20 m tall and 110 cm girth. The bark, inner bark and sapwood are dark brown, white and yellowish in colour respectively. The leaves appear with 30 cm long and up to five leaflets. The flower's colour of panicles are white in 16-30cm long with each of it has five petals and ten stamens that united at base. The fruits can be seen as oblong shaped with 2 cm long.

.


**Figure 1.2**: *W. pinnata* Hassk (a = tree, b = leaves, c = bark, d = fruits)

## 1.5 Objective

This research work involves chemical investigation and biological testing of *W. pinnata* Hassk. The genus was chosen because it was less studied but possesses interesting structures of triterpenoids and limonoids from the literature. The plant species belonged to Meliaceae family and was collected at 243 km, from Gua Musang, Kelantan to Kuala Lipis, Pahang. The objectives of this study are as follows:

1. To perform extraction, isolation and purification of the chemical constituents from the bark of *Walsura pinnata* Hassk.
2. To characterize each isolated constituents by means of various spectroscopic method, including NMR, UV, IR and Mass spectrometry.
3. To evaluate the cytotoxic activity of compounds isolated against five type of cancer cell lines namely, liver (Hep3b and HepG2), ovary (SK-OV-3), breast (MCF-7) and leukemia (Kasumi-1).

# CHAPTER 2: GENERAL CHEMICAL ASPECTS

This chapter will briefly discuss the classification and biosynthesis of triterpenoids as it is the major compound found in *Walsura* genus. In addition, a brief explanation on literature review on the chemical constituents and its biological activities of all species from genus *Walsura* were added in the last section of this chapter.

## 2.1 Terpenoids

Terpenoids represent the majority class of natural products with as many as 20,000 different forms identified in higher plant. The term terpenes and terpenoids are basically referred to different chemical class. Terpenes are mainly hydrocarbon while terpenoids are oxygen-containing analogs of terpenes (Breitmaier, 2006). All terpenoids consist of a combination of several isoprenes (five-carbon units) joint through either tail to head, head to head or head to middle. Terpenoids are classified according to the number of isoprene units from which they are formed (Bowsher et al., 2008). The following addition of isoprene units and its representative structure of each class of terpenoids were shown in Table 2.1.

**Table 2.1**: Classifications of terpenoids

| Isoprene | Class | Example | Functions |
|---|---|---|---|
| 2 | Mono terpene | Limonene (**7**) | Used in cosmetic products (Yokomaku et al., 2010) |
| 3 | Sesqui Terpene | Humulane (**8**) | Anti-inflammatory effects in mammals (Giang et al., 2009) |
| 4 | Diterpene | Kahweol (**9**) | Inhibit osteoclast differentiation on bone cell (Fumimoto et al., 2012) |
| 5 | Sesterpene | Deoxymanoalide (**10**) | Inhibitors against snake venom phospholipase $A_2$ (Uddin et al., 2009) |
| 6 | Triterpene | Oleanane (**11**) | Potent as anti-cancer agents (Gauthier et al., 2009) |
| 8 | Tetra terpene | Phytoene (**12**) | Protect the skin by acting as UV absorbers (von Oppen-Bezalel & Shaish, 2009) |

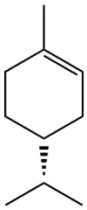

7

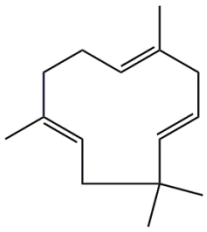

8

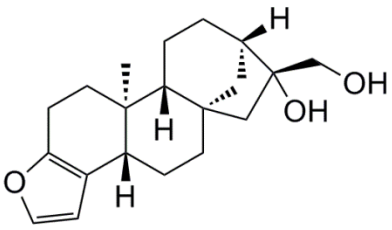


9

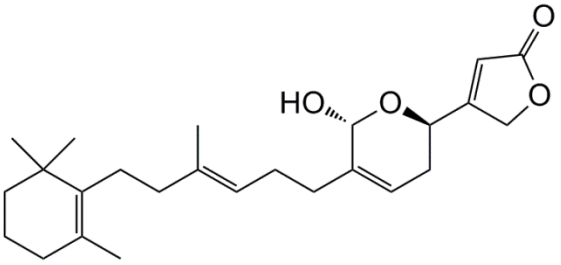


10

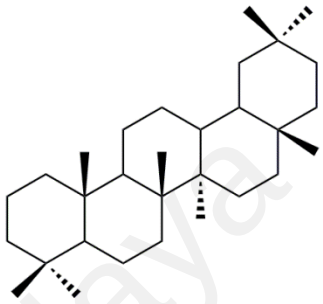

11

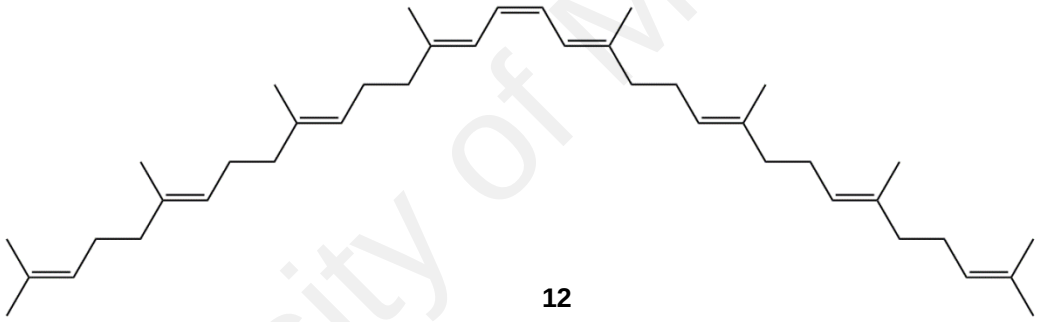

12

## 2.2 Biogenesis of terpenoids

Terpenoids are the majority and diverse groups of natural product plants. The biogenesis of this type of compounds can be divided into four main stages (Stanforth, 2006).

Firstly, the synthesis of isoprene such as isopentyl diphosphate (IPP) and dimethylallyl diphospshate (DMAPP) through mevalonic acid (MVA) pathway and deoxyxylulose phosphate (DXP) pathway. Higher plants, liverworts, marine diatoms and mosses followed both MVA and DXP pathway. In contrast, animals, fungi and the Archea used only MVA pathway while all eubacteria and green algae only followed

DXP pathway. The entire pathway of both MVA and DXP takes place in the higher plants in the cytosol and plastids respectively (Figure 2.1).

Following the synthesis of both IPP and DMAPP; either in cytosol or plastid, the next steps are repetitive addition and condensation of isoprene units to form more complex terpenoids precursors. Both IPP and DMAPP are joint by enzyme prenyltransferases to form precursors such as geranyl diphosphate (GPP) followed by farnesyl diphosphate (FPP) and geranylgeranyl diphosphate (GGPP) which then convert those to specific terpenoids. Larger terpenoids may form by joining two smaller terpenoids precursors such as triterpenoids ($C_{30}$) formed from two FPP in reaction catalyzed by squalene synthase (SQS) (Thimmappa et al., 2014). The schematic diagram for the formation of squalene was shown in Figure 2.2.

Terpene synthases such as monoterpene synthase, sesquiterpene synthase, and triterpene synthase are groups of enzyme that convert the terpenoids precursors and are ordered by the number of isoprenes (mono-, sesqui-, di- and triterpenoids). They are sometimes referred to terpene cyclases because majority of the products were in cyclic form. These enzymes were important as they are responsible for introducing diversity of structural variation into the terpenoid skeletons.

Finally, the terpenoid skeletons forms can be further modified by action of variety of enzyme including cytochrome P450 hydroxylases, reductases and glycosyl transferases to introduce a variety of final products of terpenoids by following reaction such as hydride and methyl shifts, oxidation, cyclization, loss of proton and addition of both water and sugar moiety (Stanforth, 2006).

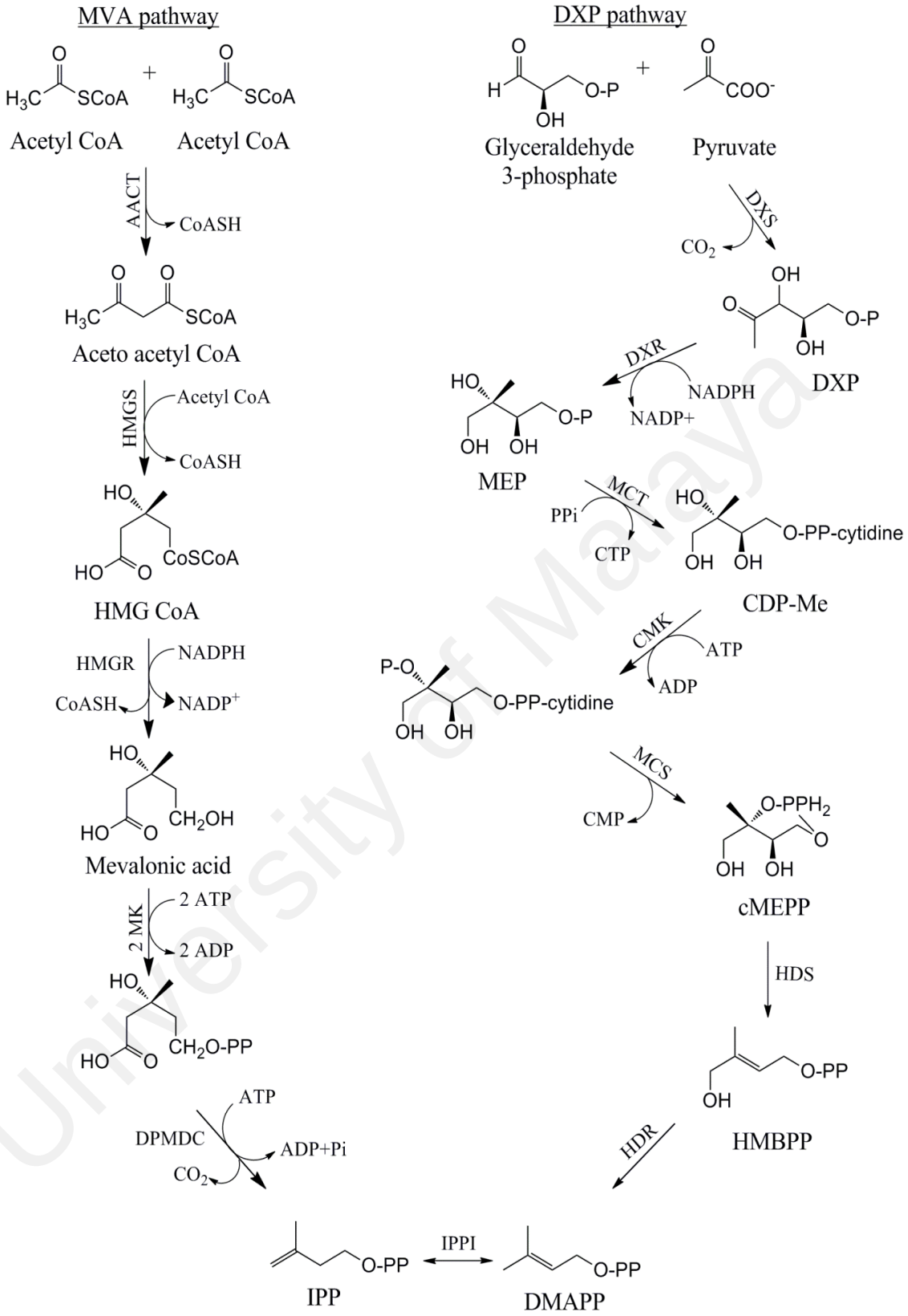


**Figure 2.1**: Biosynthetic pathway for the formation of both isopentyl diphosphate, IPP and dimethylallyl diphospshate, DMAPP

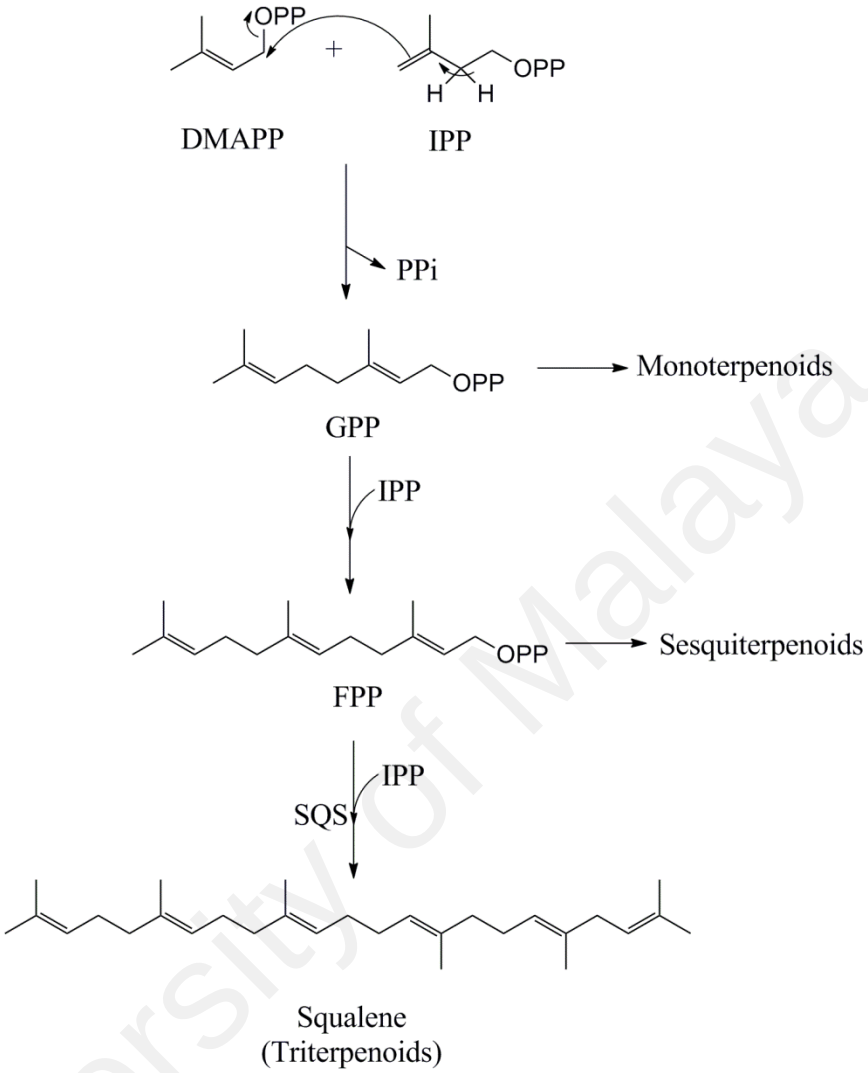


**Figure 2.2**: Biosynthetic pathway for the formation of squalene

## 2.3 Triterpenoids

Triterpenoids are thirty-carbon group of natural products derived from squalene or related acyclic thirty-carbon precursors. Triterpenoids including sterol, steroids and saponins showed wide range of commercial and biological applications such as in food and cosmetics sectors and also act as signaling molecules plus provide protections against pathogens and pests. To date, these groups have displayed nearly 200 distinct skeletons which covered a variety of pharmalogical activities (Das & Mahato, 1983).

In triterpenoids biosynthesis, the squalene (in bacteria) or 2,3-oxidosqualene (in fungi, animals, and plants) will fold to form either mono-, di-, tri-, tetra-, penta-, or acyclic triterpenoids skeletons.

The cyclization of 2,3-oxidosqualene was catalyzed by enzymes oxidosqualene cyclases (OCSs) which generated either sterols or triterpenoids structure. The sterols and triterpenoids skeletons was cyclized via the chair-boat-chair (CBC) and chair-chair-chair (CCC) conformation respectively as shown in Figure 2.3, in which the majority of triterpenoids scaffolds resembled 6/6/6/5 tetracycles, 6/6/6/6/5 and 6/6/6/6/6 pentacycles (Phillips et al., 2006).

The triterpenoids scaffolds processes (Thimmappa et al., 2014; Xu et al., 2004) involve four main stages (Figure 2.4) which are:

a) Organization and binding of substrates
b) Protonation of the epoxide (initiation).
c) Rearrangement and cyclization of carbocation species.
d) Yield of final triterpenoids by deprotonation or water capture (termination).

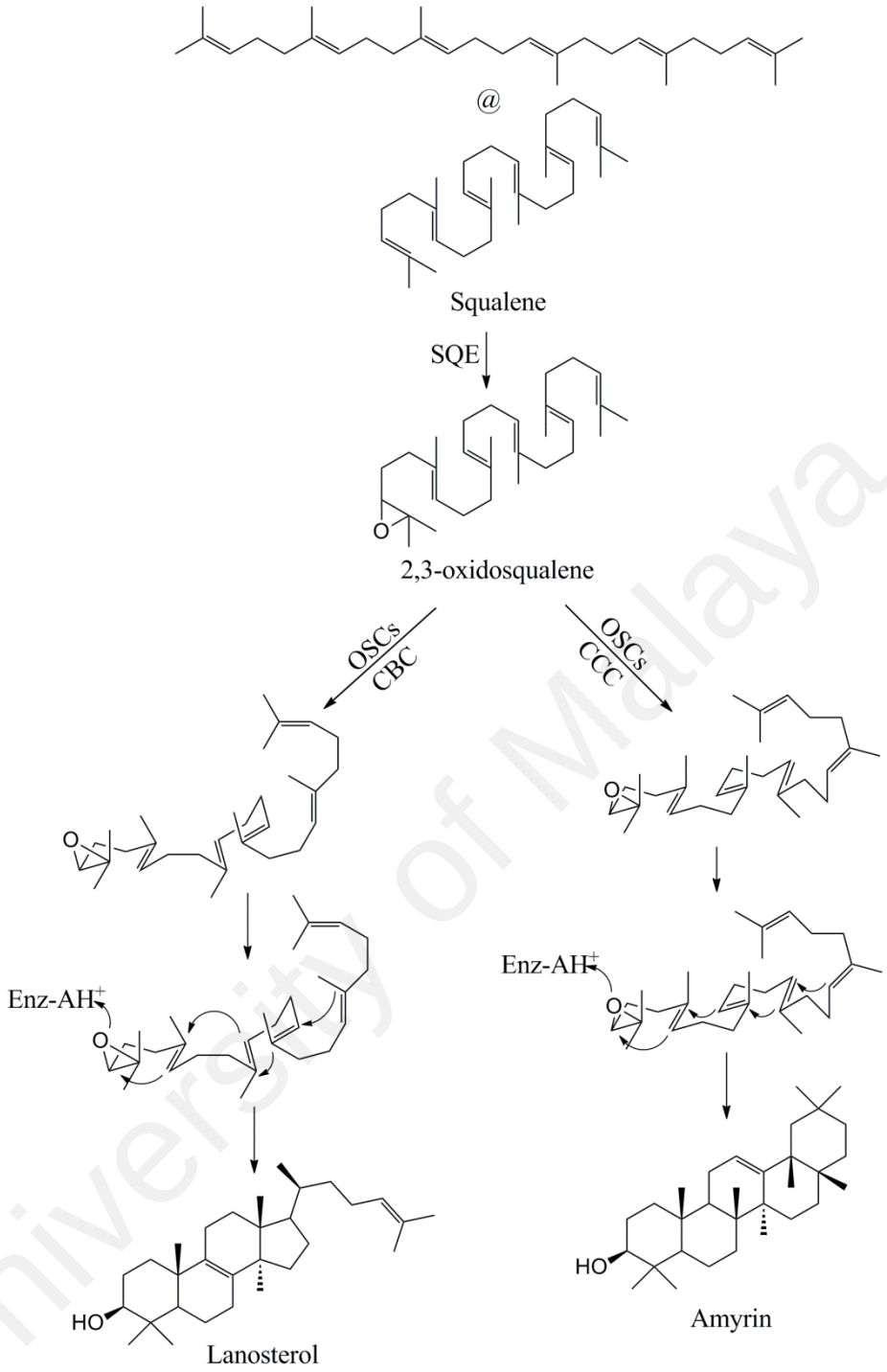


**Figure 2.3**: Formation of sterols/triterpenoids through different type of cyclization

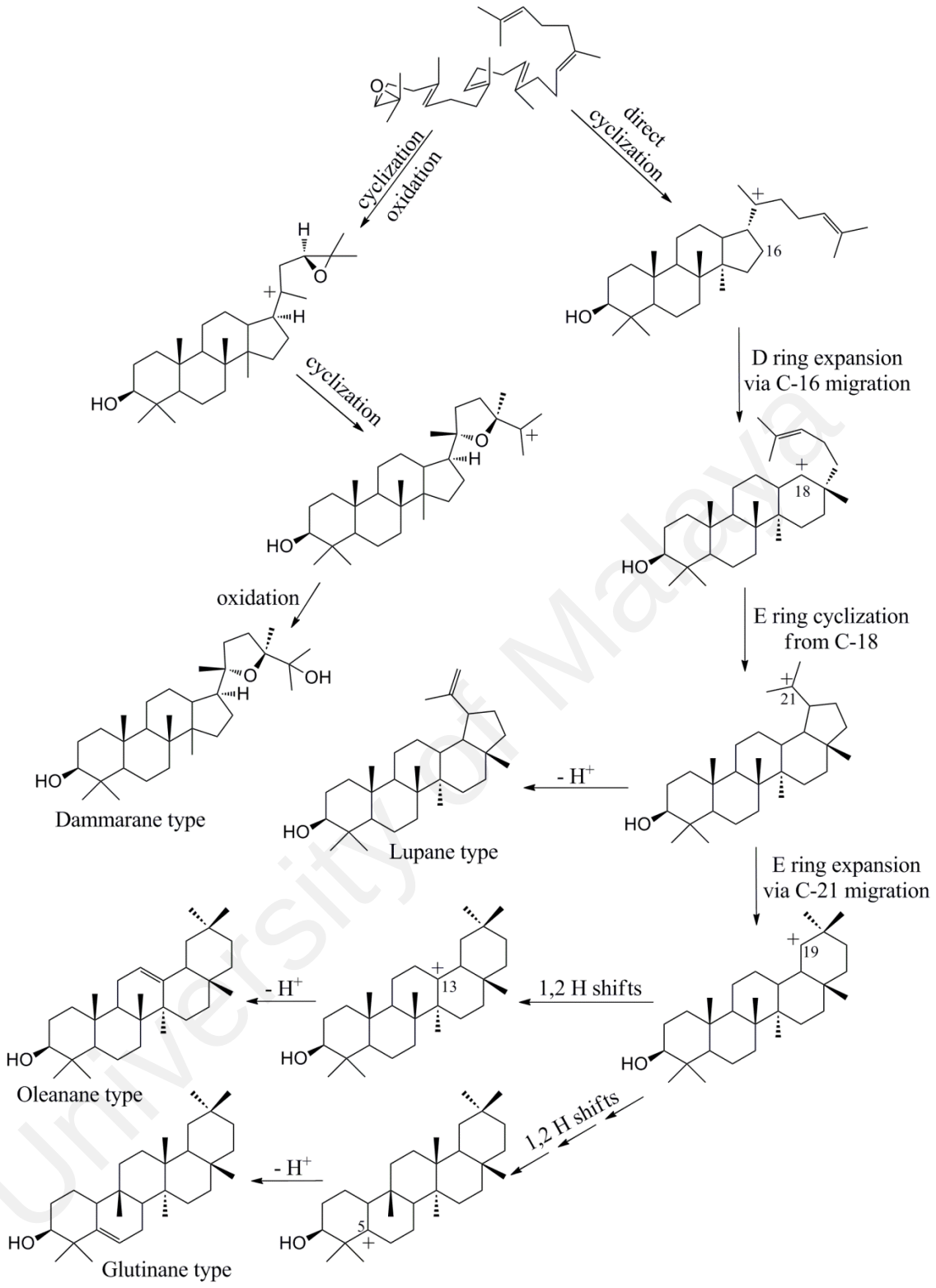


**Figure 2.4**: Biogenesis of selected type of triterpenoids

## 2.4 Tetra- and pentacycles triterpenoids

The majority of triterpenoids formed is either in 6/6/6/5 tetracycles, 6/6/6/6/5 or 6/6/6/6/6 pentacycles that those skeletons was composed of several isoprene units that linked in regular or irregular arrangement (Ruzicka, 1953) as illustrated in Figure 2.5.

Once the triterpenoids have formed, it may be modified through different type of enzymes to introduce a massive variety into the final range of triterpenoids products. Some of the enzymes and its reaction involve such as cytochrome P450 hydroxylases (oxidation), reductases (reduction), glycosyl and methyl transferases (addition of glucose and methyl). The skeletons also may performed some rearrangement to its skeletons such as cyclization, 1,2-hydride shifts and 1,2-methyl shifts (Xu et al., 2004).

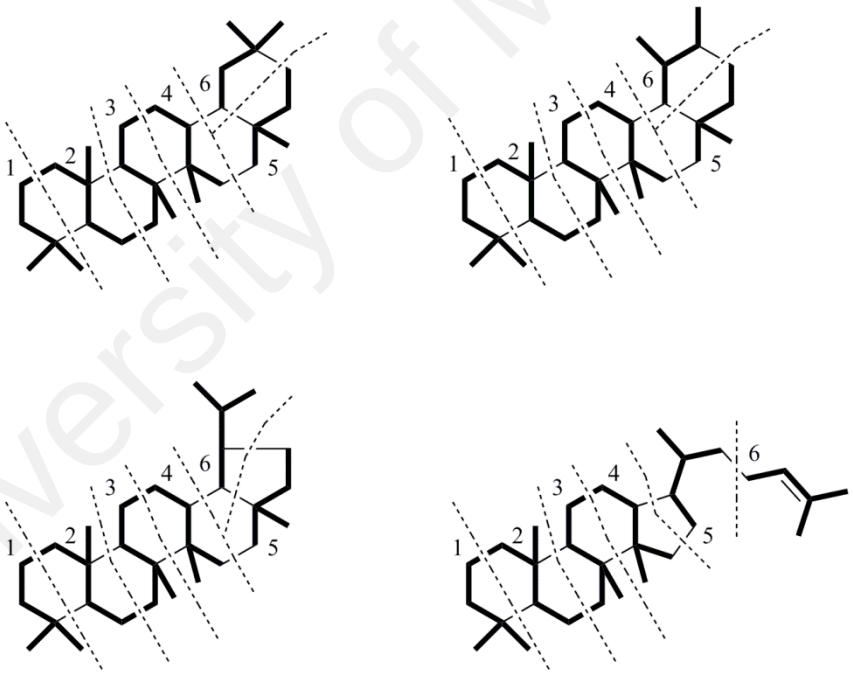


**Figure 2.5**: Different cycles of triterpenoids

## 2.5 Chemical constituents of *Walsura* species

Chemical and pharmacological of this genus have been very actively studied in the past few decades, resulting in the separation and identification of various types of compounds with promising pharmacological properties. To date, eight *Walsura* species have been studied chemically. The species are *W. robusta*, *W. tubulata*, *W. trichostemon*, *W. piscidia*, *W. cochinchinensis*, *W. yunnanensis*, *W. chrysogyne* and *W. trifoliata*. A total of 152 compounds have been reported in which limonoids formed the majority (70 compounds; 6 novel and 69 new), while the least type of compounds isolated are sesquiterpenoids with only 3 compounds. Among all the compounds, 44 compounds from triterpenoids skeleton have chemically been isolated from various part of *Walsura* species with almost half of it comes from apotirucallane type, having the largest number of compounds followed by dammarane (10 compounds), tirucallane (7 compounds), cycloartane (4 compounds) and lupane type (3 compounds). The remaining compounds isolated also belonged to sterols (6 compounds) and aromatic derivatives (20 compounds).

The interesting chemical constituents from leaves and twigs part of *W. robusta* consist of 5 limonoids, 3 novel compounds; walsuronoid A (**89**), walsuronoid B (**85**) and walsuronoid C (**86**) with 2 new compounds; (Ji et al., 2016) walsuronoid D (**87**) and walsuronoid E (**88**) (Yin et al., 2007) was the first limonoid peroxide isolated feature an unprecedented *seco*-A ring limonoids skeleton incorporating a 3, 4-peroxide bridge while remaining 2 novel limonoids share the rare 18(13-14)-*abeo*-limonoid skeleton. The two new limonoids were active with $IC_{50}$ ranging from 2.7-4.5 μM against several cancer cell line; HL-60 (human myeloid leukemia), SMMC-7721 (hepatocellular carcinoma), A-549 (lung), MCF-7 (breast) and SW480 (colon). The same species, from extracts of its leaves also gave nine new cedrelone-type limonoids (Wang et al., 2016); namely walsunoids A-I (**44-52**), with only **51** showed moderate inhibitory aginst human

11β-HSD1 with $IC_{50}$ 9.9 μM. A new sesquiterpenoid (Hou et al., 2013), 10β-nitro-isodauc-3-en-15-al (**97**) was isolated from the same part of extracts having a rare nitro group attached to the ring systems; however this compound showed no antimicrobial activity against *Staphylococcus aureus*.

The phytochemical investigation of the ethanol extracts of twigs and leaves of *W. cochinchinensis* has led to isolation of 33 compounds, including 2 novel tetranortriterpenoids, walsucochins A-B (**30-31**) (Zhou et al., 2008), 28 new limonoids, walsucochinoids A-R (Han et al., 2014) (**60-61, 32-43, 62-65**) and cochinchinoids A-J (**53-59, 82-84**) and 3 new tirucallane types, 3-epimesendanin S (**66)** and cochinchinoids K (**67**). **67** possess a potent activity against mouse 11β-HSD1 with $IC_{50}$ = 0.82 μM while **33-34** showed mild activities for mouse and human 11β-HSD1 inhibitors with $IC_{50}$ 13.4±1.7 μM and 8.25±0.69 μM respectively (Han et al., 2013). **60-61** were isolated as unique skeleton with rearranged 5-membered C rings fused with 6-membered aromatic D rings plus an extra ring F of tetrahydrofuran formed connecting C-6 and C-28 (Han et al., 2012). A significant cell protecting activities against $H_2O_2$ induced PC12 cell damage were discovered for **30-31** which featured a contracted 5-membered C ring fused with a rare phenylacetylene moiety.

The chemical investigation on the leaves of *W. piscidia* has led to the isolation of twelve new compounds (Balakrishna et al., 2003; Govindachari et al., 1995; Purushothaman et al., 1985). Those compounds were two tiruccalane type; piscidinols A-B (**68-69**), four apotiruccalane type; piscidinols C-F (**13-16**), three protolimonoids; piscidinols G (**17**), piscidofuran (**90**) and piscidenone (**23**), and two from lupane and flavone type; lup-20(29)-ene-3β,30-diol (**91**) and 5-hydroxy-7,3',4',5'-tetramethoxyfalvone (**95**). There was only one publication on *Walsura tubulata* (Chatterjee et al., 1968) from which the leaves extract afforded one new pentacyclic

triterpene alcohol, a multiflorane type namely walsurenol (**92**). No biological activity was reported from this plants species.

Eichlerianic acid (**93**) and viridiflorol (**96**) which were isolated from bark of *W. chrysogyne* showed significant ichthyotoxicity (toxic to fish or are toxins produced by fish) against zebrafish (Danio rerio) with Median Tolerance Limit ($TL_M$) of 6.7 ppm and 15 ppm respectively (Mahmod et al., 2013). A limonoid compound which was isolated from the same part of the same species namely walsogyne A (**76**), was novel compound by the *seco* of ring C that produce a unique tetrahydrofuran-2-ol ring from the cleavage of C-11/C-12 bond and presence of γ-hydroxy-α,β-unsaturated-γ-lactone ring at C-17 (Mohamad et al., 2008). **76** was tested against several cancer cell lines; HepG2 (liver), HL-60, A-549, MCF-7 together with six new limonoids; namely walsogyne B-G (**72-75, 77-78**) (Nugroho et al., 2013) isolated by the same research group. The results showed that those seven limonoids compounds possess moderate cytotoxic activities.

The chemical investigations on *W. yunnanensis* have resulted in the isolation and characterization of a total of 41 compounds (Jiang, 2013; Luo et al., 2001) . Even though twenty new limonoids were discovered, only half were tested for its biological activities. Yunnanolide A (**80**) and 11*β*-hydroxyisowalsuranolide (**81**) showed strong cytotoxic activities against several tumor cell line; HL-60, SMMC-7721, A-549, MCF-7 and SW480 which resulted in $IC_{50}$ lies between 2.2 μM - 4.2 μM (Ji et al., 2014) while 11*β*-hydroxycedrelone (**79**) possess moderate activity against human myeloid leukemia, cell line with $IC_{50}$ = 8.9 μM (Luo et al., 2000). Walsuraside (**94**), a new polyphenolic glycoside that was isolated from BuOH extract of this bark species showed significant antioxidant activities with $IC_{50}$ values 43.2 ± 2.5 μg/mL (Luo et al., 2006).

Only four new apotirucallane type; namely trichostemonoate (**70**) (Phontree et al., 2014), 11,25-dideacetyltrichostemonate (**26**), 21,24,25-triacetyl-7-deacetyl-6-hydroxylbrujavanone E (**27**) and 7-deacetylbrujavanone E (**28**) with two new tirucallane trichostemonate (**29**) and trichostemonol (**71**) were discovered from leaves and root of *W. trichostemon*. All the new compounds were tested for Human KB and HeLa cancer cell line, which only **29** (Sichaem et al., 2012) resulted in potent cytotoxicity against both cell line with an $IC_{50}$ value of 3.28 µg/mL and 0.93 µg/mL respectively while **26** only showed good cytotoxic activity against KB cells with an $IC_{50}$ value of 3.95 µg/mL (Sichaem, 2014).

Methanol, ethyl acetate and hexane extract from root of *W. trifoliata* were tested for α-glucosidase inhibition and antioxidant activities (Mini & Gajendran, 2015). Results showed that MeOH extract possess inhibitory activity of 65.47% at maximum concentration of 1000 µg/mL with $IC_{50}$ = 690±1.44 µg/mL while the same extract also showed good antioxidant activities (DPPH Radical Scavenging Assay) with $IC_{50}$ = 620±1.99 µg/mL when compared with both hexane and ethyl acetate extracts. Moderate insecticidal activities also were found from five new apotirucallane type; piscidinol H-L (**18-22**) against *Spodoptera litura* (tobacao caterpillar) and *Achaea janata* (castor semilooper). In addition, piscidinone A-B (**24-25**) was two novel apotirucallane type triterpenoids that were discovered from leaves part of this species. While most of apotirucallane skeleton has furan and/or hemiacetal ring as a side chain, both of this novel structure showed rare 6-membered conjugated pyran moiety attached at C-17 together with both 2-hydroxyisopropyl and hydroxyl group. Both of this novel compounds showed only moderate activities against selected cancer cell lines; HT-29 (colon), MCF-7, HeLa, A-549, B-16 (skin melanoma), IEC-6 (small intestine), L6 (skeletal), and PC-3 (prostate) (Rao et al., 2012).

All the triterpenoids compounds that have been isolated and identified from *Walsura* species together with their biological activities were listed in Table 2.2

**Table 2.2**: Type and bioactivities of triterpenoids from *Walsura* genus

| TYPE | COMPOUNDS | BIOACTIVITIES | REFERENCES |
|---|---|---|---|
| Apotirucallane | Piscidinols C-E (**13-15**) | nd | (Purushothaman et al., 1985) |
| | Piscidinols F (**16**) | | (Govindachari et al., 1995) |
| | Piscidinol H(**18**) | | (Rao et al., 2015) |
| | Piscidinol I (**19**) | Moderate anti-feedant towards *S. litura* and *A. janata* | |
| | Piscidinol J-K(**20, 21**) | nd | |
| | Piscidinol L (**22**) | Moderate anti-feedant towards *S. litura* and *A. janata* | |
| | Piscidinone A-B (**24, 25**) | Moderate cytotoxic ($IC_{50}$: 13.5-50.6 µg/mL) | (Rao et al., 2012) |
| | 11,25-dideacetyl trichostemonoate (**26**) | nd | (Sichaem et al., 2012) |
| | 21,24,25-triacetyl-7-deacetyl-6-hydroxyl brujavanone E (**27**) | Moderate cytotoxic ($IC_{50}$: 12.9-17.1 µg/mL) | |
| | 7-deacetyl brujavanone E (**28**) | nd | |
| | Trichostemonate (**29**) | Good cytotoxic ($IC_{50}$: 0.9-3.8 µg/mL) | |
| Tirucallane | Trichostemonoate (**70**) | Good cytotoxic ($IC_{50}$: 3.8-5.5 µg/mL) | (Phontree et al., 2014) |
| | Trichostemonol (**71**) | nd | (Sichaem et al., 2014) |
| | 3-epimesendanin S (**66**) | nd | (Han et al., 2013) |
| | Cochinchinoids K (**67**) | Good inhibitory against mouse 11β-HSD1 ($IC_{50}$: 0.82µM) | |
| | Piscidinols A-B (**68-69**) | nd | (Purushothaman et al., 1985) |
| Cyclo-artane | 3β,24,25,26-tetrolcycloartane | Weak cytotoxic ($IC_{50}$: >40µM) | (Ji et al., 2016) |
| | Cycloart-23-ene-3β,25-diol | Moderate ichthyotoxicity against zebrafish (TLM: 6.7-15ppm) | (Mahmod et al., 2013) |
| | 25-methoxycyclo art-23-ene-3β-ol | | |
| Dam-marane | Chrysura | nd | |
| | Cabraleadiol | Moderate ichthyotoxicity against zebrafish (TLM: 6.7-15ppm) | |
| | Ocotillone | | |

| | | | |
|---|---|---|---|
| | 11α,20-dihydroxy dammar-24-ene-3-one | Good cytotoxic ($IC_{50}$: 1.9-3.7 µg/mL) | (Phontree et al., 2014) |
| Lupane | Lup-20(29)-ene-3β,30-diol (**91**) | nd | (Balakrishna et al., 1995) |
| Multi-florane | Walsurenol (**92**) | nd | (Chatterjee et al., 1968) |

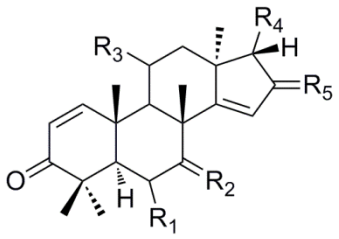


A = 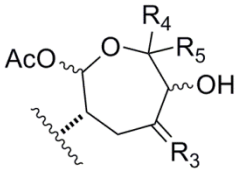


B = 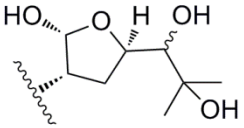


C = 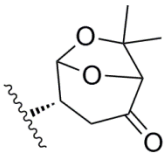


D = 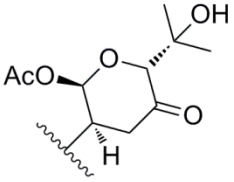


E = 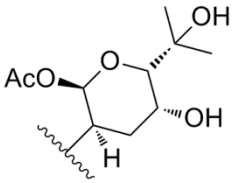


F = 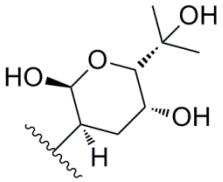


G = 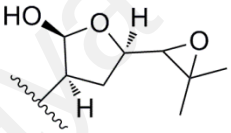


I = 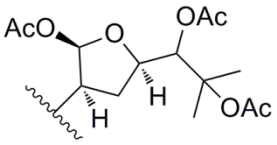


J = 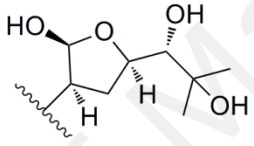


K = 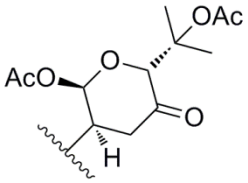


L = 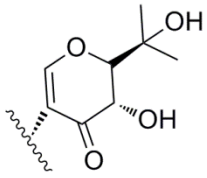


M = 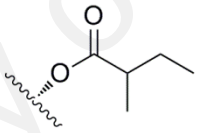


N = 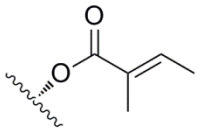


**13**: $R_1$ = H; $R_2$ = H,α-OH; $R_3$ = α-OH; $R_4$ = A; $R_5$ = $R_6$ = $R_7$ = $R_8$ = H
**14**: $R_1$ = H; $R_2$ = H,α-OH; $R_3$ = α-OH; $R_4$ = A; $R_5$ = H,α-OH; $R_6$ = $R_7$ = $R_8$ = H
**15**: $R_1$ = H; $R_2$ = O; $R_3$ = α-OH; $R_4$ = A; $R_5$ = H,α-OH; $R_6$ = $R_7$ = $R_8$ = H
**16**: $R_1$ = H; $R_2$ = H,α-OH; $R_3$ = α-OH; $R_4$ = A; $R_5$ = H,OMe; $R_6$ = $R_7$ = Me; $R_8$ = O
**17**: $R_1$ = H; $R_2$ = H,α-OH; $R_3$ = H; $R_4$ = B; $R_5$ = H
**18**: $R_1$ = H; $R_2$ = O; $R_3$ = α-OH; $R_4$ = D; $R_5$ = H
**19**: $R_1$ = H; $R_2$ = H,α-OH; $R_3$ = α-OH; $R_4$ = E; $R_5$ = H
**20**: $R_1$ = H; $R_2$ = H,α-OH; $R_3$ = M; $R_4$ = D; $R_5$ = H
**21**: $R_1$ = H; $R_2$ = H,α-OH; $R_3$ = H; $R_4$ = F; $R_5$ = H
**22**: $R_1$ = H; $R_2$ = H,α-OH; $R_3$ = H; $R_4$ = G; $R_5$ = H
**23**: $R_1$ = H; $R_2$ = O; $R_3$ = M; $R_4$ = C; $R_5$ = H
**24**: $R_1$ = H; $R_2$ = O; $R_3$ = N; $R_4$ = L; $R_5$ = H
**25**: $R_1$ = H; $R_2$ = O; $R_3$ = M; $R_4$ = L; $R_5$ = H
**26**: $R_1$ = H; $R_2$ = H,α-OAc; $R_3$ = α-OH; $R_4$ = D; $R_5$ = H
**27**: $R_1$ = α-OH; $R_2$ = H,α-OH; $R_3$ = α-OH; $R_4$ = I; $R_5$ = H
**28**: $R_1$ = H; $R_2$ = H,α-OH; $R_3$ = α-OH; $R_4$ = J; $R_5$ = H
**29**: $R_1$ = H; $R_2$ = H,α-OAc; $R_3$ = α-OAc; $R_4$ = K; $R_5$ = H

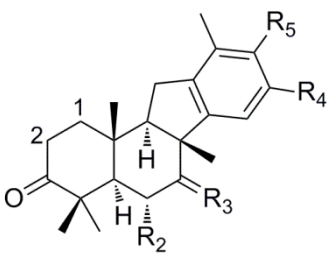


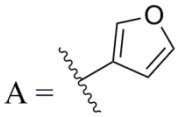


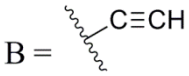


**30**: $R_1$ = O; $R_2$ = H; $R_3$ = H,OH; $R_4$ = OMe; $R_5$ = B; $\Delta^{1,2}$
**31**: $R_1$ = $R_2$ = H; $R_3$ = O; $R_4$ = OMe; $R_5$ = B
**32**: $R_1$ = O; $R_2$ = H; $R_3$ = H,α-OH; $R_4$ = OMe; $R_5$ = A
**33**: $R_1$ = O; $R_2$ = H; $R_3$ = O; $R_4$ = OMe; $R_5$ = A
**34**: $R_1$ = O; $R_2$ = H; $R_3$ = H,α-OAc; $R_4$ = OMe; $R_5$ = A
**35**: $R_1$ = O; $R_2$ = H; $R_3$ = H,α-OAc; $R_4$ = OH; $R_5$ = A
**36**: $R_1$ = O; $R_2$ = OH; $R_3$ = H,α-OAc; $R_4$ = OMe; $R_5$ = A
**37**: $R_1$ = O; $R_2$ = OH; $R_3$ = H,α-OAc; $R_4$ = OH; $R_5$ = A
**38**: $R_1$ = O; $R_2$ = α-OH; $R_3$ = H,α-OAc; $R_4$ = OMe; $R_5$ = A
**39**: $R_1$ = O; $R_2$ = α-OAc; $R_3$ = H,α-OH; $R_4$ = OMe; $R_5$ = A
**40**: $R_1$ = O; $R_2$ = α-OH; $R_3$ = H,α-OAc; $R_4$ = OH; $R_5$ = A
**41**: $R_1$ = H,α-OH; $R_2$ = H; $R_3$ = H,α-OH; $R_4$ = OMe; $R_5$ = A
**42**: $R_1$ = H,β-OH; $R_2$ = H; $R_3$ = H,α-OH; $R_4$ = OMe; $R_5$ = A
**43**: $R_1$ = H,α-OH; $R_2$ = H; $R_3$ = O; $R_4$ = OMe; $R_5$ = A

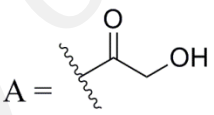


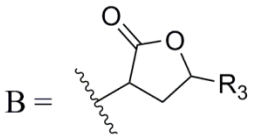


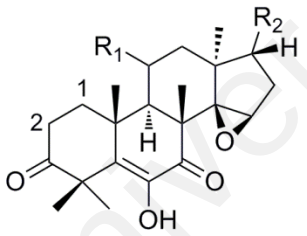


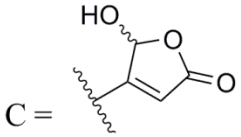


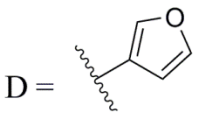


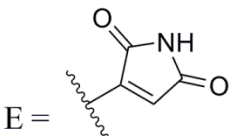


**44**: $R_1$ = β-OH; $R_2$ = A; $\Delta^{1,2}$
**45**: $R_1$ = β-OH; $R_2$ = B; $R_3$ = β-OMe; $\Delta^{1,2}$
**46**: $R_1$ = β-OH; $R_2$ = B; $R_3$ = OH; $\Delta^{1,2}$
**47**: $R_1$ = β-OH; $R_2$ = B; $R_3$ = α-OMe; $\Delta^{1,2}$
**48**: $R_1$ = β-OH; $R_2$ = B; $R_3$ = H; $\Delta^{1,2}$
**49**: $R_1$ = β-OAc; $R_2$ = C; $\Delta^{1,2}$
**50**: $R_1$ = β-OAc; $R_2$ = C
**51**: $R_1$ = β-OAc; $R_2$ = D; $\Delta^{1,2}$
**52**: $R_1$ = β-OH; $R_2$ = E; $\Delta^{1,2}$

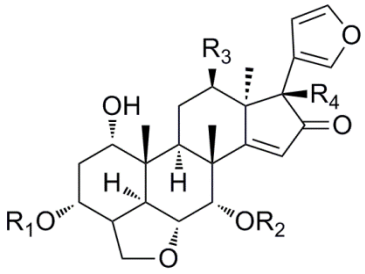


A= 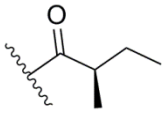

B= 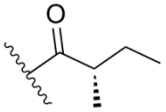

C= 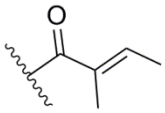

D= 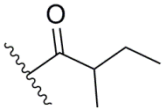

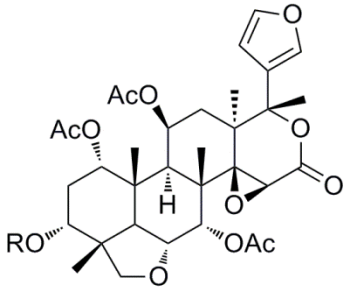


**53**: $R_1$ = A; $R_2$ = A; $R_3$ = H; $R_4$ = OH
**54**: $R_1$ = B; $R_2$ = B; $R_3$ = H; $R_4$ = OH
**55**: $R_1$ = C; $R_2$ = C; $R_3$ = $R_4$ = H
**56**: $R_1$ = C; $R_2$ = D; $R_3$ = OAc; $R_4$ = H
**57**: R = C
**58**: R = A
**59**: R = B

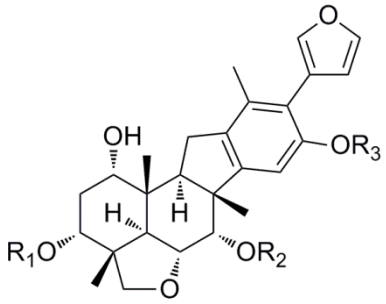


A= 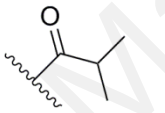

B= 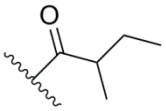

C= 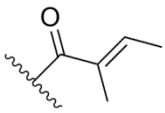

**60**: $R_1$ = A; $R_2$ = $R_3$ = H
**61**: $R_1$ = C; $R_2$ = H; $R_3$ = Me
**62**: $R_1$ = B; $R_2$ = H; $R_3$ = Me
**63**: $R_1$ = B; $R_2$ = $R_3$ = H
**64**: $R_1$ = C; $R_2$ = H; $R_3$ = Me
**65**: $R_1$ = C; $R_2$ = A; $R_3$ = H

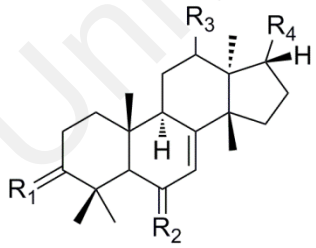


A = 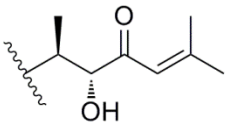

B = 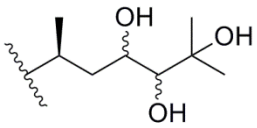

C = 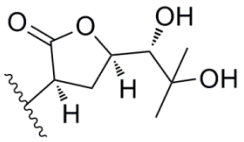

**66**: $R_1$ = H,α-OH; $R_2$ = H; $R_3$ = β-OH; $R_4$ = A
**67**: $R_1$ = H,β-OH; $R_2$ = $R_3$ = H; $R_4$ = C
**68**: $R_1$ = O; $R_2$ = H; $R_3$ = H; $R_4$ = B
**69**: $R_1$ = H,β-OH; $R_2$ = $R_3$ = H; $R_4$ = B
**70**: $R_1$ = H,OAc; $R_2$ = O; $R_3$ = β-OH; $R_4$ = A
**71**: $R_1$ = H,OH; $R_2$ = O; $R_3$ = β-OH; $R_4$ = A

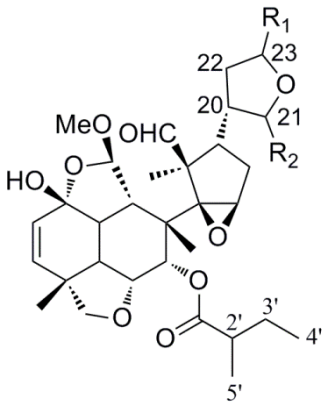


**72**: $R_1 = R_2 = H$; $\Delta^{2',3'}$; $\Delta^{20,21}$; $\Delta^{22,23}$
**73**: $R_1 = R_2 = H$; $\Delta^{20,21}$; $\Delta^{22,23}$
**74**: $R_1 = R_2 = OMe$; $\Delta^{2',3'}$; $\Delta^{20,22}$
**75**: $R_1 = R_2 = OMe$; $\Delta^{20,22}$

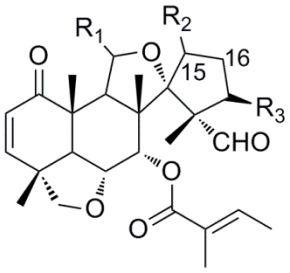


A = 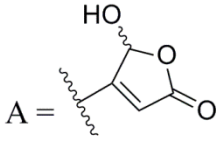


B = 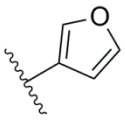


**76**: $R_1 = OH$; $R_2 = \beta$-OH; $R_3 = A$
**77**: $R_1 = \beta$-OH; $R_2 = H$; $R_3 = B$; $\Delta^{15,16}$
**78**: $R_1 = \alpha$-OH; $R_2 = H$; $R_3 = B$; $\Delta^{15,16}$

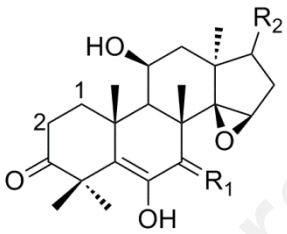


A = 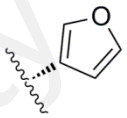


B = 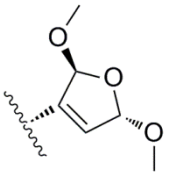


C = 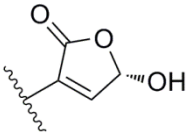


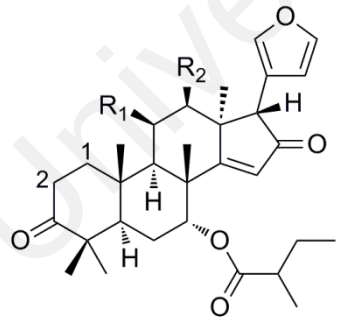


**79**: $R_1 = O$; $R_2 = A$
**80**: $R_1 = H$; $R_2 = B$; $\Delta^{1,2}$
**81**: $R_1 = H$; $R_2 = C$; $\Delta^{1,2}$
**82**: $R_1 = OAc$; $R_2 = H$; $\Delta^{1,2}$
**83**: $R_1 = H$; $R_2 = OAc$; $\Delta^{1,2}$
**84**: $R_1 = H$; $R_2 = OAc$

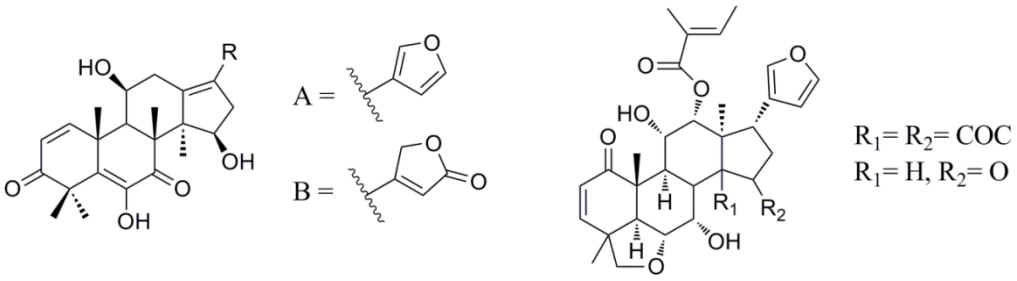


**85**: R = A **87**: $R_1 = R_2$ =COC
**86**: R = B **88**: $R_1$ = H; $R_2$ = O

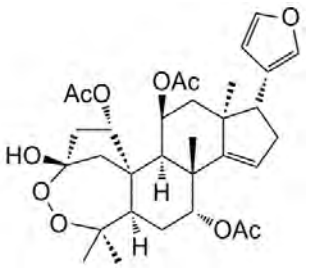


**89**

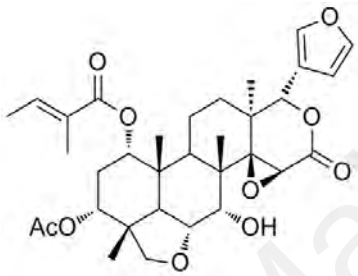


**90**

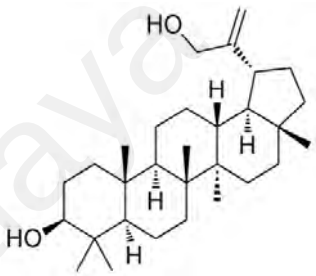


**91**

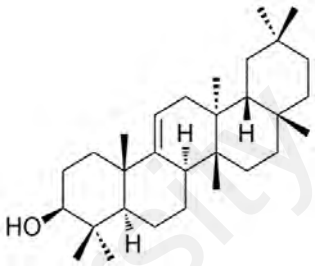


**92**

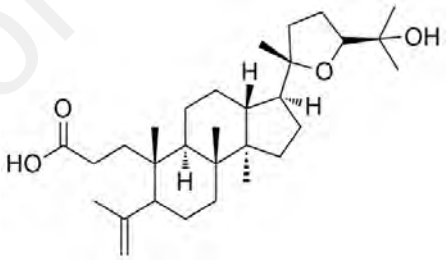


**93**

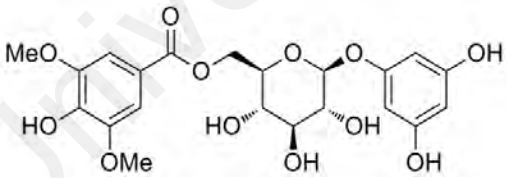


**94**

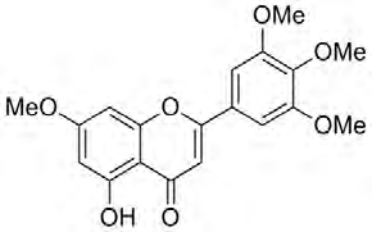


**95**

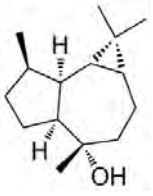


**96**

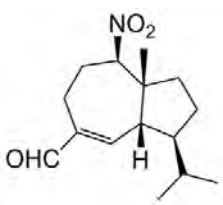


**97**

# CHAPTER 3: RESULTS AND DISCUSSION

*W. pinnata* Hassk. (Meliaceae), coded KL 4571, was collected from Hutan Kuala Lipis, Pahang was investigated for the chemical constituents. The dichloromethane extract was chosen because of its medium polarity extracts. The extract has been subjected to extensive chromatographic separation such as column chromatography, preparative TLC and recycling HPLC to yield ten pure compounds; five triterpenoids, one sesquiterpenoid, two sterols and two phenolic compounds.

The structural elucidation of all compounds will be discussed in detail through spectroscopic methods, principally NMR experiments. The elucidated compounds have been arranged according to their skeletal types and presented in **Table 3.1**. Of the compounds isolated, one is new natural product compound (**100**). Complete $^{1}H$, $^{13}C$, DEPT, COSY and HMBC spectral data were given for all compounds and whenever necessary, the NMR data of relevant compounds was included as comparisons to further validate the proposed structure.

**Table 3.1**: Compounds isolated from *Walsura pinnata* Hassk

| Compounds | Type | Classes |
|---|---|---|
| 3-oxo-lup-20(29)-en-28-oic acid, **97** | Triterpenoid | Lupane |
| 3*β*-hydroxy-5-glutinen-28-oic acid, **98** | Triterpenoid | Glutinane |
| 3-oxo-olean-11-en-28,13*β*-olide, **99** | Triterpenoid | Oleanane |
| 3-oxo-olean-9(11),12-dien-28-oic acid, **100** | Triterpenoid | Oleanane |
| 3-oxo-20(24)-epoxy-12*β*,25-dihydroxydammarane, **101** | Triterpenoid | Dammarane |
| 2(3),6(7)-diepoxy-9-humulene, **102** | Sesquiterpenoid | Humulane |
| Stigmasterol, **103** | Sterol | - |
| *β*-sitosterol glycoside, **104** | Sterol | - |
| 4-hydroxy-3-methoxybenzoic acid, **105** | Phenolic compounds | - |
| 4-hydroxy-4,8-dimethyl-1-tetralone, **106** | Phenolic compounds | - |

### 3.1 Compound 97: 3-oxo-lup-20(29)-en-28-oic acid

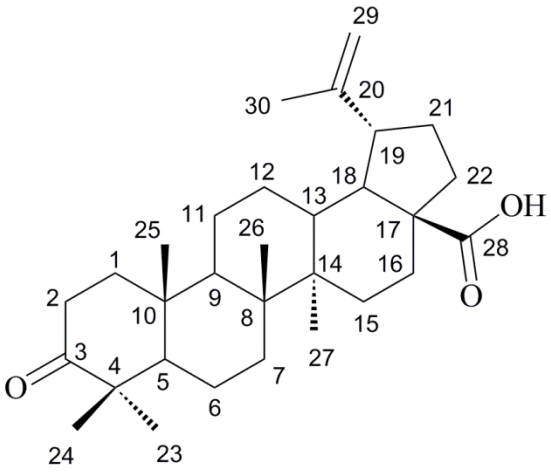


3-oxo-lup-20(29)-en-28-oic acid, **97** was isolated as white amorphous powder. It's molecular formula is $C_{30}H_{46}O_3$ as deduced from its positive LCMS-IT-TOF ($[M+H]^+$, m/z 455.3581; calcd. for $C_{30}H_{47}O_3$; 455.3525) spectrum, consistent with eight degrees of unsaturation. The IR spectrum showed strong absorption bands for hydroxyl group from –COOH moiety (3440 $cm^{-1}$), C-H alkene (2942 $cm^{-1}$) and carbonyl (1701 $cm^{-1}$) functionalities (Gary et al., 2010).

The $^1$H NMR spectrum (Figure 3.2) revealed the presence of six tertiary methyls of which five of them gave methyl signals within close proximity; δ 0.94 (Me-25), 0.99 (Me-26), 1.00 (Me-27), 1.03 (Me-24) and 1.08 (Me-23) while the more downfield methyl at δ 1.70 (Me-30). The geminal olefinic protons signal of C-29 appeared as two broad singlets at δ 4.62 and δ 4.75, the coupling constant for the geminal olefinic protons is too small compared to the width of the singlet peak. Therefore, it was observed as broad singlet rather than a doublet signal. The features mentioned were typical of a lupane triterpenoid skeleton (Chaturvedula et al., 2003; Zhang et al., 2014) Also observed, was the non-equivalent methylene signals at δ 2.42 (*m*, H-2a) and δ 2.50 (*m*, H-2b), which were particularly deshielded suggesting that it is close to an electron withdrawing group (C=O).

The $^{13}C$ NMR (Figure 3.3) and DEPT (Figure 3.4) spectra of 3-oxo-lup-20(29)-en-28-oic acid, **97** coupled with HSQC (Figure 3.6) analysis revealed the presence of thirty carbons among which are six methyl resonated at δ 14.6 (C-27), 15.8 (C-26), 16.0 (C-25), 19.4 (C-30), 21.0 (C-24) and 26.6 (C-23). Two carbonyl signals appeared at δ 180.8 (C-28) and 218.2 (C-3) while an olefinic moiety was observed as methylene and quaternary carbon resonated at δ 109.8 (C-29) and δ 150.3 (C-20) respectively.

In the COSY experiment (Figures 3.1 and 3.5), the methine of H-19 (δ 3.02, *td*, *J* = 10.7, 4.8 Hz) showed cross correlation with H-18 and H-21 while H-13 (δ 2.23, *m*) showed interaction with H-12 and H-18.

From the analysis of HMBC experiments (Figures 3.1 and 3.7), the position of ketone group at C-3 (δ 218.2) was supported from correlation with H-2a (δ 2.42, *m*), H-2b (δ 2.50, *m*), Me-23 (δ 1.08, *s*) and Me-24 (δ 1.03, *s*). Both methyls were deduced as geminal signals through cross correlations between them and C-4. A double bond at C-20(29) position was confirmed on the basis of correlation with Me-30 (δ 1.70, *s*) and H-19 (δ 3.02, *td, J* = 10.7, 4.8 Hz*)* while the existence of carboxyl moiety at C-28 (δ 180.8) was established through interaction with H-13 (δ 2.23, *m*) and H-18 (δ 1.64, *m*). The stereochemistry of compound **97** was established by comparing with the optical rotation and coupling constant from the literature.

Based on the complete assignments of 1D and 2D NMR spectra (Table 3.2), **97** was concluded to be 3-oxo-lup-20(29)-en-28-oic acid, trivially named as betulonic acid (Kuroyanagi et al., 1986).

**Table 3.2**: $^{1}H$ (600 MHz) and $^{13}C$ (150 MHz) NMR data of 3-oxo-lup-20(29)-en-28-oic acid (**97**) in $CDCl_3$

| Position | Compound **97** | | (Kuroyanagi et al., 1986) | |
|---|---|---|---|---|
| | $\delta_H$ (ppm), *J (Hz)* | $\delta_C$ (ppm) | $\delta_H$ (ppm), *J (Hz)* | $\delta_C$ (ppm) |
| 1 | 1.38, *m*<br>1.91, *m* | 39.6 | 1.31, m<br>1.90, *ddd* (8.4, 4.9, 2.9) | 39.6 |
| 2 | 2.42, *m*<br>2.50, *m* | 34.1 | 2.40, *ddd* (10.4, 5.0, 2.8)<br>2.49, *ddd* (15.8, 6.4, 5.2) | 34.1 |
| 3 | - | 218.2 | - | 218.2 |
| 4 | - | 47.3 | - | 47.3 |
| 5 | 1.35, *m* | 54.9 | 1.31, *m* | 54.9 |
| 6 | 1.52, *m* | 20.6 | 1.41, *m* | 19.6 |
| 7 | 1.44, *m* | 33.6 | 1.41, *m* | 33.6 |
| 8 | - | 40.6 | - | 42.5 |
| 9 | 1.38, *m* | 49.9 | 1.40, *m* | 49.9 |
| 10 | - | 36.9 | - | 36.9 |
| 11 | 1.34, *m*<br>1.44, *m* | 21.4 | 1.33, *m*<br>1.44, *m* | 21.4 |
| 12 | 1.06, *m*<br>1.73, *m* | 25.4 | 1.31, *m*<br>1.73, *m* | 25.5 |
| 13 | 2.23, *m* | 38.5 | 2.22,*m* | 38.5 |
| 14 | - | 42.5 | - | 40.6 |
| 15 | 1.22, *m*<br>1.54, *m* | 29.7 | 1.21, *m*<br>1.53, *m* | 29.7 |
| 16 | 1.44, *m*<br>2.28, *m* | 32.1 | 1.43, *m*<br>2.28, *m* | 32.1 |
| 17 | - | 56.3 | - | 56.4 |
| 18 | 1.64, *m* | 49.2 | 1.63, *t* (7.6) | 49.2 |
| 19 | 3.02, *td* (10.7, 4.8) | 46.9 | 3.01,*m* | 46.9 |
| 20 | - | 150.3 | - | 150.3 |
| 21 | 1.42, *m*<br>1.99, *m* | 30.5 | 1.99, *m* | 30.5 |
| 22 | 1.47, *m*<br>1.99, *m* | 37.0 | 1.48, *m* | 37.0 |
| 23 | 1.08, *s* | 26.6 | 1.07, *s* | 26.6 |
| 24 | 1.03, *s* | 21.0 | 1.01, *s* | 21.0 |
| 25 | 0.94, *s* | 16.0 | 0.92, *s* | 16.0 |
| 26 | 0.99, *s* | 15.8 | 0.97, *s* | 15.8 |
| 27 | 1.00, *s* | 14.6 | 0.99, *s* | 14.6 |
| 28 | - | 180.8 | - | 181.7 |
| 29 | 4.62, *br s*<br>4.75, *br s* | 109.8 | 4.61, *br s*<br>4.74, *br s* | 109.8 |
| 30 | 1.70, *s* | 19.4 | 1.69, *s* | 19.4 |

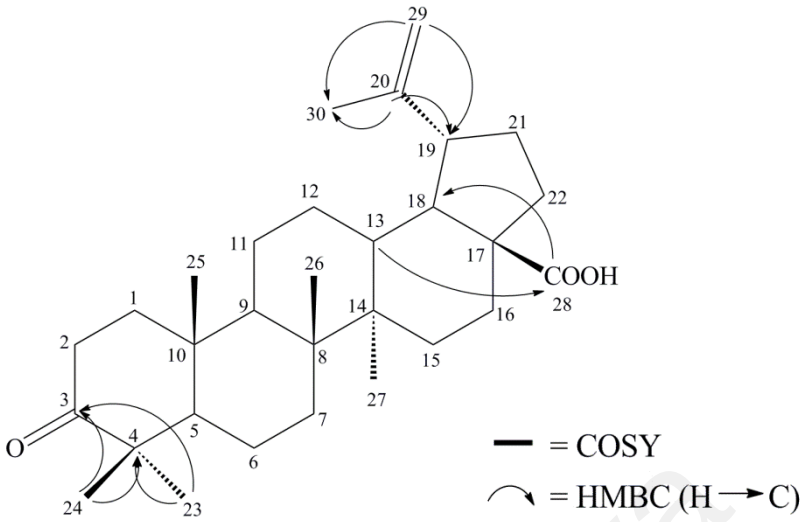


**Figure 3.1**: Selected COSY and HMBC correlations of 3-oxo-lup-20(29)-en-28-oic acid (**97**)

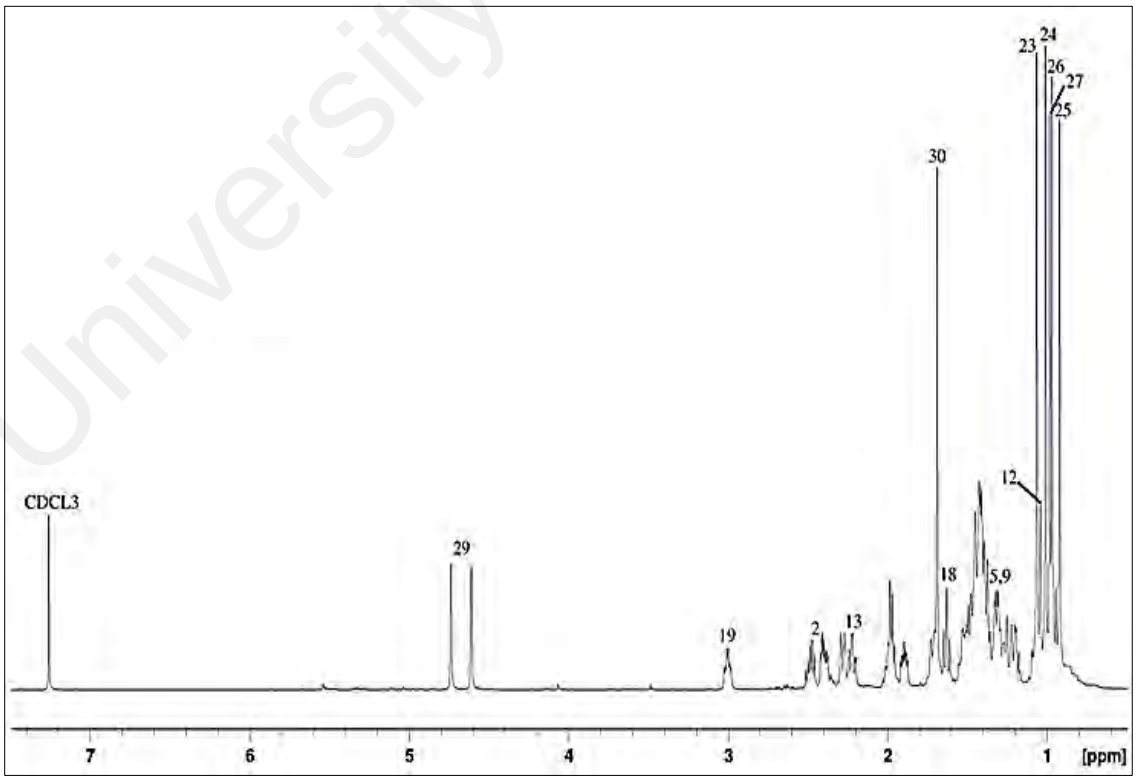


**Figure 3.2**: $^{1}$H (600 MHz) NMR spectrum of 3-oxo-lup-20(29)-en-28-oic acid (**97**)

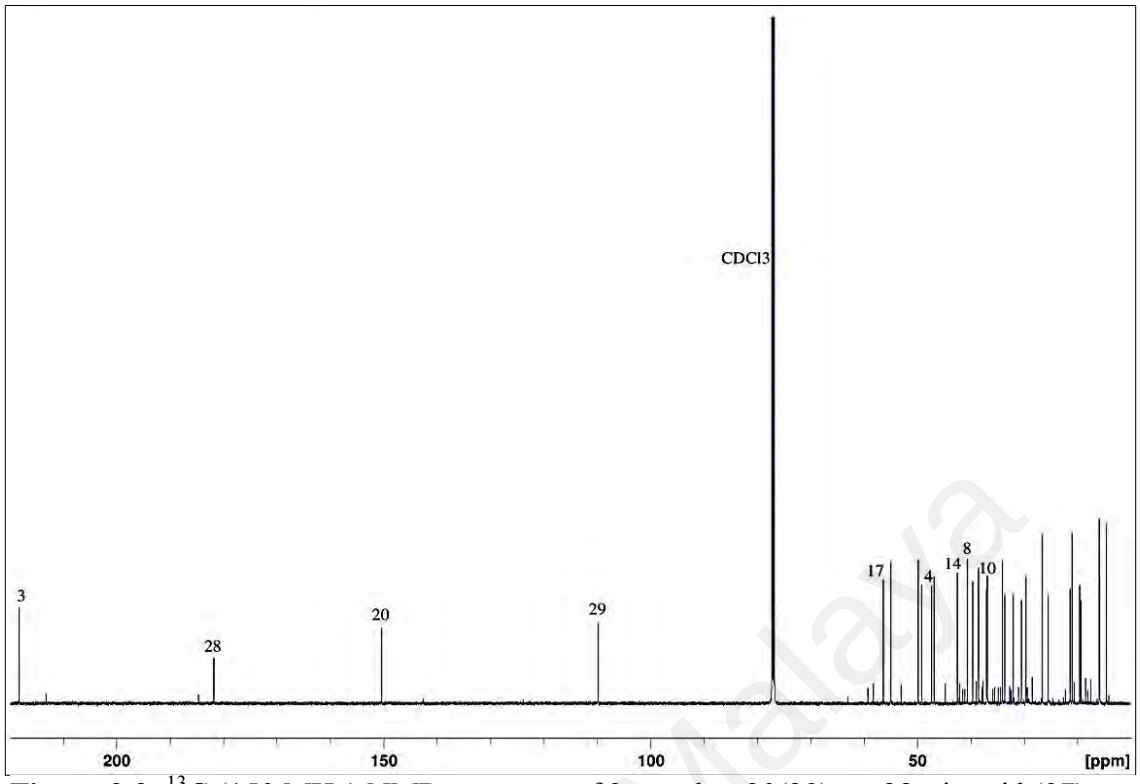


**Figure 3.3**: $^{13}C$ (150 MHz) NMR spectrum of 3-oxo-lup-20(29)-en-28-oic acid (**97**)

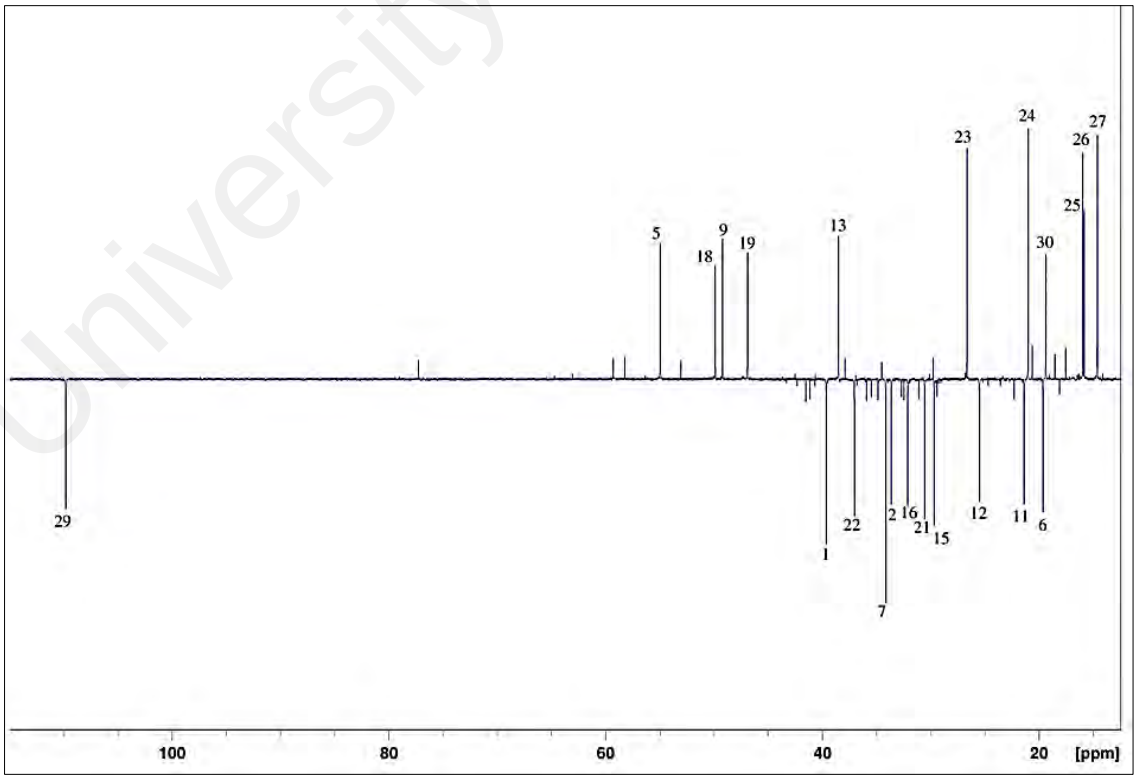


**Figure 3.4**: DEPT-135 spectrum of 3-oxo-lup-20(29)-en-28-oic acid (**97**)

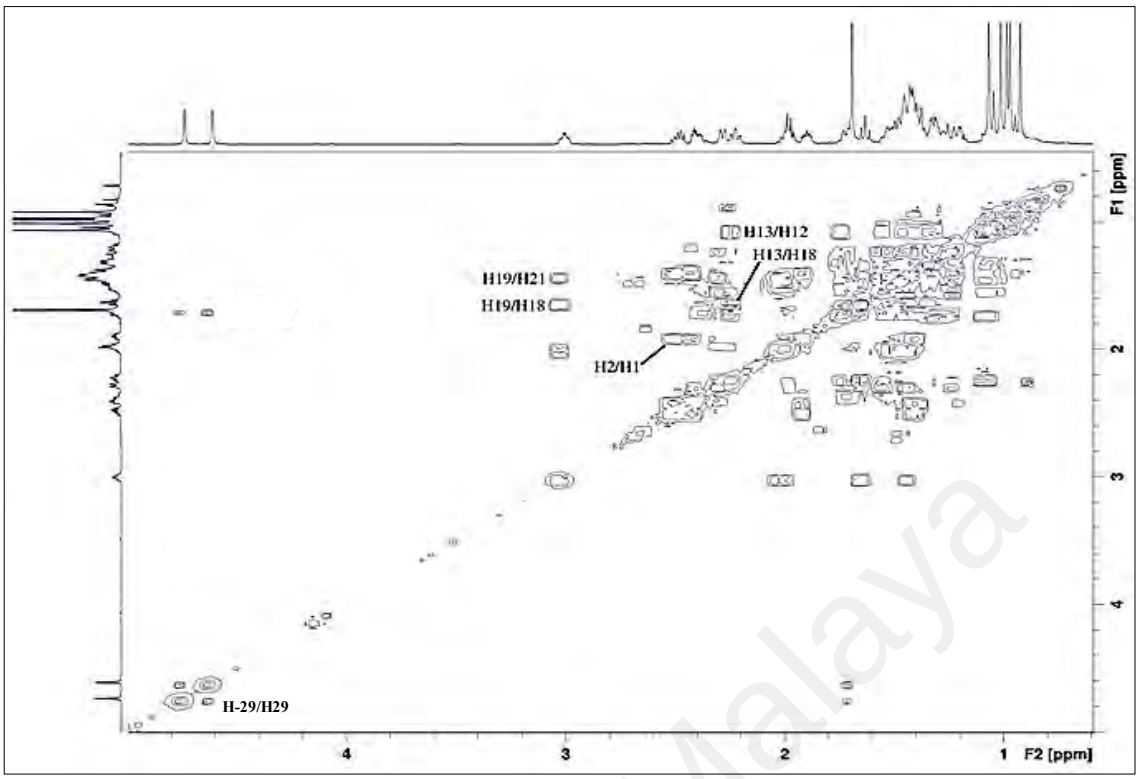


**Figure 3.5**: COSY spectrum of 3-oxo-lup-20(29)-en-28-oic acid (**97**)

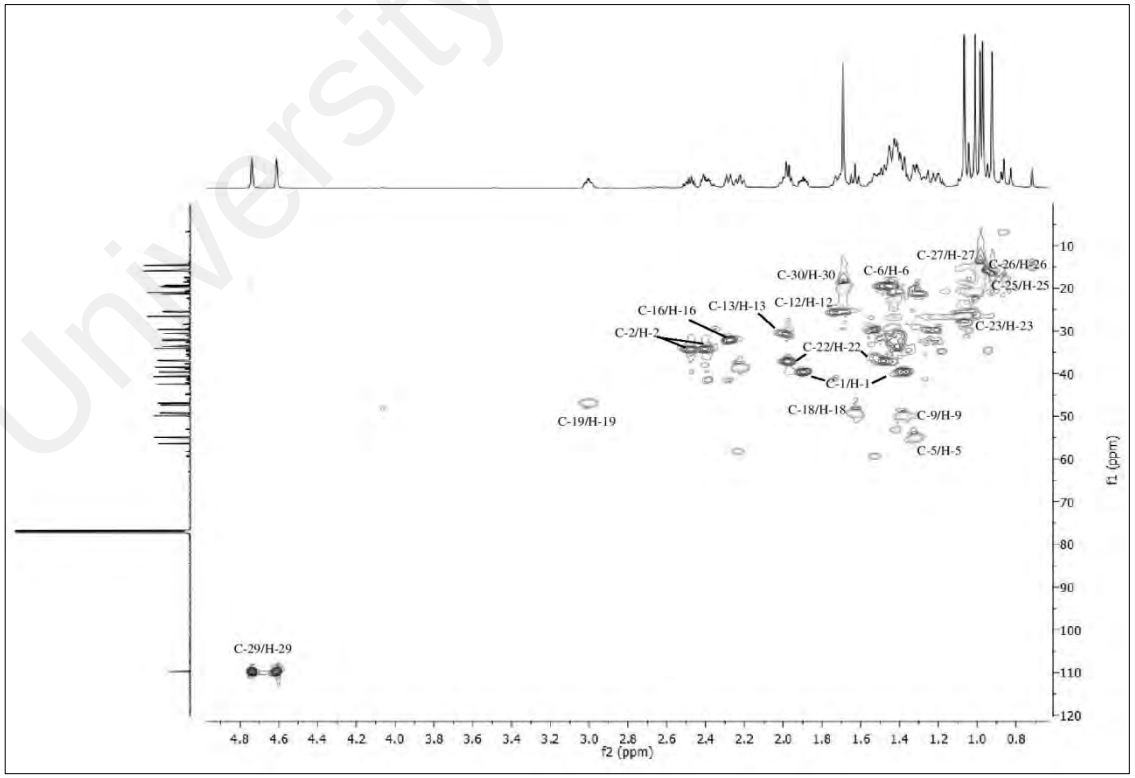


**Figure 3.6:** HSQC spectrum of 3-oxo-lup-20(29)-en-28-oic acid (**97**)

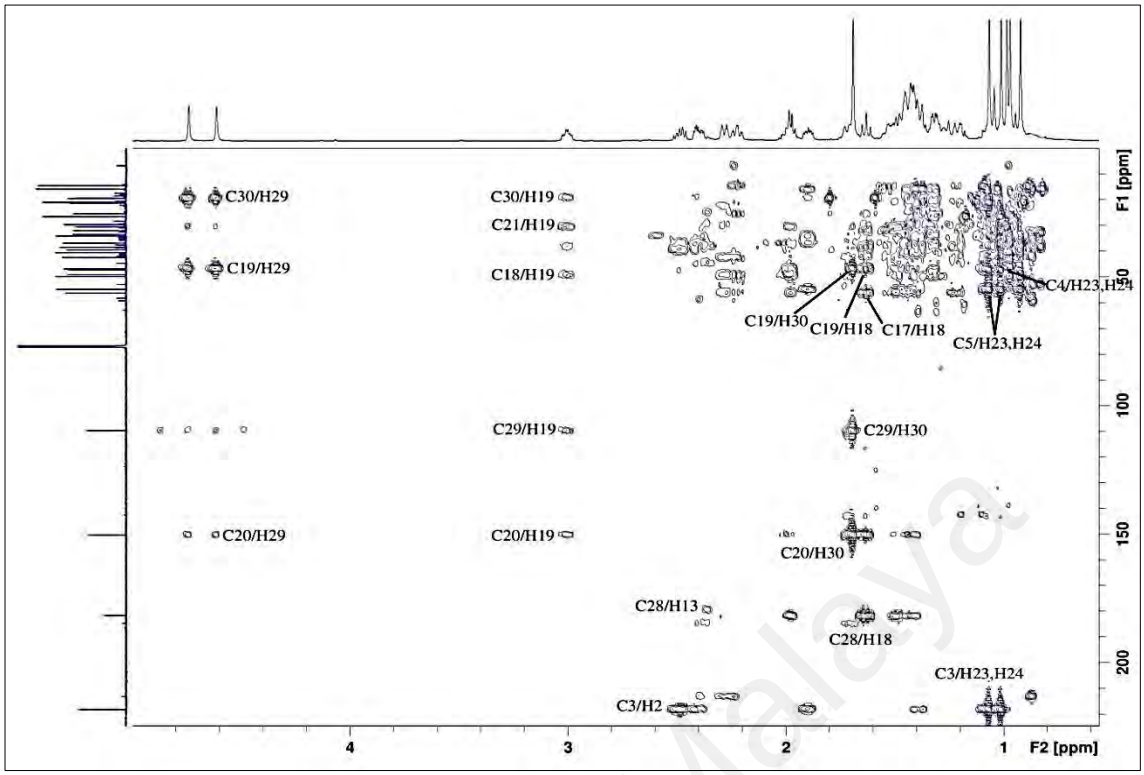


**Figure 3.7**: HMBC spectrum of 3-oxo-lup-20(29)-en-28-oic acid (**97**)

## 3.2 Compound 98: 3*β*-hydroxy-5-glutinen-28-oic acid

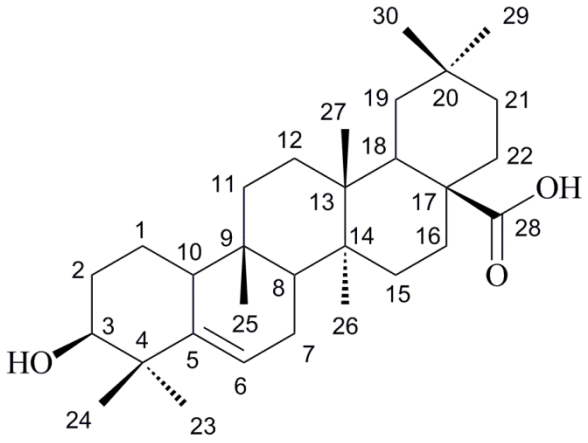


3*β*-hydroxy-5-glutinen-28-oic acid, **98** was afforded as white crystals with melting point 306$^0$C. It was assigned a molecular formula of $C_{30}H_{48}O_3$ as deduced from its negative HRESIMS ([M-H]$^-$, m/z 456.3603; calcd. for $C_{30}H_{47}O_3$; 455.3525), consistent with seven degrees of unsaturation. The IR spectrum exhibits a broad band for hydroxyl (3396 cm$^{-1}$) and olefinic (2933 cm$^{-1}$) structure. Both intensive and medium intensity band for carbonyl (1695 cm$^{-1}$) and C-O stretch (1180 cm$^{-1}$) were observed (Gary et al., 2010).

The $^1$H NMR spectrum (Figure 3.9) showed seven singlets of methyl groups resonated in close proximity at δ 0.82 (Me-25), 0.93 (Me-26), 0.94 (Me-30), 0.98 (Me-29), 1.04 (Me-23), 1.04 (Me-27) and 1.14 (Me-24). An olefinic methine with oxymethine signals were observed at δ 5.64 (*d*, *J* = 5.8 Hz, H-6) and at δ 3.47 (*dd, J* = 3.2, 2.3 Hz) respectively. The olefinic methine was observed as doublet signal because the coupling constant is too small compared to the width of the doublet peak. Therefore, it was observed as doublet signal rather than doublet of doublet (*dd*) signal.

The $^{13}$C NMR (Figure 3.10), DEPT (Figure 3.11) and HSQC experiment of 3β-hydroxy-5-glutinen-28-oic acid, **98** revealed the presence of thirty carbon signals, among which seven methyls resonated at δ 15.6 (C-25), 18.2 (C-27), 20.3 (C-26), 25.4 (C-24), 28.9 (C-23), 28.9 (C-30) and 34.3 (C-29). A hydroxyl, olefinic moiety (methine

and quaternary carbon) and carbonyl carbon were identified resonated at δ 76.3 (C-3), δ 121.7 (C-6), δ 141.6 (C-5) and δ 182.6 (C-28).

The correlation in COSY spectrum (Figures 3.8 and 3.12) between H-10 (δ 2.00, *m*) and H-1 (δ 1.45, *m* and δ 1.50, *m*) confirmed that C-10 is not methylated thus suggesting that compound **98** possess a glutinane triterpenoid skeleton (Atta-ur et al., 2002). Other correlations observed were H-3/H-2, H-6/H-7 and H-18/H-19.

Through analysis of HMBC experiments (Figures 3.8 and 3.13), the location of hydroxyl group at H-3 (δ 3.47, *dd, J* = 3.2, 2.3 Hz) was supported from correlation with C-23 (δ 28.9), C-24 (δ 25.4) and C-5 (δ 141.6). Both sets of methyls Me-23 (δ 1.04, *s*)/Me-24 (δ 1.14, *s*) and Me-29 (δ 0.98, *s*)/Me-30 (δ 0.94, *s*) was observed as geminal on cross correlation between them together with C-4 (δ 40.8) and C-20 (δ 28.5) respectively. A double bond at C-5(6) was confirmed on the basis correlation of C-5 with H-10 (δ 2.00, *m*), H-3, Me-23 and Me-24; and C-6 (δ 121.7) with H-7 (δ 1.77, *m* and δ 1.95, *m*), H-8 (δ 1.52, *m*) and H-10. The existence of carboxyl moiety at C-28 (δ 182.6) position was verified on basis correlation with H-16 (δ 1.50, *m*), H-18 (δ 2.43, *dd*, *J* = 13.2, 4.5 Hz) and H-22 (δ 1.67, *m* and δ 2.29, *dd*, *J* = 14.9, 9.7 Hz).

The in depth analysis of 1D and 2D NMR spectra (Table 3.3) suggested that **98** was 3*β*-hydroxy-5-glutinen-28-oic acid, trivially named as Pinnatane A (Elfita et al., 2009; Mohamad et al., 2009).

**Table 3.3**: $^{1}H$ (600 MHz) and $^{13}C$ (150 MHz) NMR data of 3*β*-hydroxy-5-glutinen-28-oic acid (**98**) in $CDCl_3$

| Position | Compound **98** | | (Elfita et al., 2009) | |
|---|---|---|---|---|
| | $\delta_H$ (ppm), *J (Hz)* | $\delta_C$ (ppm) | $\delta_H$ (ppm), *J (Hz)* | $\delta_C$ (ppm) |
| 1 | 1.45, *m*<br>1.50, *m* | 18.3 | 1.44<br>1.52 | 18.3 |
| 2 | 1.67, *m*<br>1.85, *m* | 27.8 | 1.67<br>1.82 | 27.8 |
| 3 | 3.47, *dd* (3.2, 2.3) | 76.3 | 3.45, *br s* | 76.3 |
| 4 | - | 40.8 | - | 40.8 |
| 5 | - | 141.6 | - | 141.5 |
| 6 | 5.64, *d* (5.8) | 121.7 | 5.6 | 121.7 |
| 7 | 1.77, *m*<br>1.95, *m* | 23.5 | 1.75<br>1.95 | 23.4 |
| 8 | 1.52, *m* | 47.7 | 1.5 | 47.7 |
| 9 | - | 35.1 | - | 35.1 |
| 10 | 2.00, *m* | 49.4 | 1.98 | 49.9 |
| 11 | 1.36, *m*<br>1.53, *m* | 34.5 | 1.36<br>1.51 | 34.5 |
| 12 | 1.39, *m*<br>1.47, *m* | 30.9 | 1.35<br>1.45 | 30.9 |
| 13 | - | 38.7 | - | 38.6 |
| 14 | - | 37.2 | - | 37.1 |
| 15 | 1.21, *m*<br>1.25, *m* | 32.5 | 1.2 | 32.4 |
| 16 | 1.50, *m* | 35.8 | 1.48 | 35.8 |
| 17 | - | 44.7 | - | 44.7 |
| 18 | 2.43, *dd* (13.2, 4.5) | 37.8 | 2.37, *dd* (13.1, 3.8) | 37.7 |
| 19 | 1.17, *m*<br>1.31, *m* | 34.9 | 1.14<br>1.29 | 34.8 |
| 20 | - | 28.5 | - | 28.5 |
| 21 | 1.47, *m* | 32.8 | 1.46 | 32.8 |
| 22 | 1.67, *m*<br>2.29, *dd* (14.9, 9.7) | 29.4 | 1.65<br>2.29, *dd* (14.7, 9.5) | 29.2 |
| 23 | 1.04, *s* | 28.9 | 1.01, *s* | 28.9 |
| 24 | 1.14, *s* | 25.4 | 1.12, *s* | 25.4 |
| 25 | 0.82, *s* | 15.6 | 0.80, *s* | 15.6 |
| 26 | 0.93, *s* | 20.3 | 0.89, *s* | 20.3 |
| 27 | 1.04, *s* | 18.2 | 0.96, *s* | 18.2 |
| 28 | - | 182.6 | - | 184.8 |
| 29 | 0.98, *s* | 34.3 | 0.91, *s* | 34.3 |
| 30 | 0.94, *s* | 29.8 | 1.01, *s* | 29.7 |

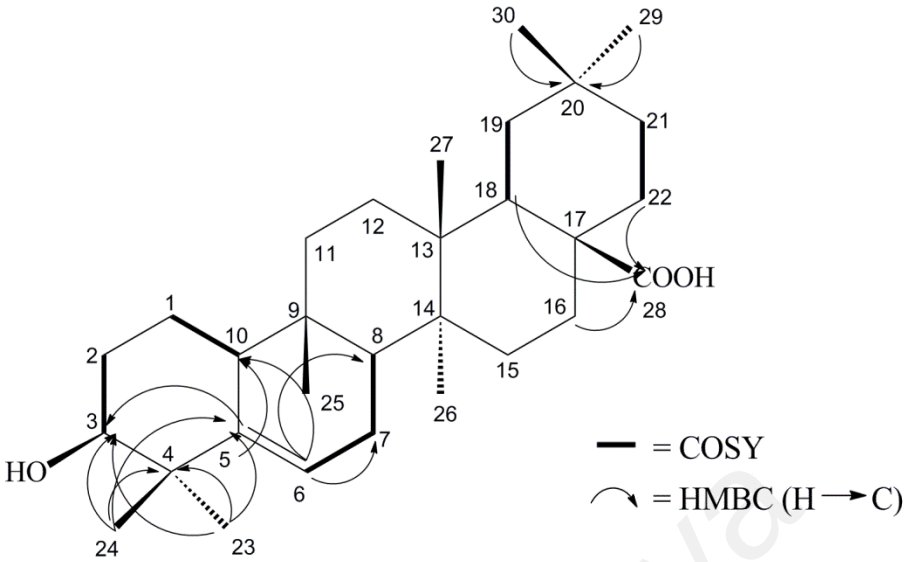


**Figure 3.8**: Selected COSY and HMBC correlations of 3*β*-hydroxy-5-glutinen-28-oic acid (**98**)

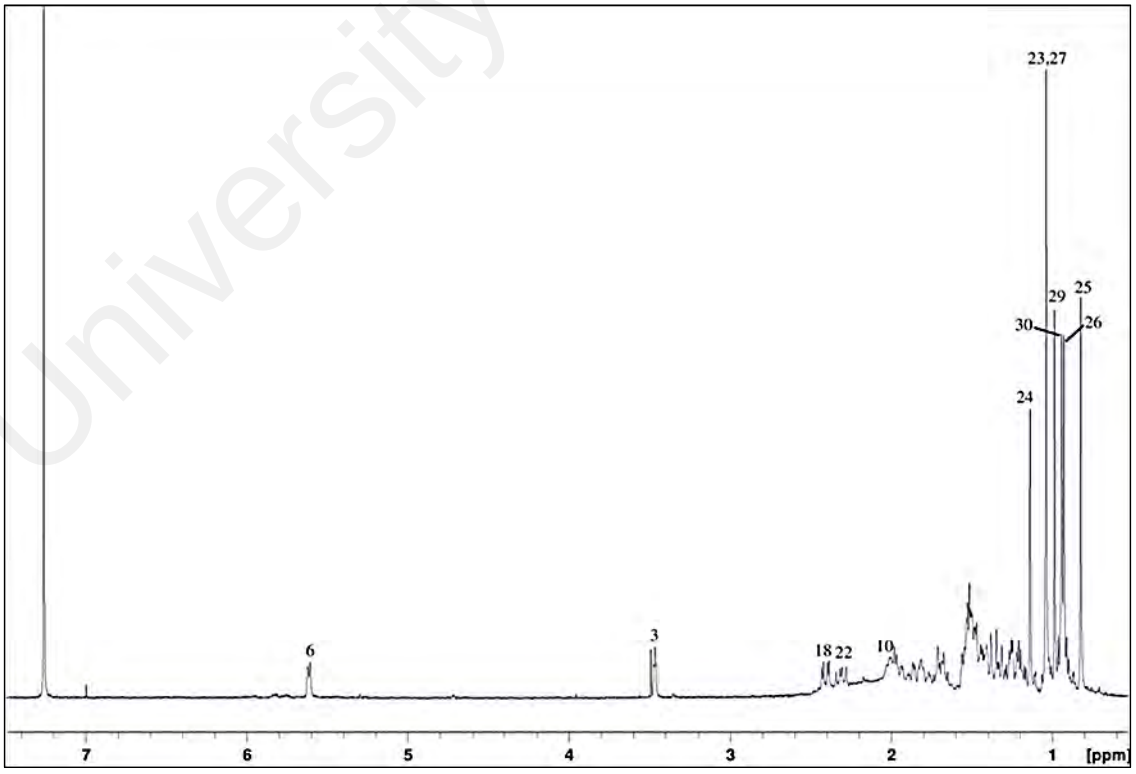


**Figure 3.9**: $^{1}$H (600 MHz) NMR spectrum of 3*β*-hydroxy-5-glutinen-28-oic acid (**98**)

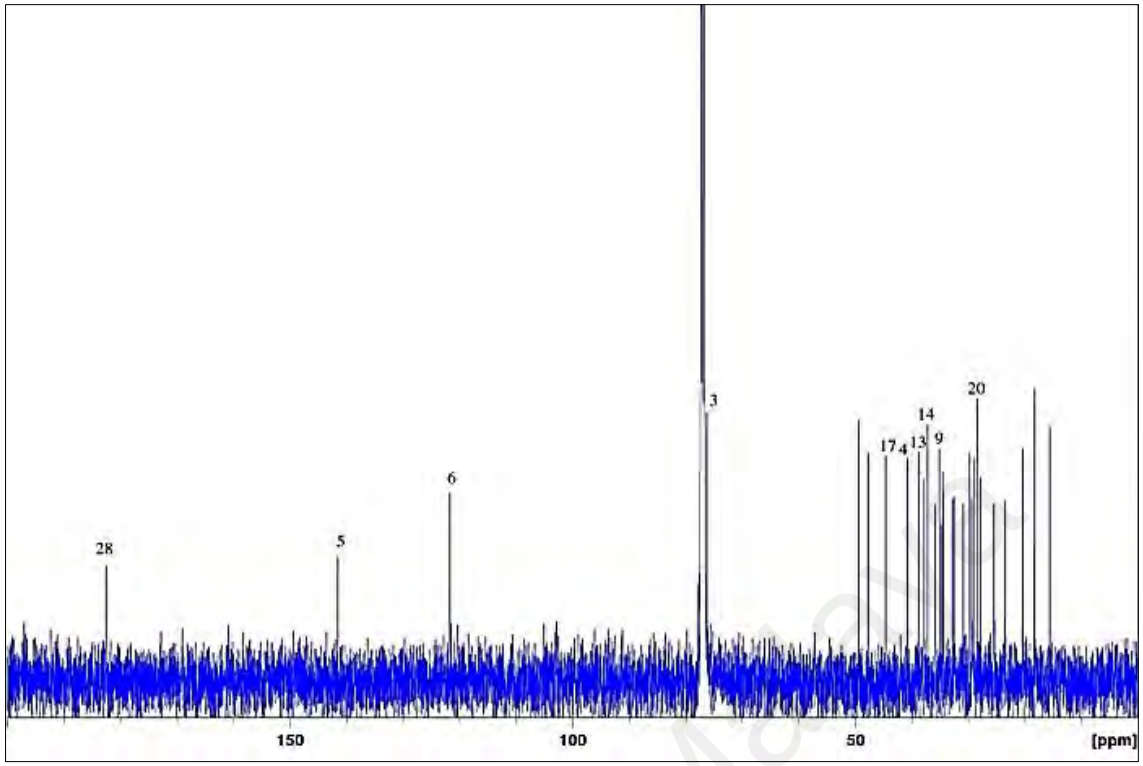


**Figure 3.10**: $^{13}C$ (150 MHz) NMR spectrum of 3$\beta$-hydroxy-5-glutinen-28-oic acid (**98**)

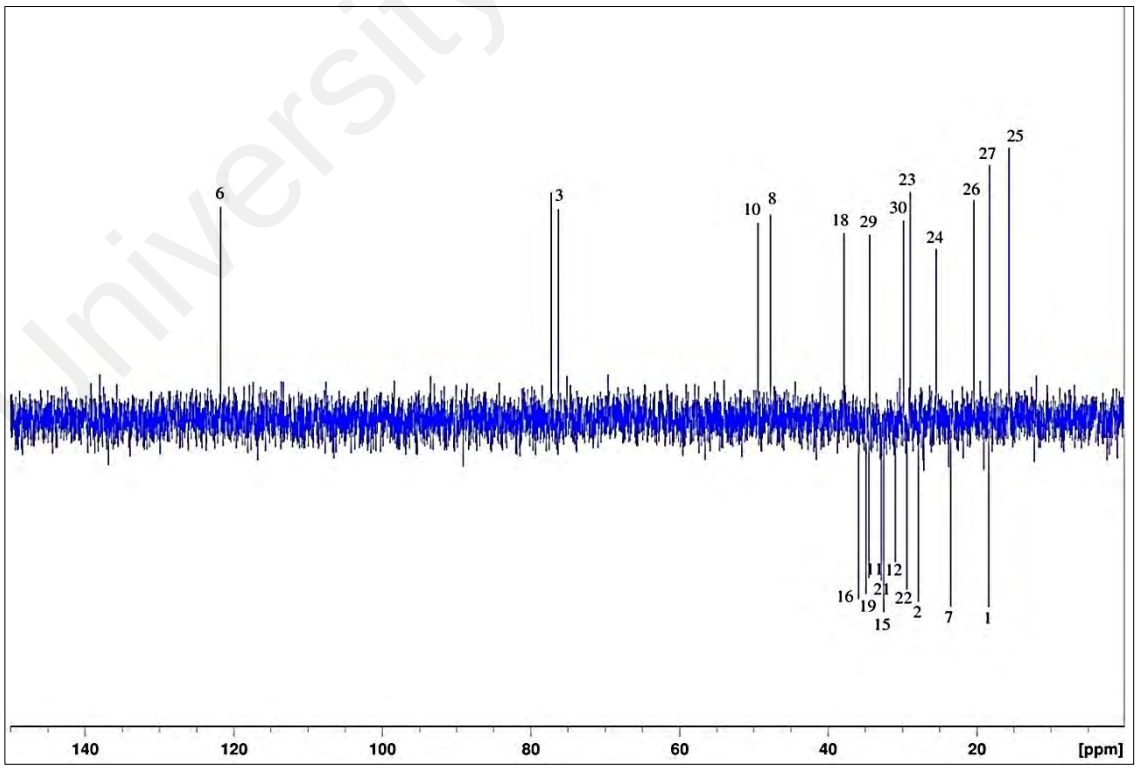


**Figure 3.11**: DEPT-135 spectrum of 3$\beta$-hydroxy-5-glutinen-28-oic acid (**98**)

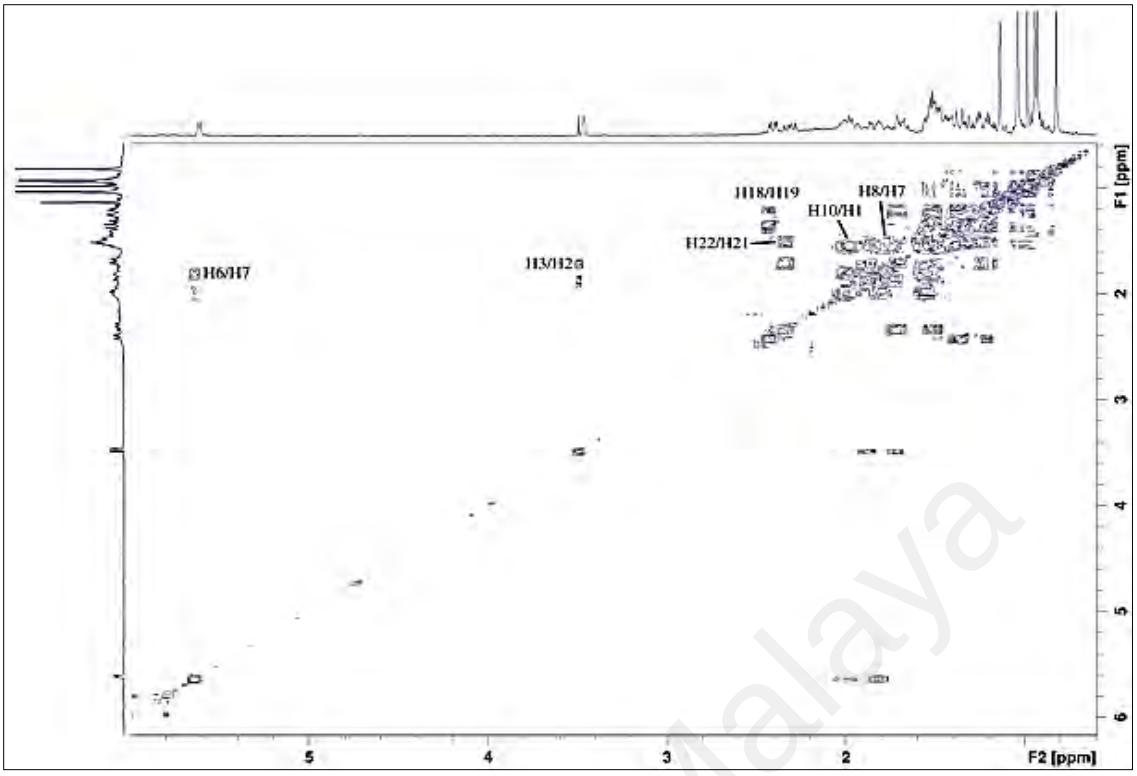


**Figure 3.12**: COSY spectrum of 3$\beta$-hydroxy-5-glutinen-28-oic acid (**98**)

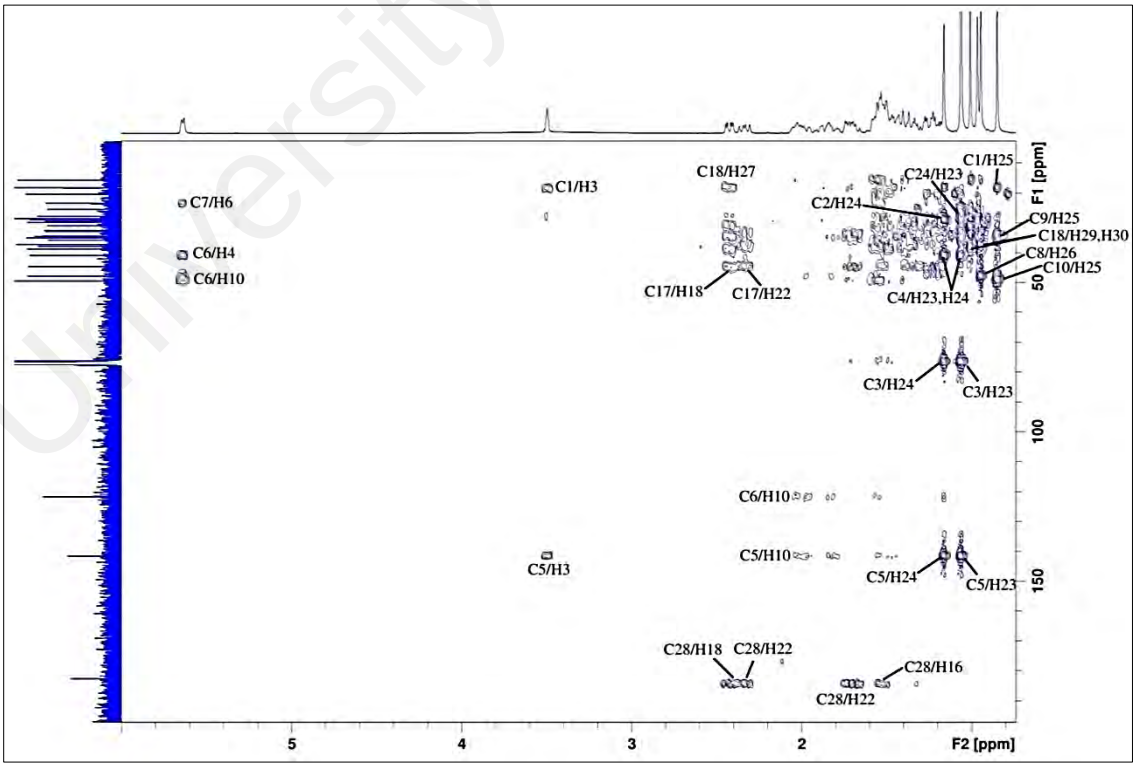


**Figure 3.13**: HMBC spectrum of 3$\beta$-hydroxy-5-glutinen-28-oic acid (**98**)

### 3.3 Compound 99: 3-oxo-olean-11-en-28,13*β*-olide

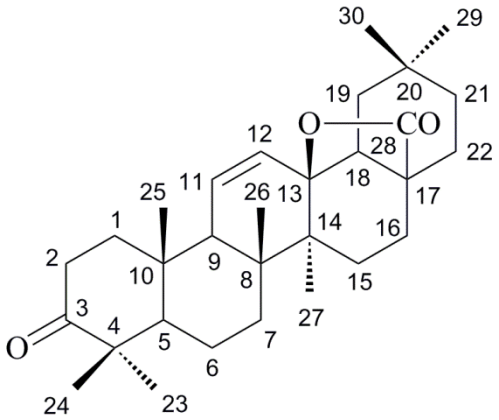


3-oxo-olean-11-en-28,13*β*-olide, **99** was isolated as white amorphous solid. The HRESIMS revealed a pseudo-molecular ion peak $[M+H]^+$ at m/z 453.3434 (calcd. for $C_{30}H_{45}O_3$, 453.3369), thus suggested that **99** possess a molecular formula of $C_{30}H_{44}O_3$ and nine degrees of unsaturation. The IR absorptions implied the presence of lactone ring (1765 $cm^{-1}$), carbonyl (1705 $cm^{-1}$) and olefinic (1640 $cm^{-1}$) functionalities (Gary et al., 2010).

The $^1$H NMR spectrum (Figure 3.15) indicate the presence of seven singlets for methyl groups resonating in close proximity to each other; δ 0.81 (Me-30), 0.93 (Me-29), 0.95 (Me-25), 1.03 (Me-24), 1.07 (Me-27), 1.16 (Me-23) and 1.23 (Me-26). This observation suggested that compound **99** could be a triterpenoid with pentacyclic skeleton (Ageta et al., 1995). An olefinic functionality was observed at δ 5.88 (*dd*, *J* = 10.1, 2.9 Hz, H-11) and δ 6.08 (*d*, *J* = 10.4 Hz, H-12). The more downfield shift of the methylene protons resonated at δ 2.45 (*ddd*, *J* = 15.8, 6.6, 3.5 Hz, H-2a) and δ 2.63 (*ddd*, *J* = 17.6, 10.8, 7.3 Hz, H-2b) suggesting it is close to an electron withdrawing group.

The $^{13}$C NMR (Figure 3.16), DEPT (Figure 3.17) and HSQC analysis of 3-oxo-olean-11-en-28,13*β*-olide, **99** revealed the presence of thirty carbons, among which seven methyls resonated at δ 17.0 (C-25), 17.9 (C-27), 18.7 (C-26), 20.7 (C-24), 23.2 (C-30), 25.9 (C-23) and 32.9 (C-29). An oxygenated, olefinic methine and carbonyl

carbons were observed resonating at δ 89.1 (C-13), $\delta_C$ 127.6 (C-11), δ 135.6 (C-12) and δ 215.2 (C-3).

From the COSY experiment (Figures 3.14 and 3.18), an olefinic group was deduced at H-11/H-12 position from correlation of H-11 (δ 5.58, *dd*, *J* = 10.1, 2.9 Hz) with H-9 (δ 2.03, *brs*) and H-12 (δ 6.08, *d*, *J* = 10.4 Hz). Others correlations observed were H-2/H-1, H-6/H-7, H-15/H-16 and H-18/H-19.

In depth analysis of HMBC experiments (Figures 3.14 and 3.19), the position of carbonyl group at C-3 (δ 215.2) was supported from correlation with Me-23 (δ 1.16), Me-24 (δ 1.03) and H-2. The presence of two sets of geminal methyls which is a characteristic features of an oleanane skeleton were deduced from the cross correlation between Me-23 (δ 1.16, *s*)/Me-24 (δ 1.03, *s*) and Me-29 (δ 0.93, *s*)/Me-30 (δ 0.81, *s*) with C-4 (δ 47.3) and C-20 (δ 31.2), respectively. A double bond at C-11(12) positon was confirmed on the basis correlation of H-11 with C-8 (δ 41.5) and C-9 (δ 52.5); and H-12 with C-9, C-10 (δ 35.9), C-13 (δ 89.1) and C-14 (δ 41.5). The existence of lactone linkage was verified between cross correlation of C-28 (δ 179.2) with H-18 (δ 2.23, *dd, J* = 13.9, 3.0 Hz) and C-13 (δ 89.1) with H-12, H-15, H-18 and Me-27.

The complete assignments of 1D and 2D NMR spectra (Table 3.4) led to the conclusion that **99** is 3-oxo-olean-11-en-28,13*β*-olide (Castellanos et al., 2002).

**Table 3.4**: $^{1}H$ (600 MHz) and $^{13}C$ (150 MHz) NMR data of 3-oxo-olean-11-en-28,13*β*-olide (**99**) in $C_5D_5N$

| Position | Compound **99** | | (Castellanos et al., 2002) | |
|---|---|---|---|---|
| | $\delta_H$ (ppm), *J (Hz)* | $\delta_C$ (ppm) | $\delta_H$ (ppm), *J (Hz)* | $\delta_C$ (ppm) |
| 1 | 1.97, *ddd* (12.5, 7.0, 3.5)<br>1.32, *m* | 38.6 | | 39.0 |
| 2 | 2.45, *ddd* (15.8, 6.6, 3.5)<br>2.63, *ddd* (17.6, 10.8, 7.3) | 33.8 | 2.44, *ddd* (16.0, 6.7, 3.7)<br>2.65, *ddd* (16.0, 11.1, 7.2) | 33.8 |
| 3 | - | 215.2 | - | 216.8 |
| 4 | - | 47.3 | - | 47.6 |
| 5 | 1.34, *m* | 54.1 | | 54.6 |
| 6 | 2.15, *dt* (26.3, 13.1, 5.8) | 21.4 | | 18.8 |
| 7 | 1.31, *m*<br>1.52, *d*t (25.4, 12.9, 3.4) | 18.8 | | 30.4 |
| 8 | - | 41.5 | - | 41.4 |
| 9 | 2.03, *brs* | 52.5 | 2.00, *brs* | 52.5 |
| 10 | - | 35.9 | - | 36.1 |
| 11 | 5.58, *dd* (10.1, 2.9) | 127.6 | 5.46, *dd* (10.2, 3.1) | 127.4 |
| 12 | 6.08, *d* (10.4) | 135.6 | 6.04, *dd* (10.2, 1.3) | 135.2 |
| 13 | - | 89.1 | - | 89.6 |
| 14 | - | 41.5 | - | 41.5 |
| 15 | 1.19, *m*<br>1.76, *d* (5.3) | 25.5 | | 25.4 |
| 16 | 1.72, *td* (16.7, 13.4, 3.5)<br>1.79, *dd* (16.0, 6.8) | 27.9 | | 21.2 |
| 17 | - | 44.1 | - | 44.0 |
| 18 | 2.23, *dd* (13.9, 3.0) | 50.5 | | 50.5 |
| 19 | 1.39, *m*<br>1.86, *t* (13.5) | 37.1 | 1.81, *t* (13.5) | 37.3 |
| 20 | - | 31.2 | - | 31.4 |
| 21 | 1.20, *m*<br>1.38, *m* | 34.2 | | 34.3 |
| 22 | 1.19, *m*<br>1.42, *m* | 30.3 | | 27.1 |
| 23 | 1.16, *s* | 25.9 | 1.08, *s* | 26.0 |
| 24 | 1.03, *s* | 20.7 | 1.06, *s* | 20.8 |
| 25 | 0.95, *s* | 17.0 | 1.05, *s* | 17.3 |
| 26 | 1.23, *s* | 18.7 | 1.10, *s* | 18.1 |
| 27 | 1.07, *s* | 17.9 | 1.11, *s* | 18.6 |
| 28 | - | 179.2 | - | 180.0 |
| 29 | 0.93, *s* | 32.9 | 0.98, *s* | 33.3 |
| 30 | 0.81, *s* | 23.2 | 0.89,*s* | 23.5 |

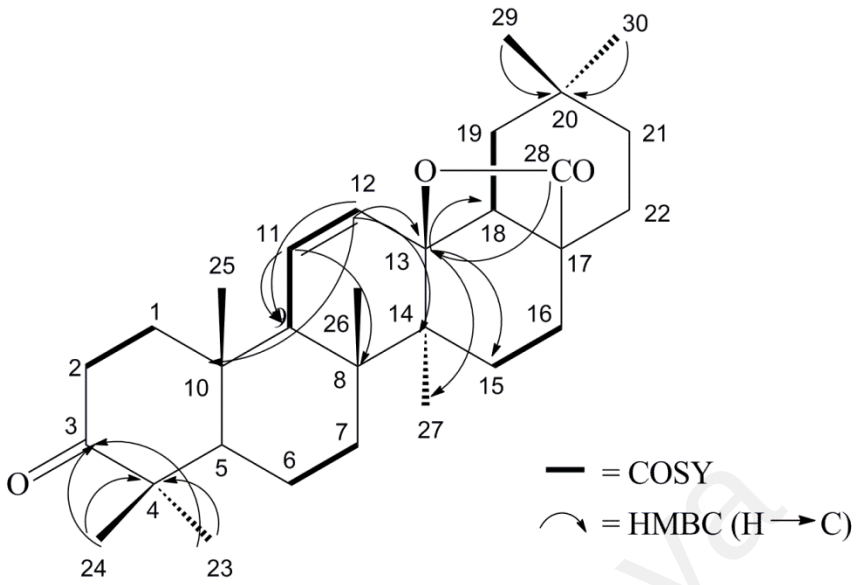


**Figure 3.14**: Selected COSY and HMBC correlations of 3-oxo-olean-11-en-28,13*β*-olide (**99**)

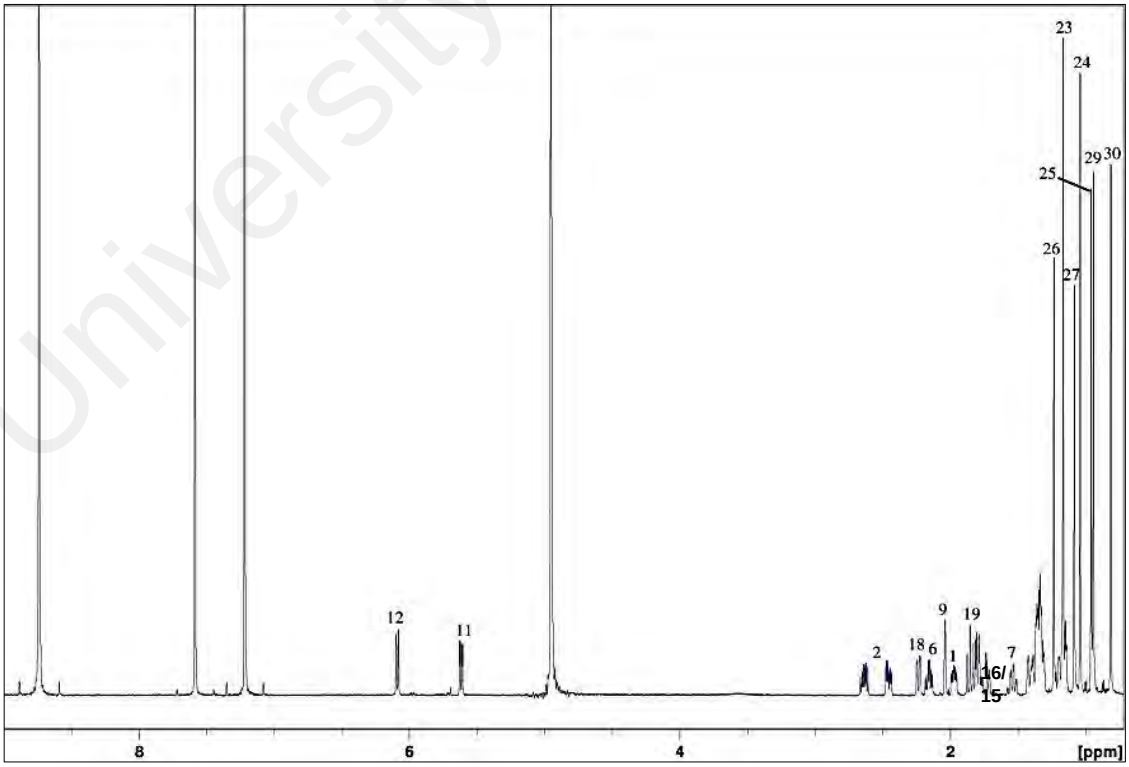


**Figure 3.15**: $^{1}$H (600 MHz) NMR spectrum of 3-oxo-olean-11-en-28,13*β*-olide (**99**)

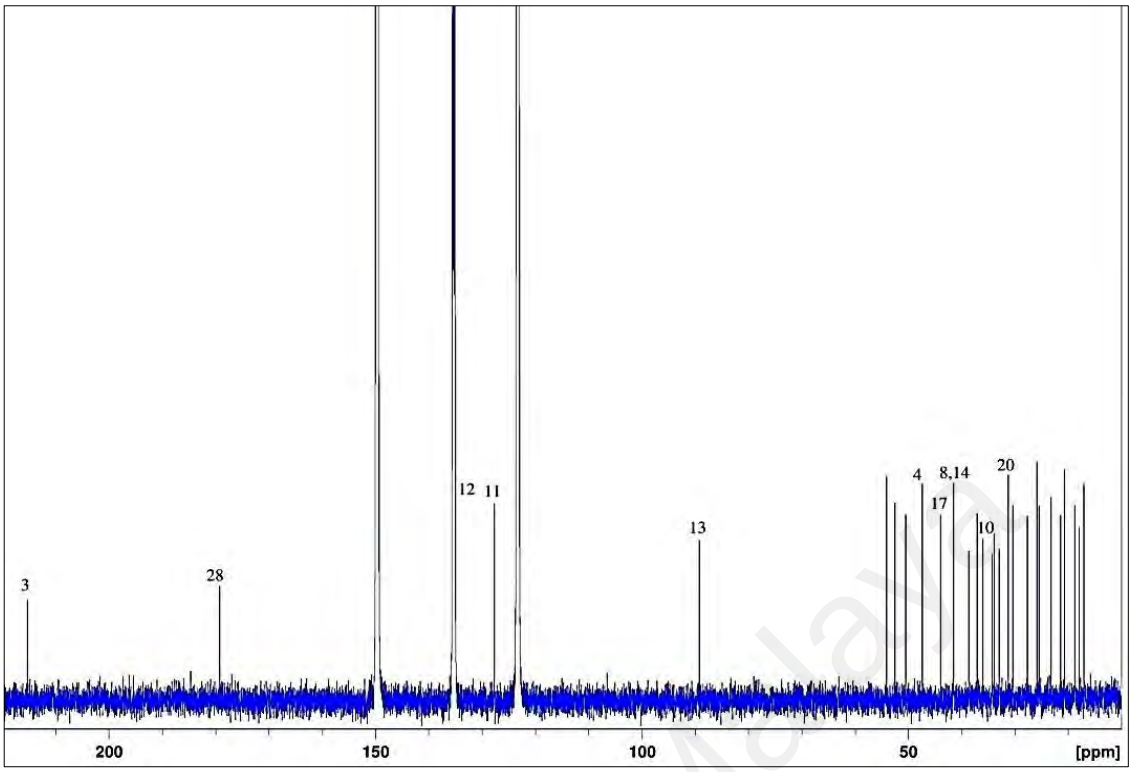


**Figure 3.16**: $^{13}C$ (150 MHz) NMR spectrum of 3-oxo-olean-11-en-28,13$\beta$-olide (**99**)

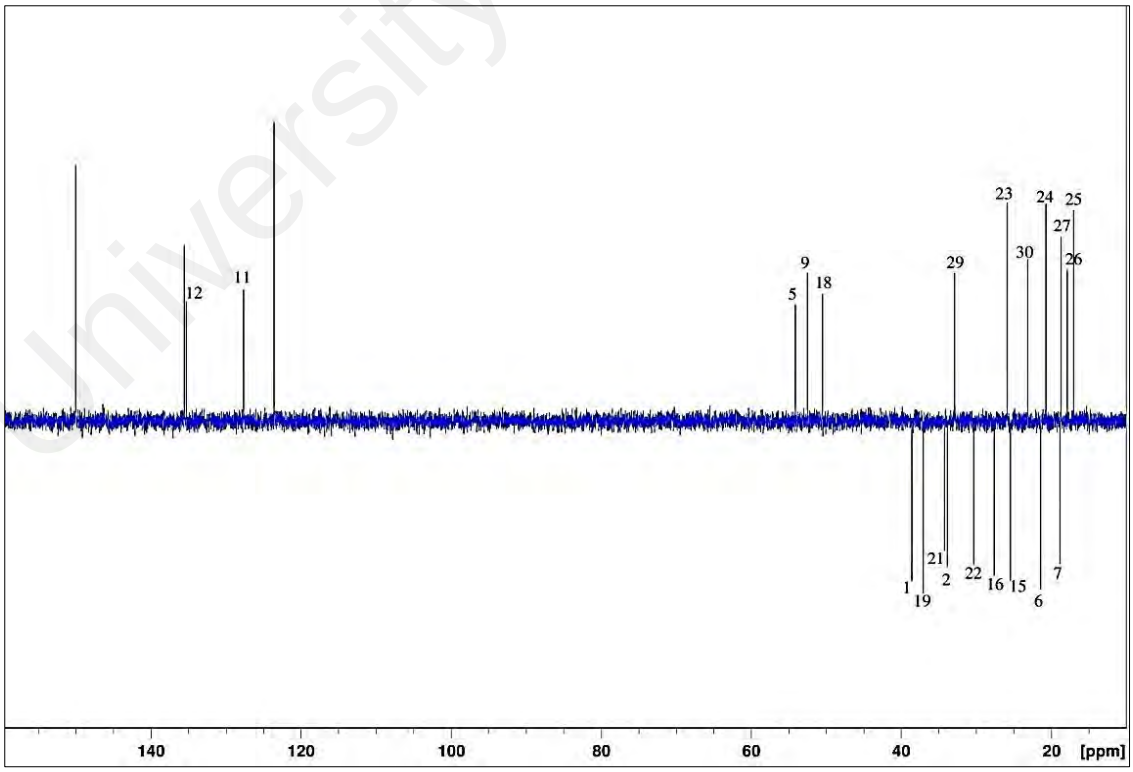


**Figure 3.17**: DEPT-135 spectrum of 3-oxo-olean-11-en-28,13$\beta$-olide (**99**)

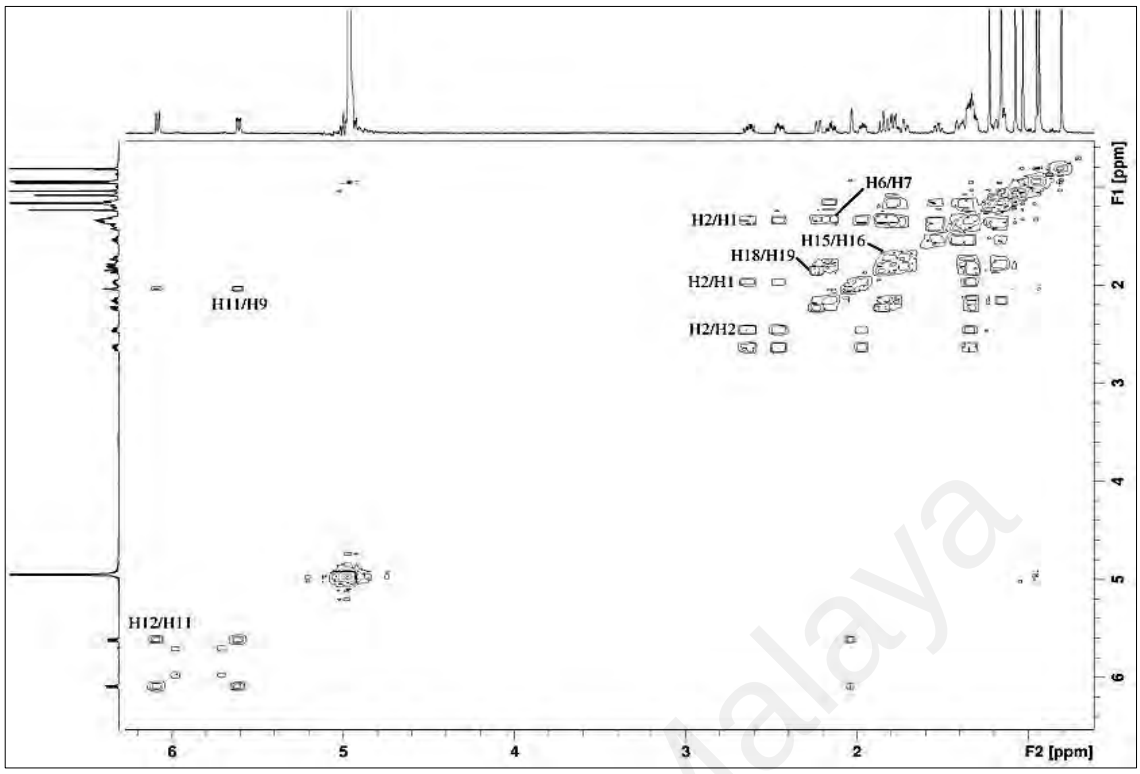


**Figure 3.18**: COSY spectrum of 3-oxo-olean-11-en-28,13$\beta$-olide (**99**)

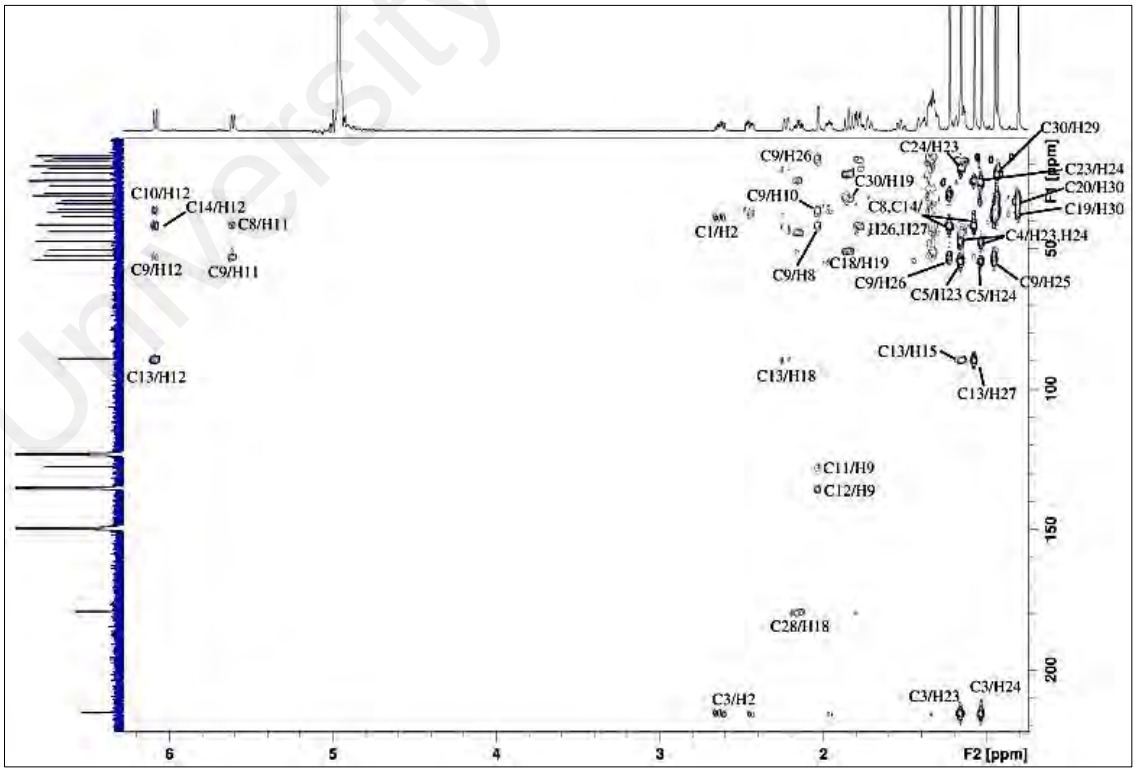


**Figure 3.19**: HMBC spectrum of 3-oxo-olean-11-en-28,13$\beta$-olide (**99**)

### 3.4 Compound 100: 3-oxo-olean-9(11),12-dien-28-oic acid

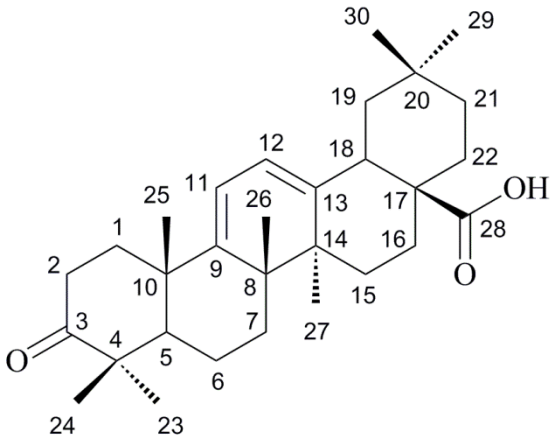


3-oxo-olean-9(11),12-dien-28-oic acid, **100** was obtained as white amorphous powder. The molecular formula of **100** was determined as $C_{30}H_{44}0_3$ by HR-ESI-MS, which provided a molecular ion peak at m/z 453.3434 $[M+H]^+$ (calcd. m/z at 453.3369) corresponding to nine degree of unsaturation. The IR spectrum indicated a strong absorption bands for hydroxyl (3436 $cm^{-1}$), an olefinic (2941 $cm^{-1}$) and carbonyl (1701 $cm^{-1}$) functionalities (Gary et al., 2010).

The $^1$H NMR spectrum (Figure 3.21) showed seven singlets for the methyl groups resonated at δ 0.91 (Me-29), 0.95 (Me-30), 1.01 (Me-26), 1.04 (Me-27), 1.06 (Me-24), 1.11 (Me-23), and 1.23 (Me-25). This observation suggested that compound **99** could be a triterpenoid with pentacyclic skeleton (Ageta et al., 1995). Two olefinic methine signals resonated at δ 5.65 (*d*, *J* = 5.8 Hz, H-11) and 5.59 (*d*, *J* = 5.8 Hz, H-12) respectively. The more downfield chemical shift of the methylene protons of δ 2.49 (*ddd*, *J* = 16.0, 7.9, 4.1 Hz, H-2a) and δ 2.58 (*ddd*, *J* = 16.0, 9.8, 7.9 Hz, H-2b) suggested that the vicinal C-3 position is an electron withdrawing group.

The $^{13}$C NMR (Figure 3.22) and DEPT spectra (Figure 3.23) of 3-oxo-olean-9(11),12-dien-28-oic acid, **100** coupled with HSQC (Figure 3.25) analysis revealed the presence of thirty carbons, among which seven methyls at δ 20.0 (C-26, C-27), 21.3 (C-24), 23.5 (C-30), 25.2 (C-25), 26.9 (C-23), 32.9 (C-29), two olefinic methine carbons at

δ 117.4 (C-11) and 120.6 (C-12), two olefinic quaternary carbon at δ 152.7 (C-9) and 145.3 (C-13) and two carbonyl carbons at δ 182.1 (C-28) and 217.7 (C-3) were included.

In the COSY experiment (Figures 3.20 and 3.24), the olefinic methines of H-11(δ 5.65, *d*, *J* = 5.8 Hz) and H-12 (δ 5.59, *d*, *J* = 5.8 Hz) showed cross correlations and thus suggested to have adjacent positions.

The in depth analysis of HMBC experiments (Figures 3.20, 3.26 and 3.27) supported the location of ketone group at C-3 (δ 217.7) from its correlation with H-1 (δ 1.84, *m* and δ 2.21, *ddd*, *J* = 13.2, 7.7, 4.1 Hz), H-2a, H-2b, Me-23, and Me-24. The presence of two sets of geminal methyls which is a characteristic features of an oleanane skeleton between Me-23 (δ 1.11, *s*)/Me-24 (δ 1.06, *s*) and Me-29 (δ 0.91, *s*)/Me-30 (δ 0.95, *s*) were deduced from the cross correlation between them. Careful analysis of this experiments suggested that both olefinic moieties were located at C-9/C-11 and C-12/C-13 positions. The first double bond was deduced from the correlations of C-9 (δ 152.7) with H-12 (δ 5.59, *d*, *J* = 5.8 Hz), H-25 (δ 1.23, *s*) and H-26 (δ 1.01, *s*); and H-11 (δ 5.65, *d*, *J* = 5.8 Hz) with C-10 (δ 38.3), C-13 (δ 145.3) and C-14 (δ 42.6) while the position of other double bond was established through the correlations of H-12 (δ 5.59, *d*, *J* = 5.8 Hz) with C-9 (δ 152.7) and C-18 (δ 39.5); and C-13 (δ 145.3) with H-11 (δ 5.65, *d*, *J* = 5.8 Hz), H-18 (δ 2.99, *dd*, *J* = 13.5, 4.3 Hz) and H-27 (δ 1.04, *s*). The position of the carboxyl moiety which was attached to C-17 was established from the correlation of C-28 (δ 182.1) with H-18 (δ 2.99, *dd*, *J* = 13.5, 4.3 Hz) and H-16 (δ 1.67, *m* and δ 1.99, *dt*, *J* = 27.4, 13.7, 3.9 Hz).This carboxyl presence is another characteristic feature of an oleanane classes.

The relative stereochemistry of **100** was proposed based on those of oleanonic acid triterpene, previously isolated from *Cedrela odorata* (Meliaceae) and also by the

interpretation of NOE data. The configuration of A, B, C, D and E rings were assumed to be the same as that of the several known oleanane triterpenoids, bearing the same skeleton. NOE correlations of H-5/H-23, H-18/H-27 and H-18/H-29 established the configuration of all these protons as α-oriented. Similarly, the presence of NOE cross peak between H-24/H-25, H-25/H-26 confirmed the *β*-orientation of H-24, H-25, and H-26, H-30 which appears in all of the oleanane type triterpenoids possessing pentacyclic ring systems.

Based on the above data, compound **100** was concluded to be a unique oleanane triterpenoid possessing a conjugated diene at ring C and trivially name 3-oxo-olean-9(11),12-dien-28-oic acid. The complete assignments of 1D and 2D NMR spectra were shown in Table 3.5.

**Table 3.5**: $^{1}H$ (400 MHz) and $^{13}C$ (100 MHz) NMR data of 3-oxo-olean-9(11),12-dien-28-oic acid (**100**) in $CDCl_3$

| Position | $\delta_H$ (ppm), *J (Hz)* | $\delta_C$ (ppm) |
|---|---|---|
| 1 | 1.84, *m*<br>2.21, *ddd* (13.2, 7.7, 4.1) | 37.7 |
| 2 | 2.49, *ddd* (16.0, 7.9, 4.1)<br>2.58, *ddd* (16.0, 9.8, 7.9) | 34.5 |
| 3 | - | 217.7 |
| 4 | - | 47.3 |
| 5 | 1.48, *dd* (7.0, 4.4) | 51.8 |
| 6 | 1.54, *m* | 19.5 |
| 7 | 1.37, *m*<br>1.71, *m* | 31.3 |
| 8 | - | 40.7 |
| 9 | - | 152.7 |
| 10 | - | 38.3 |
| 11 | 5.65, *d* (5.8) | 117.4 |
| 12 | 5.59, *d* (5.8) | 120.6 |
| 13 | - | 145.3 |
| 14 | - | 42.6 |
| 15 | 1.65, *m*<br>1.82, *m* | 27.0 |
| 16 | 1.67, *m*<br>1.99, *dt* (27.4, 13.7, 3.9) | 23.6 |
| 17 | - | 30.7 |
| 18 | 2.99, *dd* (13.5, 4.3) | 39.5 |
| 19 | 1.19, *m*<br>1.59, *m* | 45.8 |
| 20 | - | 45.9 |
| 21 | 1.22, *m*<br>1.35, *m* | 33.7 |
| 22 | 1.68, m<br>1.77, m | 32.1 |
| 23 | 1.11, *s* | 26.9 |
| 24 | 1.06, *s* | 21.3 |
| 25 | 1.23, *s* | 25.2 |
| 26 | 1.01, *s* | 20.0 |
| 27 | 1.04, *s* | 20.0 |
| 28 | - | 182.1 |
| 29 | 0.91, *s* | 32.9 |
| 30 | 0.95, *s* | 23.5 |

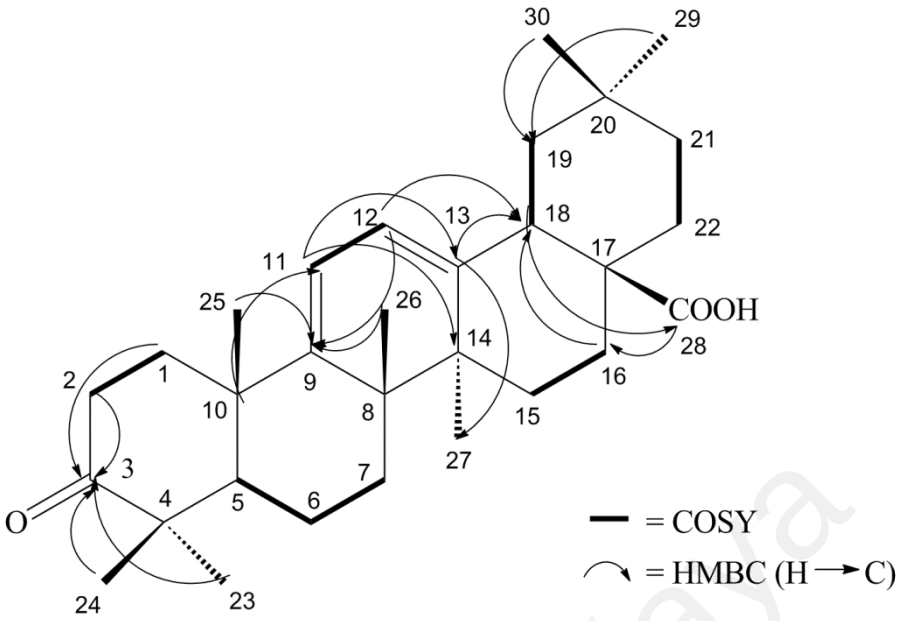


**Figure 3.20**: Selected COSY and HMBC correlations of 3-oxo-olean-9(11),12-dien-28-oic acid (**100**)

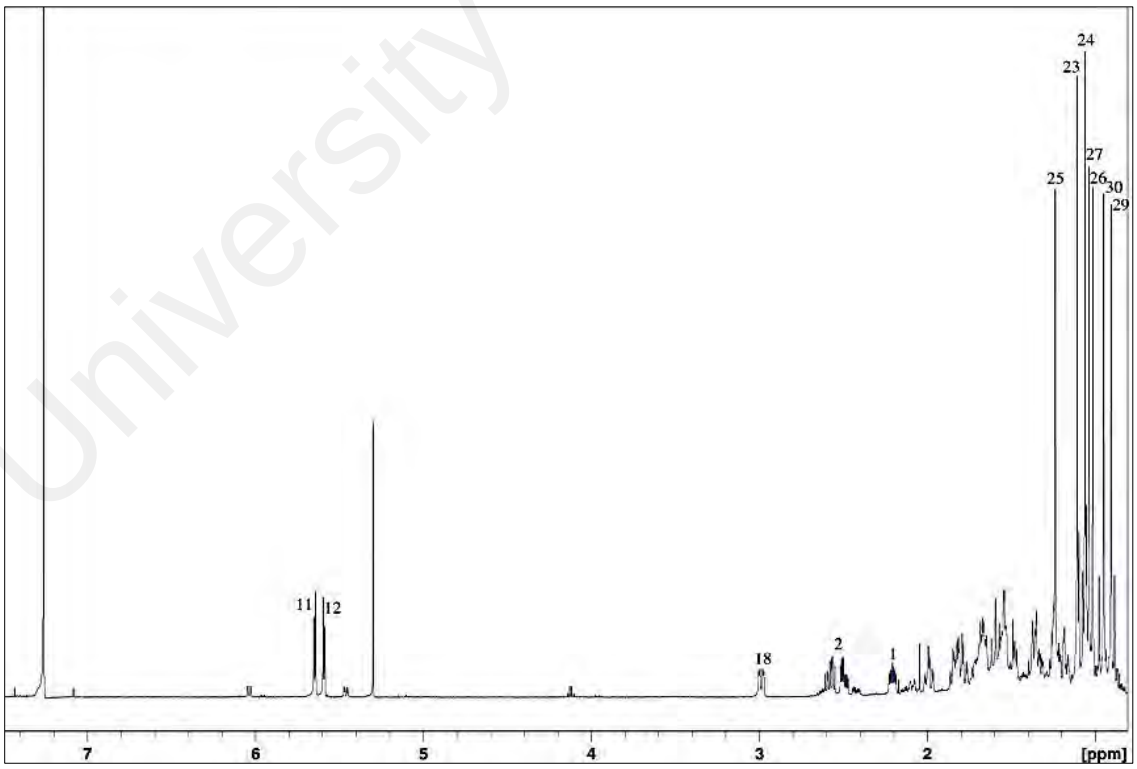


**Figure 3.21**: $^{1}$H (400 MHz) NMR spectrum of 3-oxo-olean-9(11),12-dien-28-oic acid (**100**)

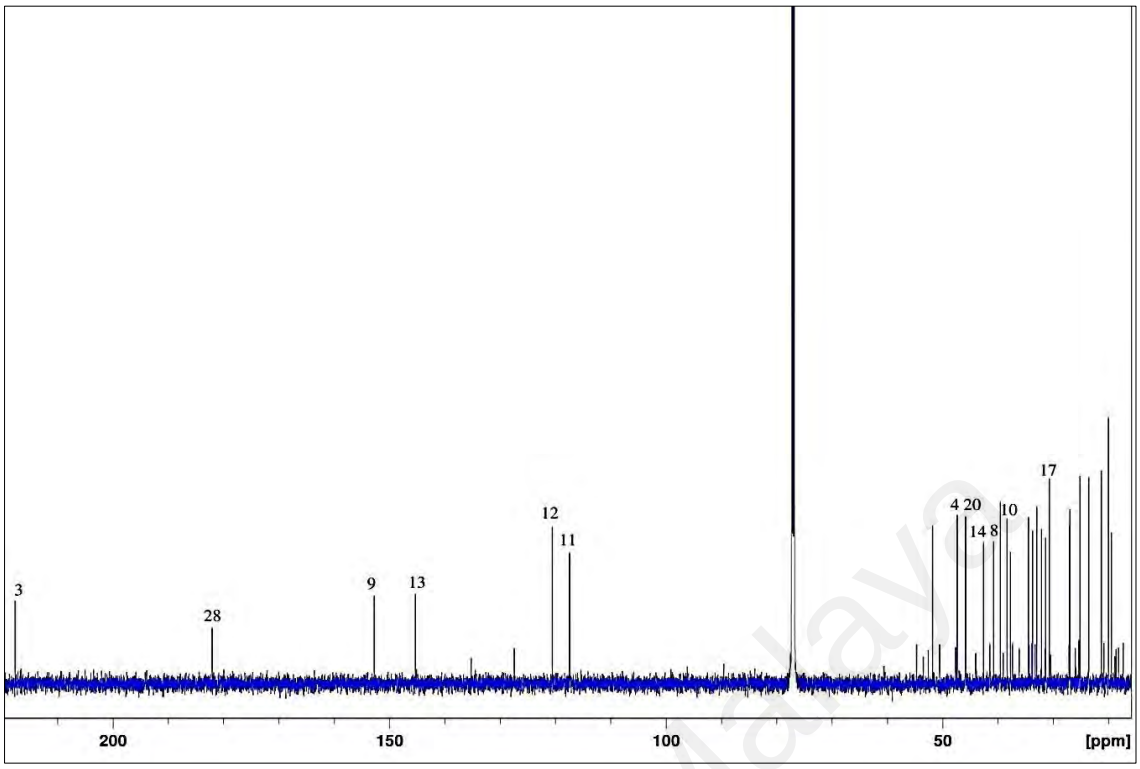


**Figure 3.22**: $^{13}C$ (100 MHz) NMR spectrum of 3-oxo-olean-9(11),12-dien-28-oic acid (**100**)

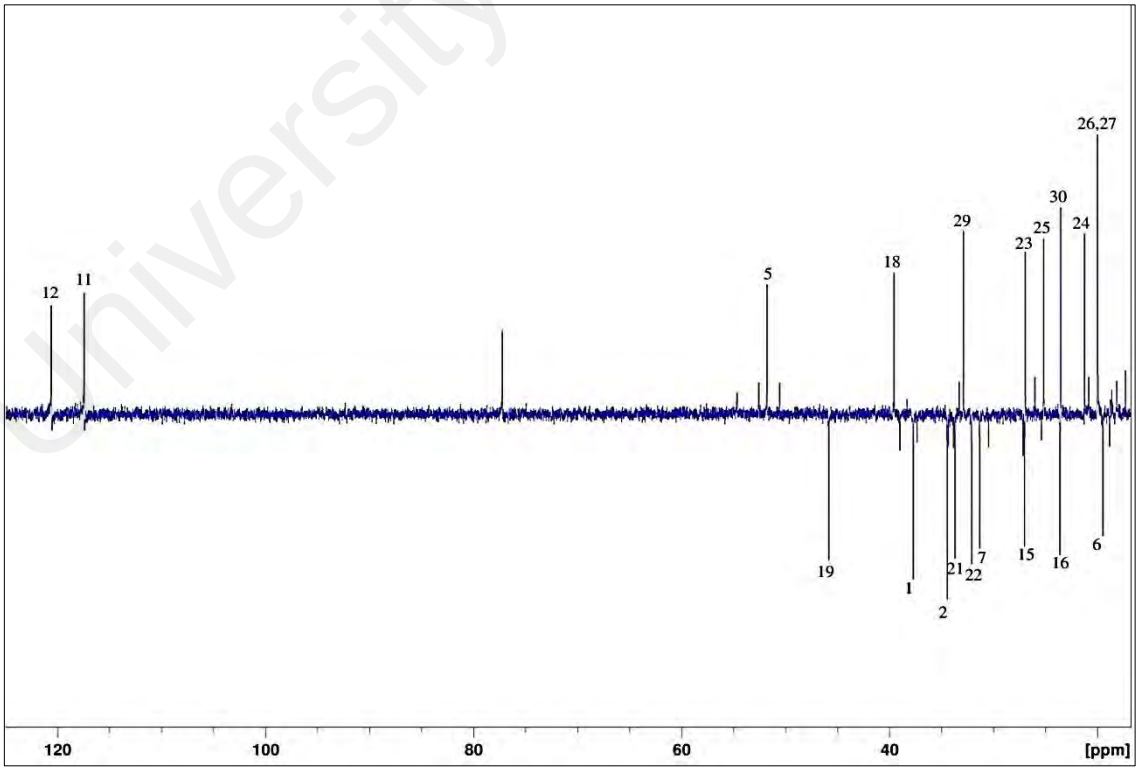


**Figure 3.23**: DEPT-135 spectrum of 3-oxo-olean-9(11),12-dien-28-oic acid (**100**)

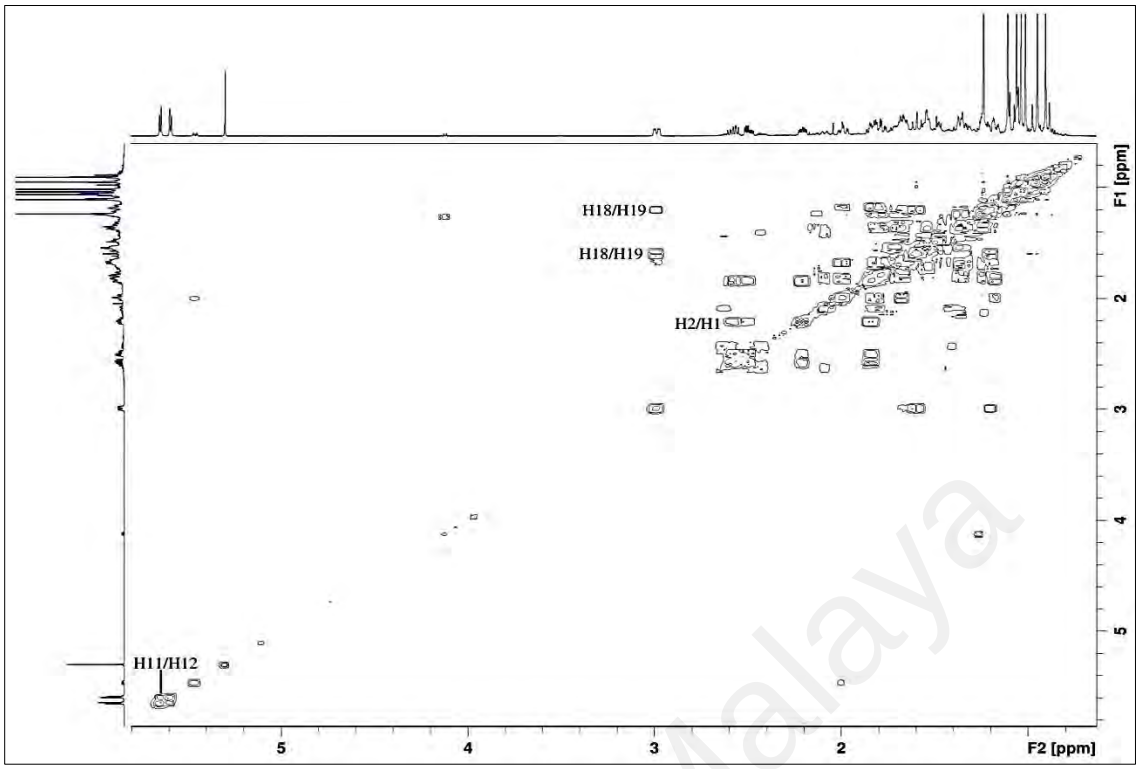


**Figure 3.24**: COSY spectrum of 3-oxo-olean-9(11),12-dien-28-oic acid (**100**)

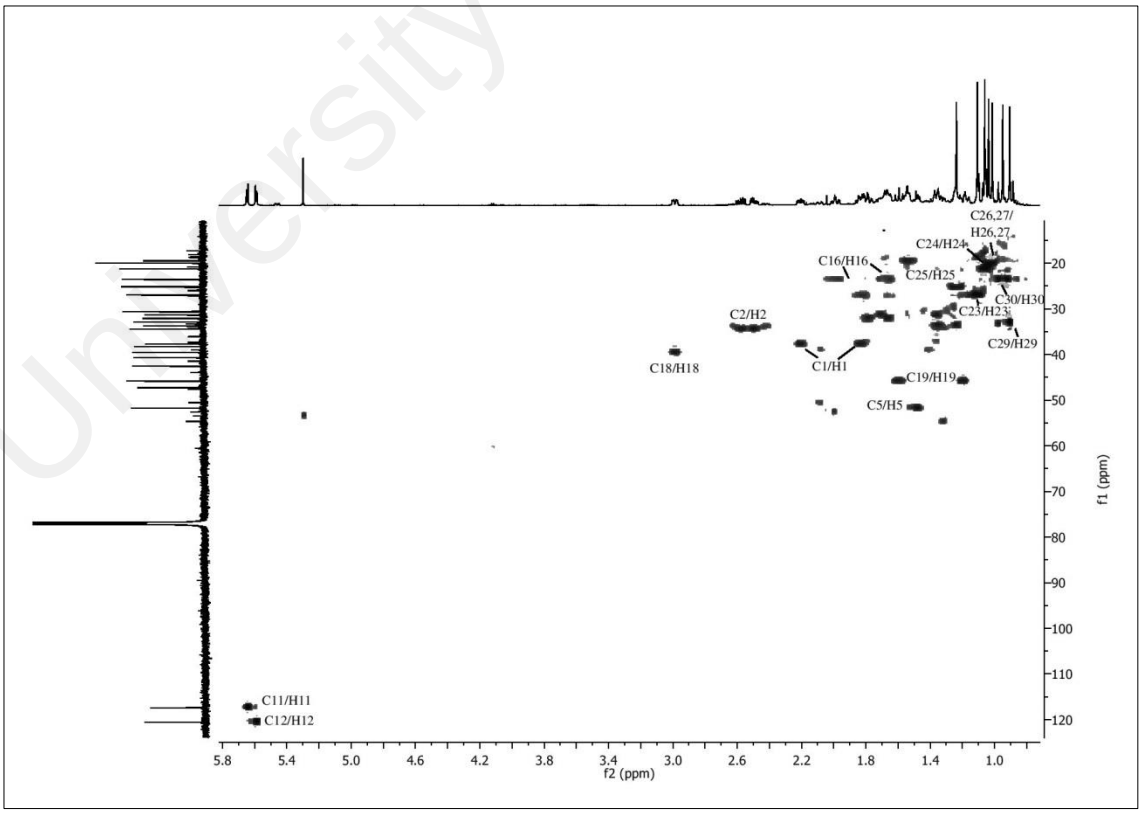


**Figure 3.25**: HSQC spectrum of 3-oxo-olean-9(11),12-dien-28-oic acid (**100**)

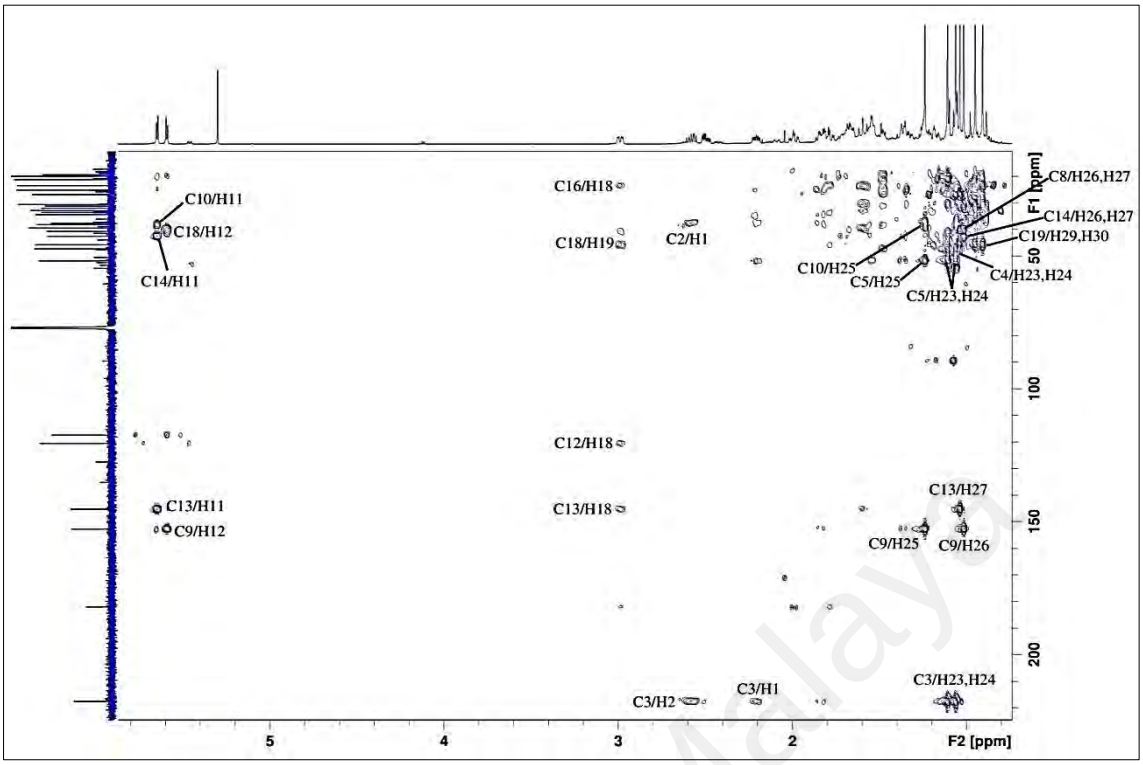


**Figure 3.26:** HMBC spectrum of 3-oxo-olean-9(11),12-dien-28-oic acid (**100**)

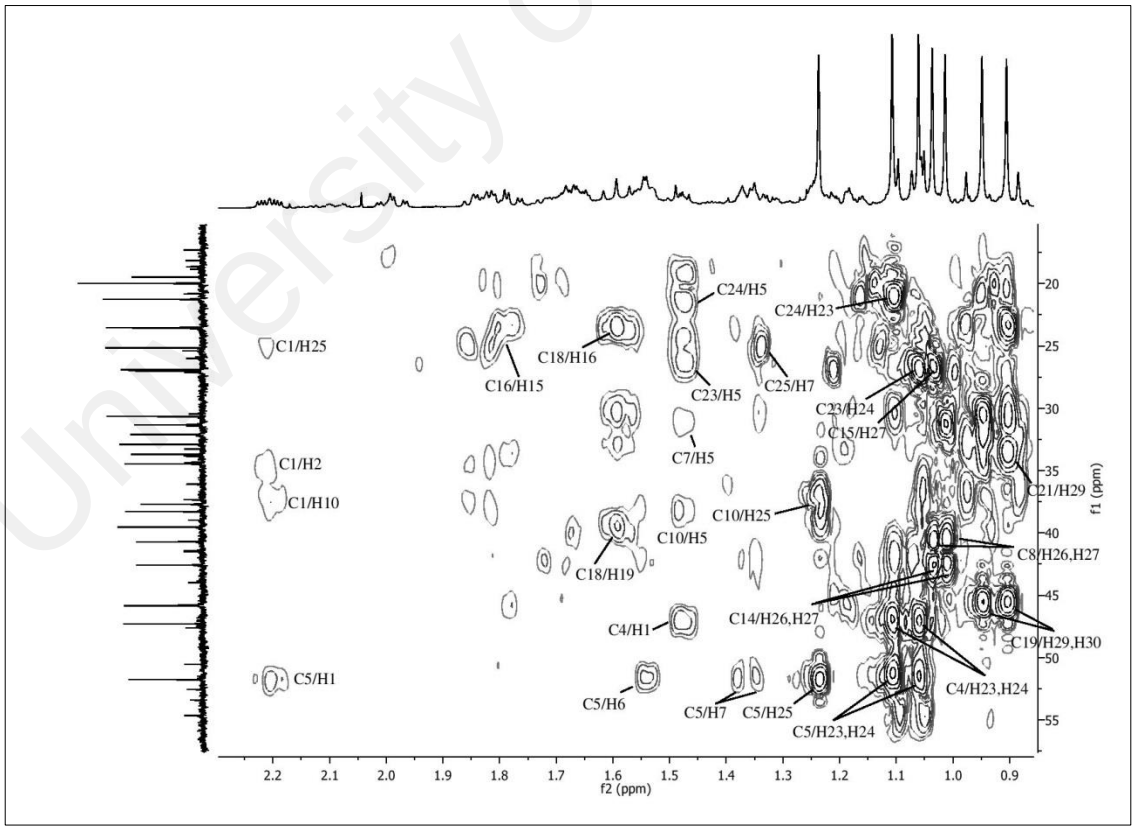


**Figure 3.27**: HMBC spectrum expanded of 3-oxo-olean-9(11),12-dien-28-oic acid (**100**)

## 3.5 Compound 101: 3-oxo-20(24)-epoxy-12*β*,25 dihydroxydammarane

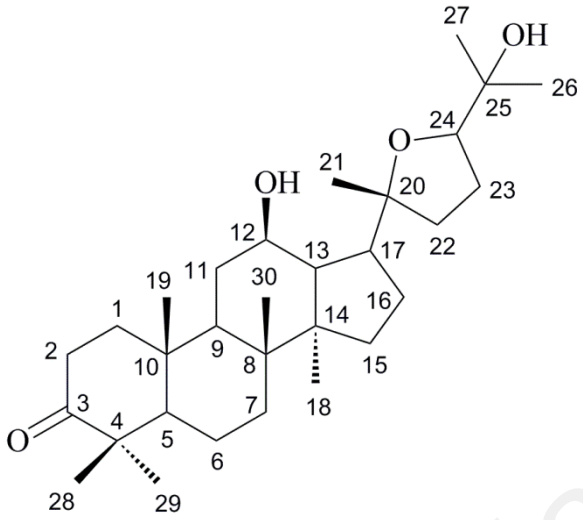


3-oxo-20(24)-epoxy-12*β*,25-dihydroxydammarane (**101**) was afforded as colourless white needles. The molecular formula was assigned a molecular formula of $C_{30}H_{50}O_4$ as deduced from its positive HRESIMS ($[M+H]^+$, m/z 474.3709; calcd. for $C_{30}H_{51}O_4$; 475.3787), consistent with six degrees of unsaturation. The IR spectrum showed a broad band for hydroxyl group (3433cm$^{-1}$), a strong sp$^3$ C-H alkane stretch (2953cm$^{-1}$) and carbonyl (1706cm$^{-1}$) functionalities (Gary et al., 2010).

The $^1$H NMR spectrum (Figure 3.29) showed eight singlets of methyl groups resonated at δ 0.95 (Me-30), 1.07 (Me-19 and Me-29), 1.01 (Me-18), 1.11 (Me-28), 1.13 (Me-27), 1.26 (Me-26) and 1.30 (Me-21). Two oxymethine signals resonated at δ 3.57 (*td*, *J* = 10.3, 4.8 Hz, H-12) and δ 3.91 (*dd*, *J* = 10.8, 5.4 Hz, H-24) were also observed. The more downfield shifts of methylene proton signals at δ 2.48 (*m*, H-2a) and δ 2.52 (*m*, H-2b) suggesting that the vicinal C-3 position is an electron withdrawing group.

The $^{13}$C NMR (Figure 3.30), DEPT (Figure 3.31) and HSQC experiments of 3-oxo-20(24)-epoxy-12*β*,25-dihydroxydammarane, **101** showed the presence of thirty carbons, among which eight methyl resonated at δ 16.1 (C-18), 15.2 (C-19), 17.7 (C-30),

20.9 (C-29), 24.2 (C-27), 26.7 (C-28), 28.0 (C-26) and 28.9 (C-21). Two oxymethine and two oxygenated quaternary carbon at δ 70.4 (C-12), 70.1 (C-25) and δ 87.2 (C-20), 87.5 (C-24) together with a carbonyl carbon resonated at δ 217.9 (C-3) were spotted.

From the COSY experiment (Figures 3.28 and 3.32), the position of hydroxyl proton at H-12 (δ 3.57, td, *J* = 10.3, 4.8 Hz) was deduced from the correlation with H-11 (δ 1.28, *m* and δ 1.57, *m*) and H-13 (δ 1.74, *t*, J= 10.0 Hz) while a methine proton at H-17 (δ 2.29, *td*, *J* = 10.5, 4.4 Hz) was detected from interaction with H-13 and H-16 (δ 1.36, *m* and δ 2.03, *m*). Other correlations observed were between H-24 with H-23 and H-2 with H-1.

In depth analysis of HMBC experiments (Figures 3.28, 3.33 and 3.34), the location of carbonyl group at C-3 (δ 217.9) was supported from correlation with Me-28 (δ 1.11, *s*), Me-29 (δ 1.07, *s*), H-1 and H-2. The tetrahydrofuran and *tert*-butyl alcohol structure was prove by the correlation of C-20 (δ 87.2) with H-17 (δ 2.29, *td*, *J* = 10.5, 4.4 Hz), Me-21 (δ 1.30, *s*) and C-23 (δ 25.1), C-24 (δ 87.5) with H-22, Me-26 (δ 1.26, *s*) and Me-27 (δ 1.13, *s*), and C-25 (δ 70.1) with H-24 (δ 3.91, *dd, J* = 10.8, 5.4 Hz), Me-26 and Me-27. The hydroxyl at position C-12 (δ 70.4) was confirmed based on interaction with H-13 (δ 1.74, *t*, *J* = 10.0 Hz) and H-17 (δ 2.29, *td*, *J* = 10.5, 4.4 Hz). The absence of correlations between C-12 (δ 70.4)/H-12 (δ 3.57, *td*, *J* = 10.3, 4.8 Hz) with Me-18, Me-19, Me-30 and C-8, C-10, C-14 respectively supported the position of hydroxyl at C-12.

Extensive analysis of 1D and 2D NMR spectra (Table 3.6) suggested that **101** was 3-oxo-20(24)-epoxy-12*β*,25-dihydroxydammarane (Valverde et al., 1985).

**Table 3.6**: $^{1}H$ (400 MHz) and $^{13}C$ (100 MHz) NMR data of 3-oxo-20(24)-epoxy-12*β*,25-dihydroxydammarane (**101**) in $CDCl_3$

| Position | Compound **101** | | (Valverde et al., 1985) | |
|---|---|---|---|---|
| | $\delta_H$ (ppm), *J (Hz)* | $\delta_C$ (ppm) | $\delta_H$ (ppm), *J (Hz)* | $\delta_C$ (ppm) |
| 1 | 1.52, *m*<br>2.00, *m* | 39.7 | | 39.8 |
| 2 | 2.48, *m*<br>2.52, *m* | 34.1 | | 34.0 |
| 3 | - | 217.9 | - | 217.5 |
| 4 | - | 47.3 | - | 47.3 |
| 5 | 1.42, *m* | 55.3 | | 55.3 |
| 6 | 1.07, *m*<br>1.53, *m* | 19.7 | | 19.6 |
| 7 | 1.38, *m*<br>1.53, *m* | 34.1 | | 34.1 |
| 8 | - | 39.6 | - | 39.6 |
| 9 | 1.61, *m* | 49.6 | | 49.5 |
| 10 | - | 36.9 | - | 36.8 |
| 11 | 1.28, *m*<br>1.57, *m* | 32.1 | | 31.2 |
| 12 | 3.57, *td* (10.3, 4.8) | 70.4 | 3.53, *sxt* (10.4, 10.4, 4.5) | 70.8 |
| 13 | 1.74, *t* (10.0) | 48.9 | | 47.9 |
| 14 | - | 52.2 | - | 52.0 |
| 15 | 1.14, *m*<br>1.23, *m* | 32.2 | | 31.7 |
| 16 | 1.36, *m*<br>2.03, *m* | 28.5 | | 25.0 |
| 17 | 2.29, *td* (10.5, 4.4) | 48.9 | | 49.8 |
| 18 | 1.01, *s* | 16.1 | 1.02, *s* | 16.1 |
| 19 | 1.07, *s* | 15.2 | 1.07, *s* | 15.1 |
| 20 | - | 87.2 | - | 86.5 |
| 21 | 1.30, *s* | 28.9 | 1.10, *s* | 26.1 |
| 22 | 1.80, *m*<br>1.96, *m* | 31.7 | | 32.6 |
| 23 | 1.89, *m*<br>2.08, *m* | 25.1 | | 28.6 |
| 24 | 3.91, *dd* (10.8, 5.4) | 87.5 | 3.85, *q* (7.8, 6.8) | 85.5 |
| 25 | - | 70.1 | - | 70.1 |
| 26 | 1.26, *s* | 28.0 | 1.28, *s* | 27.9 |
| 27 | 1.13, *s* | 24.2 | 1.27, *s* | 27.6 |
| 28 | 1.11, *s* | 26.7 | 0.96, *s* | 26.6 |
| 29 | 1.07, *s* | 20.9 | 1.04, *s* | 20.9 |
| 30 | 0.95, *s* | 17.7 | 0.91, *s* | 18.0 |

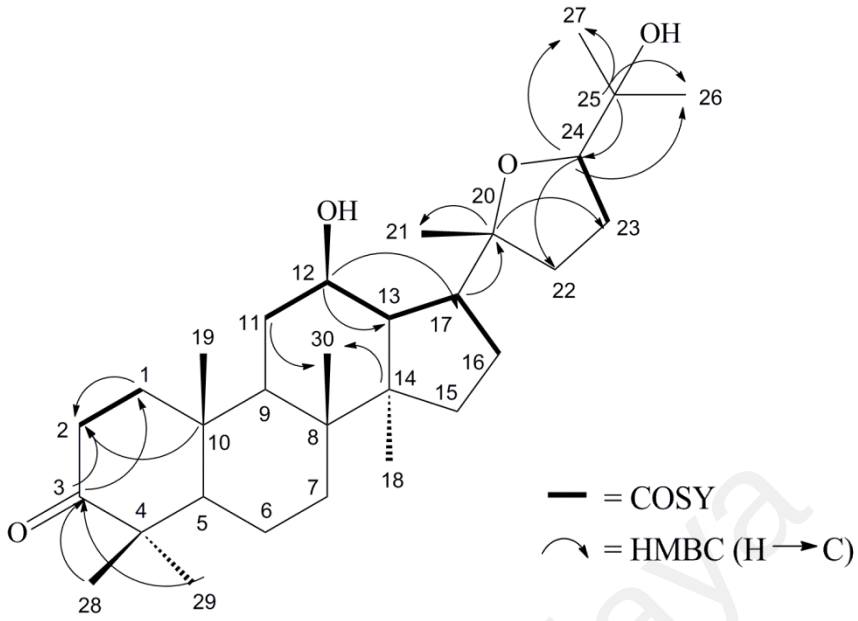


**Figure 3.28**: Selected COSY and HMBC correlations of 3-oxo-20(24)-epoxy-12*β*,25-dihydroxydammarane (**101**)

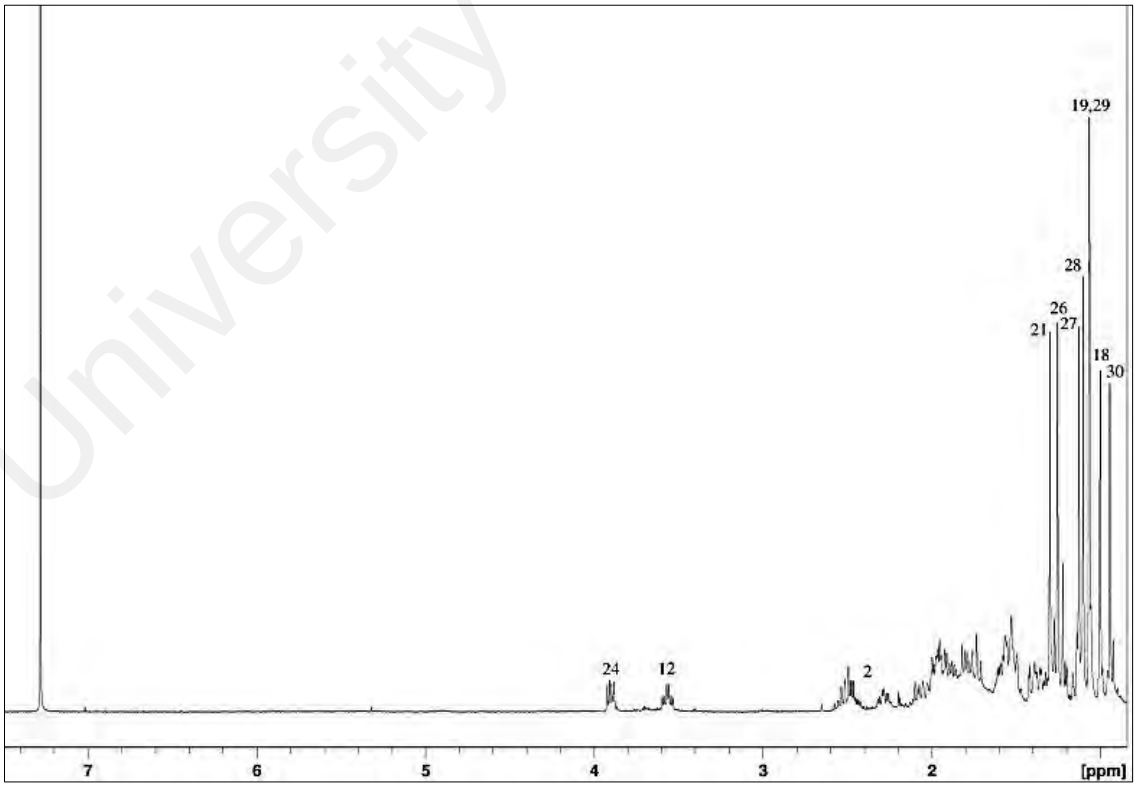


**Figure 3.29**: $^{1}$H (400 MHz) NMR spectrum of 3-oxo-20(24)-epoxy-12*β*,25-dihydroxydammarane (**101**)

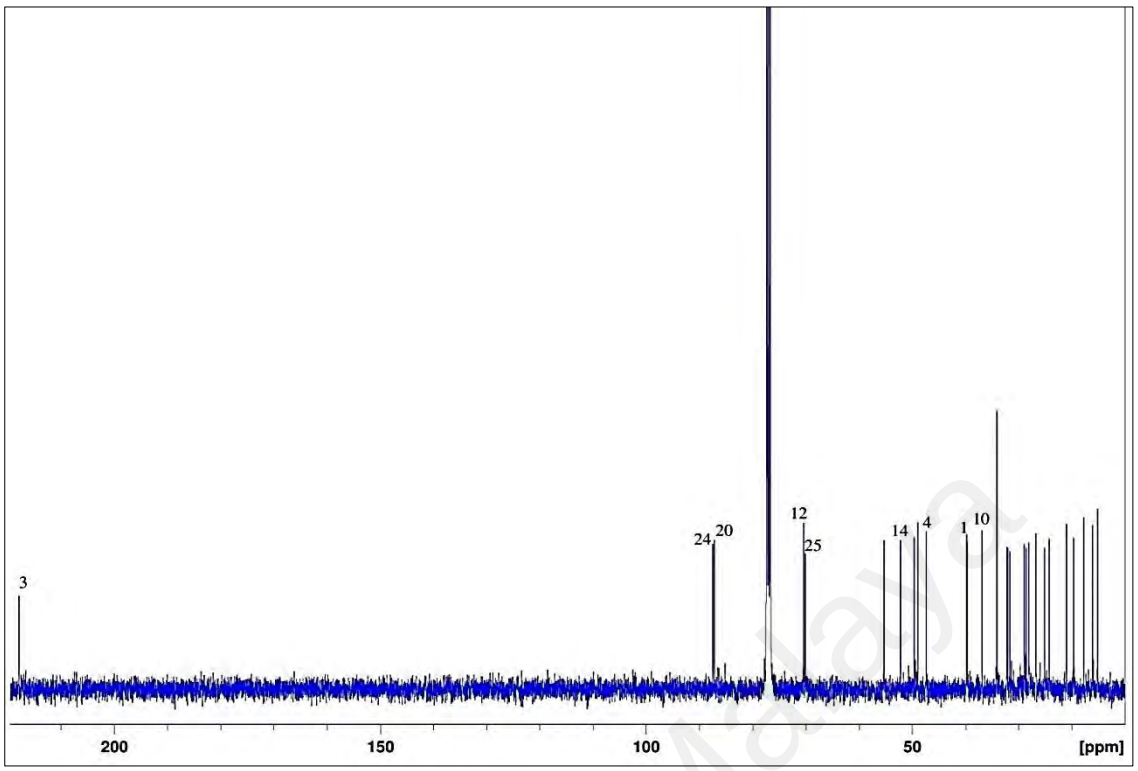


**Figure 3.30**: $^{13}C$ (100 MHz) NMR spectrum of 3-oxo-20(24)-epoxy-12*β*,25-dihydroxydammarane (**101**)

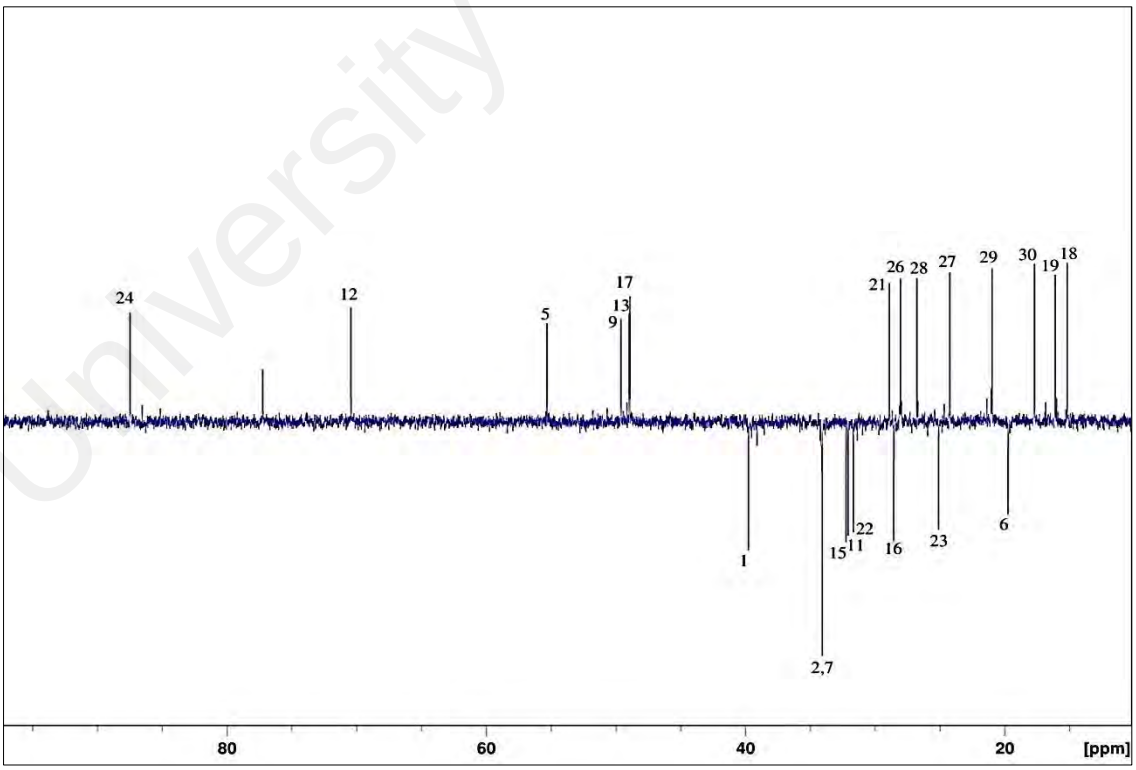


**Figure 3.31**: DEPT-135 spectrum of 3-oxo-20(24)-epoxy-12*β*,25-dihydroxydammarane (**101**)

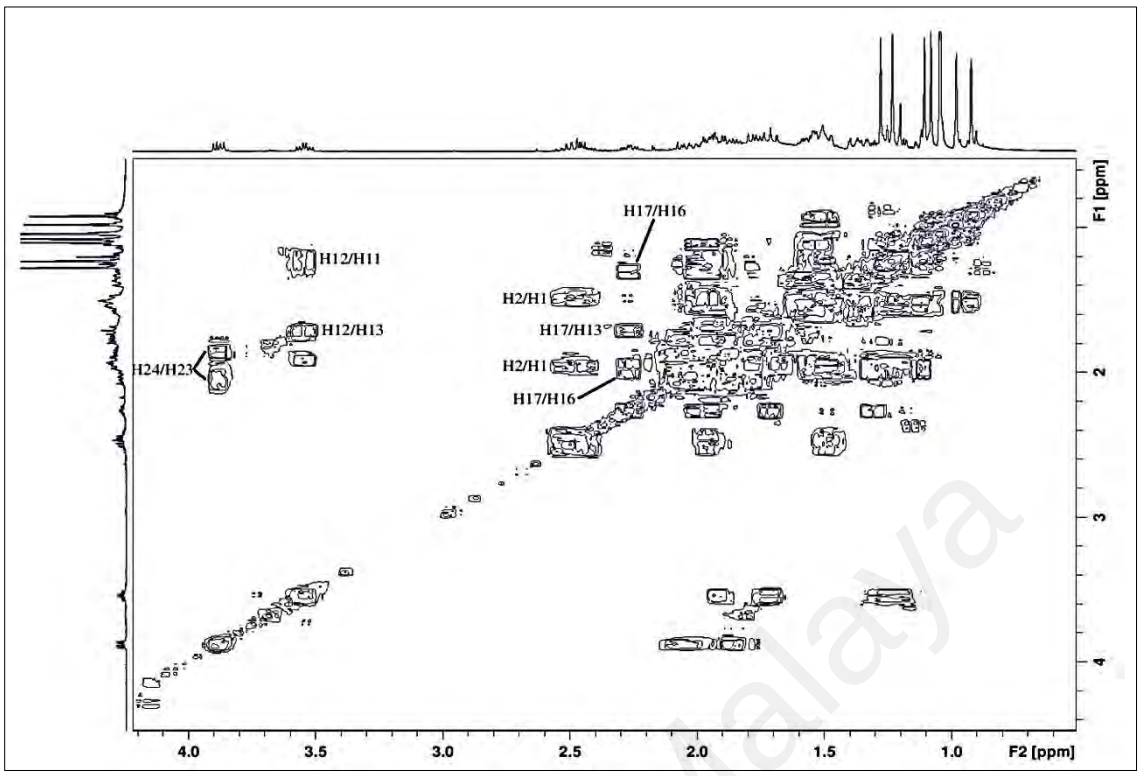


**Figure 3.32**: COSY spectrum of 3-oxo-20(24)-epoxy-12*β*,25-dihydroxydammarane (**101**)

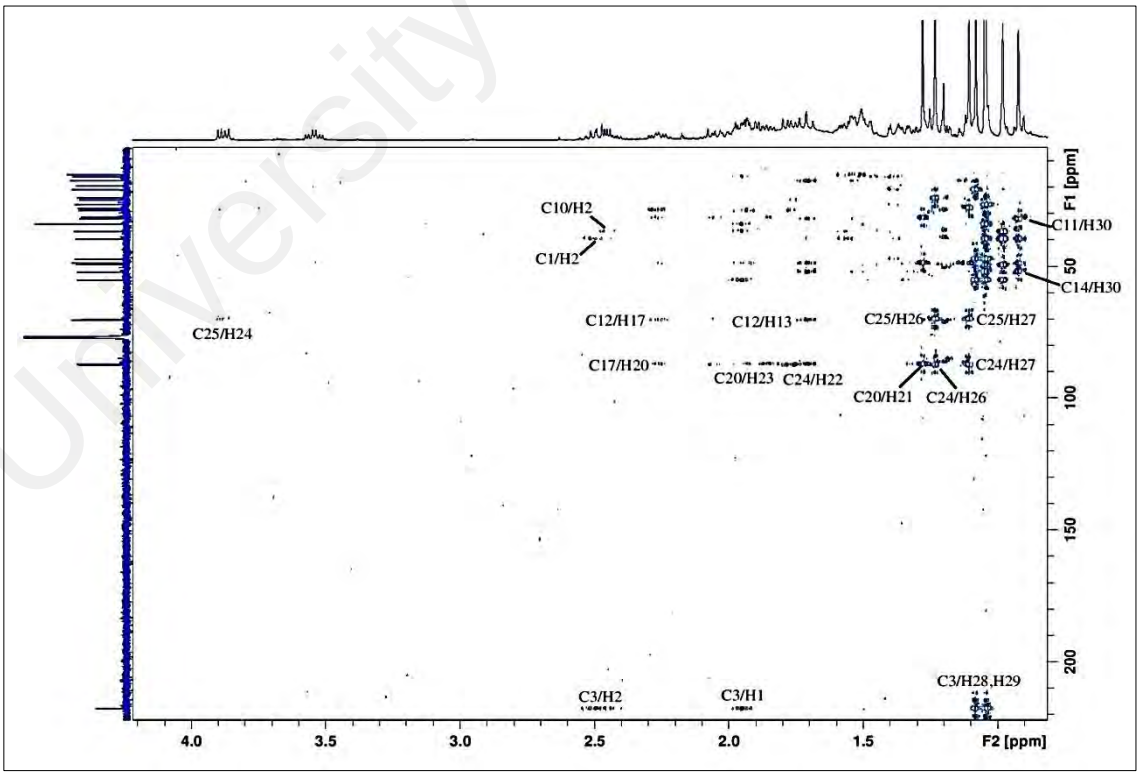


**Figure 3.33**: HMBC spectrum of 3-oxo-20(24)-epoxy-12*β*,25-dihydroxydammarane (**101**)

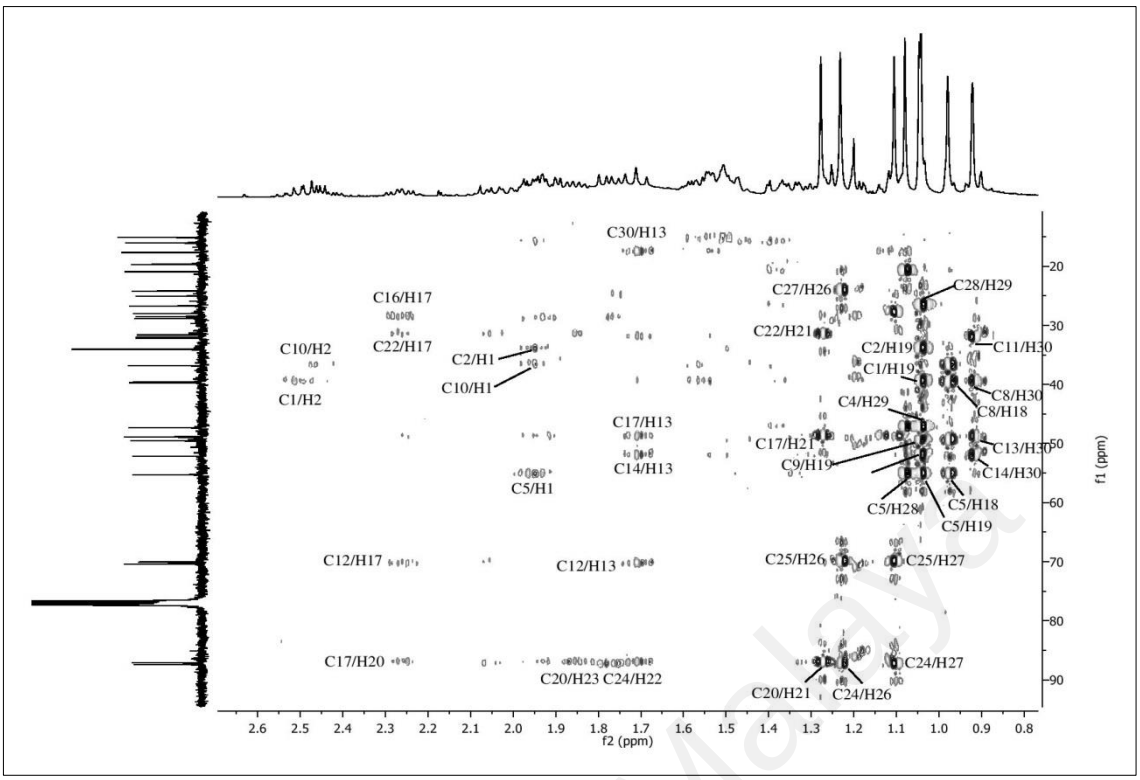


**Figure 3.34**: HMBC spectrum expanded of 3-oxo-20(24)-epoxy-12*β*,25-dihydroxydammarane (**101**)

### 3.6 Compound 102: 2(3),6(7)-diepoxy-9-humulene

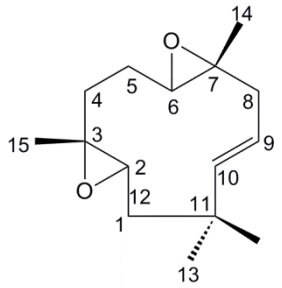


2(3),6(7)-diepoxy-9-humulene, **102** was obtained as white amorphous powder. Its molecular formula of $C_{15}H_{22}O_2$ with four degree of unsaturation was determined from the quasi-molecular ion peak $[M+H]^+$ at m/z 233.1755 (calcd. for $C_{15}H_{21}O_2$, 233.1542) by HR-ESI-MS. The IR spectrum exhibited strong band from C-O stretch (976 $cm^{-1}$) and olefinic (1657 $cm^{-1}$) functionalities (Gary et al., 2010).

The $^1H$ NMR spectrum (Figure 3.36) showed four singlets of methyl groups resonated at δ 1.09 (Me-12), 1.20 (Me-13) and 1.31 (Me-14, Me-15) which is a characteristic of sesquiterpenoid skeleton. Two olefinic proton signals resonated at δ 5.50 (*ddd*, *J* = 15.6, 10.5, 5.0 Hz, H-9) and δ 5.32 (*d*, *J* = 15.6 Hz, H-10) together with two oxymethine signals for H-2 and H-6 at δ 2.48 (*d*, *J* = 9.5 Hz) and δ 2.74 (*dd*, *J* = 10.2, 5.0 Hz), respectively.

The $^{13}C$ NMR (Figure 3.37) and DEPT spectra (Figure 3.38) of 2(3),6(7)-diepoxy-9-humulene, **102** coupled with HSQC experiments showed the presence of fifteen carbon signals, among which four methyls at δ 16.4 (C-14), 16.5 (C-15), 23.3 (C-13) and 30.7 (C-12). An olefinic carbon and two oxymethine signals resonated at δ 122.6 (C-9), 142.9 (C-10) and δ 60.3 (C-6), 64.6 (C-2) were observed while two oxygenated quaternary carbon was present at δ 60.1 (C-3) and 63.3 (C-7).

Through the COSY experiment (Figures 3.35 and 3.39), both oxymethine signals at H-2 (δ 2.48, *d*, *J* = 9.5 Hz) and H-6 (δ 2.74, *dd*, *J* = 10.2, 5.0 Hz) showed

interactions with methylene signals H-1 (δ 1.39, *m* and δ1.67, *m*) and H-5 (δ 1.37, *m*), respectively. Other correlations observed in COSY were between H-4/H-5 and H-8/H-9.

Thorough analysis of HMBC experiment (Figures 3.35 and 3.40), two epoxide rings systems at C2(3) and C6(7) were built on basis interrelationships between C-2 (δ 64.6)/C-3 (δ 60.1) with H-1, H-2, $H_2$-4, H-5 and Me-15 while C-6 (δ 60.3)/C-7 (δ 63.3) with H-5, H-6, H-8 and Me-14. Methyl positions at Me-14 and Me-15 were deduced at both epoxide on basis correlation of Me-14 (δ 16.4) with C-6 and C-7 while Me-15 (δ 16.5) with C-2 and C-3. Me-12 and Me-13 were deduced as geminal methyl position from cross correlation between them with C-1 (δ 38.3), C-10 (δ 142.9) and C-11 (δ 35.6). Careful analysis of this experiments suggested that an olefinic moiety were located at C-9(10) from interactions of H-9 (δ 5.50, *ddd*, *J* = 15.6, 10.5, 5.0 Hz) and H-10 (δ 5.32, *d*, *J* = 15.6 Hz) with C-8, C-9, C-10, C-11, C-12 and C-13.

In depth analysis of 1D and 2D NMR spectra (Table 3.7) suggested that **102** was 2(3),6(7)-diepoxy-9-humulene (Heymann et al., 1994).

**Table 3.7**: $^{1}H$ (400 MHz) and $^{13}C$ (100 MHz) NMR data of 2(3),6(7)-diepoxy-9-humulene (**102**) in $CDCl_3$

| Position | Compound **102** | | (Heymann et al., 1994) | |
|---|---|---|---|---|
| | $\delta_H$ (ppm), *J* (Hz) | $\delta_C$ (ppm) | $\delta_H$ (ppm), *J* (Hz) | $\delta_C$ (ppm) |
| 1 | 1.39, *m*<br>1.67, *m* | 38.3 | 1.38, *dd* (9.5)<br>1.61, *d* (14.0) | 38.4 |
| 2 | 2.48, *d* (9.5) | 64.6 | 2.48, *d* (9.5) | 64.7 |
| 3 | - | 60.1 | - | 60.1 |
| 4 | 1.09, *m*<br>2.14, *m* | 34.8 | 1.08, *td* (13.0, 5.0)<br>2.13, *ddd* (13.0, 6.0, 2.5) | 34.9 |
| 5 | 1.37, *m* | 25.2 | 1.38, *dddd*<br>(12.5, 10.0, 4.0, 2.5) | 25.2 |
| 6 | 2.22, *m*<br>2.74, *dd* (10.2, 5.0) | 60.3 | 2.21, *t* (13.5, 5.0)<br>2.73, *dd* (10.5) | 60.4 |
| 7 | - | 63.3 | - | 60.1 |
| 8 | 1.62, *m*<br>2.65, *dd* (12.2, 5.1) | 43.3 | 1.65, *t* (10.5)<br>2.64, *dd* (10.5, 5.0) | 43.4 |
| 9 | 5.50, *ddd*<br>(15.6, 10.5, 5.0) | 122.6 | 5.49, *ddd*<br>(16.0, 10.5, 5.0) | 122.6 |
| 10 | 5.32, *d* (15.6) | 142.9 | 5.31, *d* (16.0) | 142.9 |
| 11 | - | 35.6 | - | 35.7 |
| 12 | 1.09, *s* | 30.7 | 1.08, *s* | 30.8 |
| 13 | 1.20, *s* | 23.3 | 1.20, *s* | 23.4 |
| 14 | 1.31, *s* | 16.4 | 1.31, *s* | 16.6 |
| 15 | 1.31, *s* | 16.5 | 1.31, *s* | 16.6 |

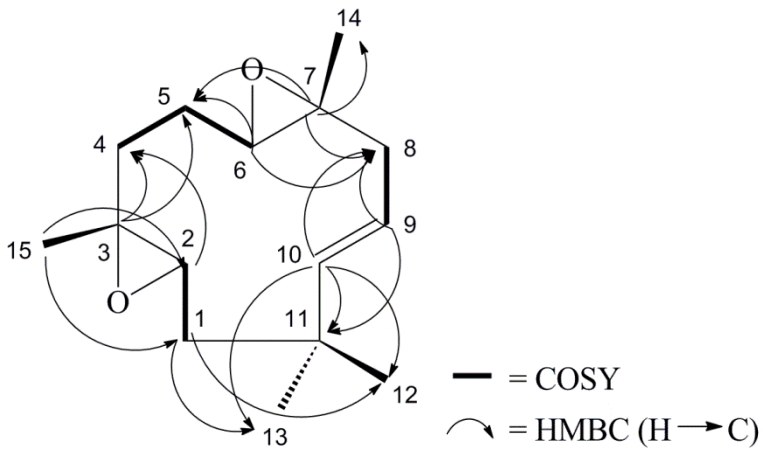


**Figure 3.35**: Selected COSY and HMBC correlations of 2(3),6(7)-diepoxy-9-humulene (**102**)

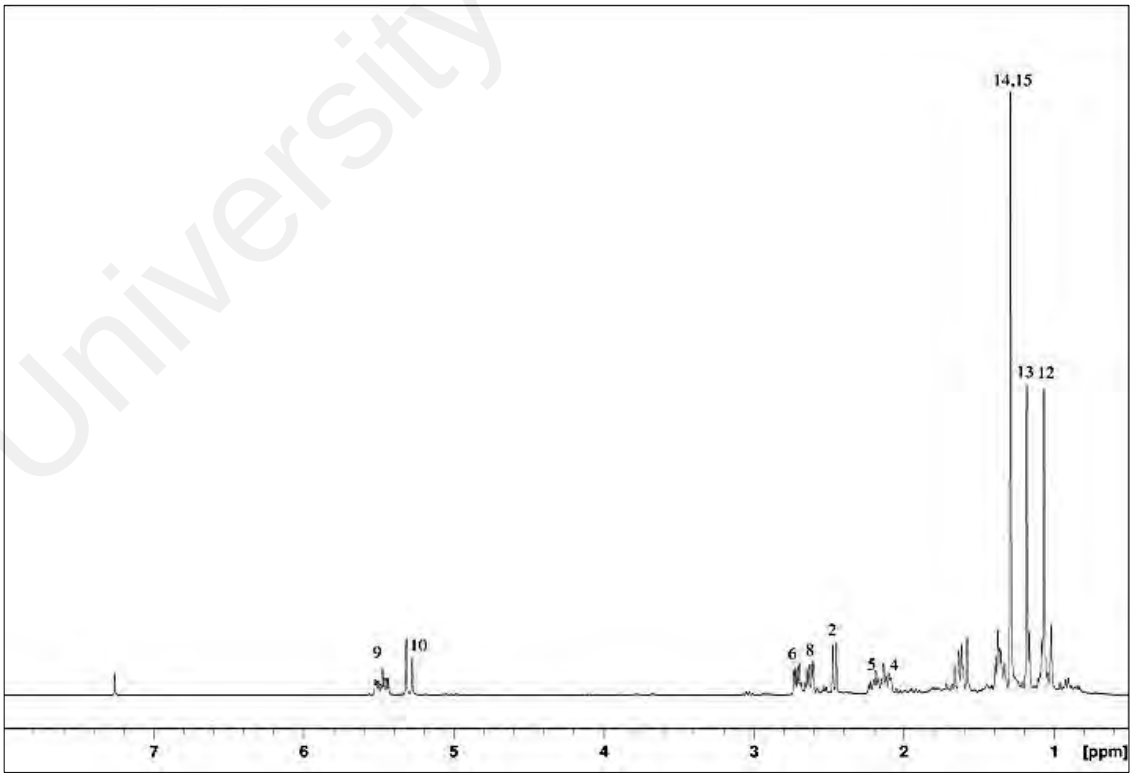


**Figure 3.36**: $^{1}$H (400 MHz) NMR spectrum of 2(3),6(7)-diepoxy-9-humulene (**102**)

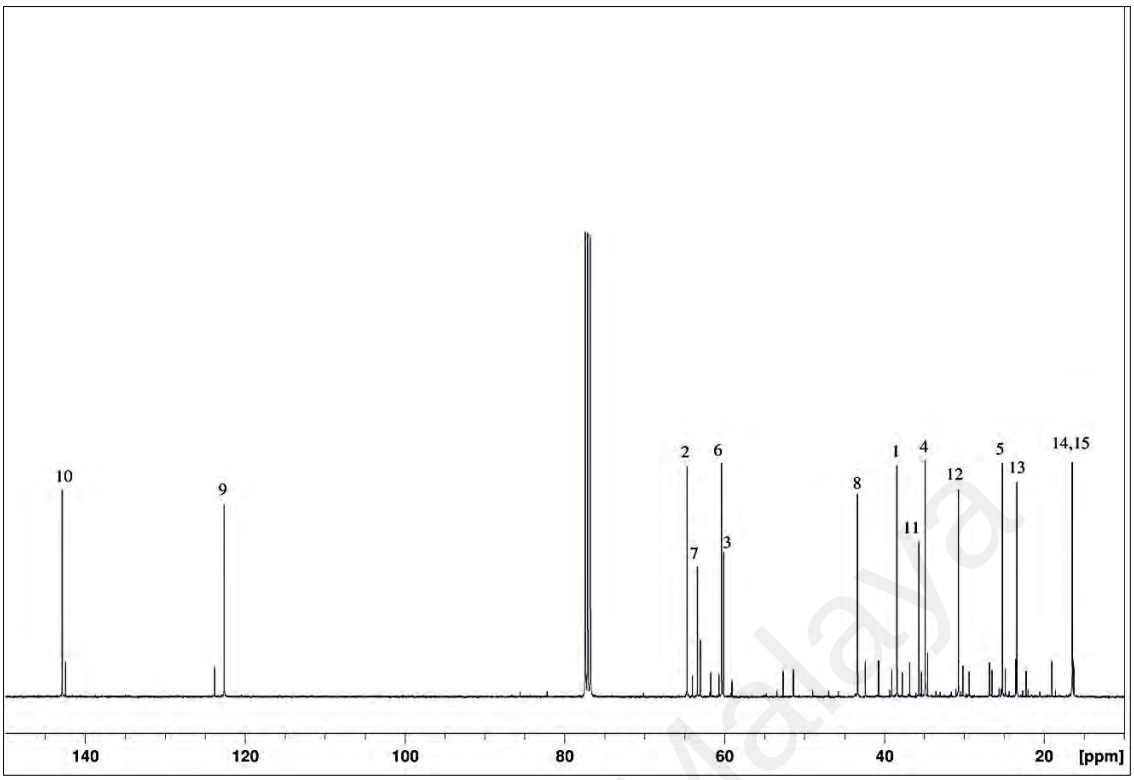


**Figure 3.37**: $^{13}C$ (100 MHz) NMR spectrum of 2(3),6(7)-diepoxy-9-humulene (**102**)

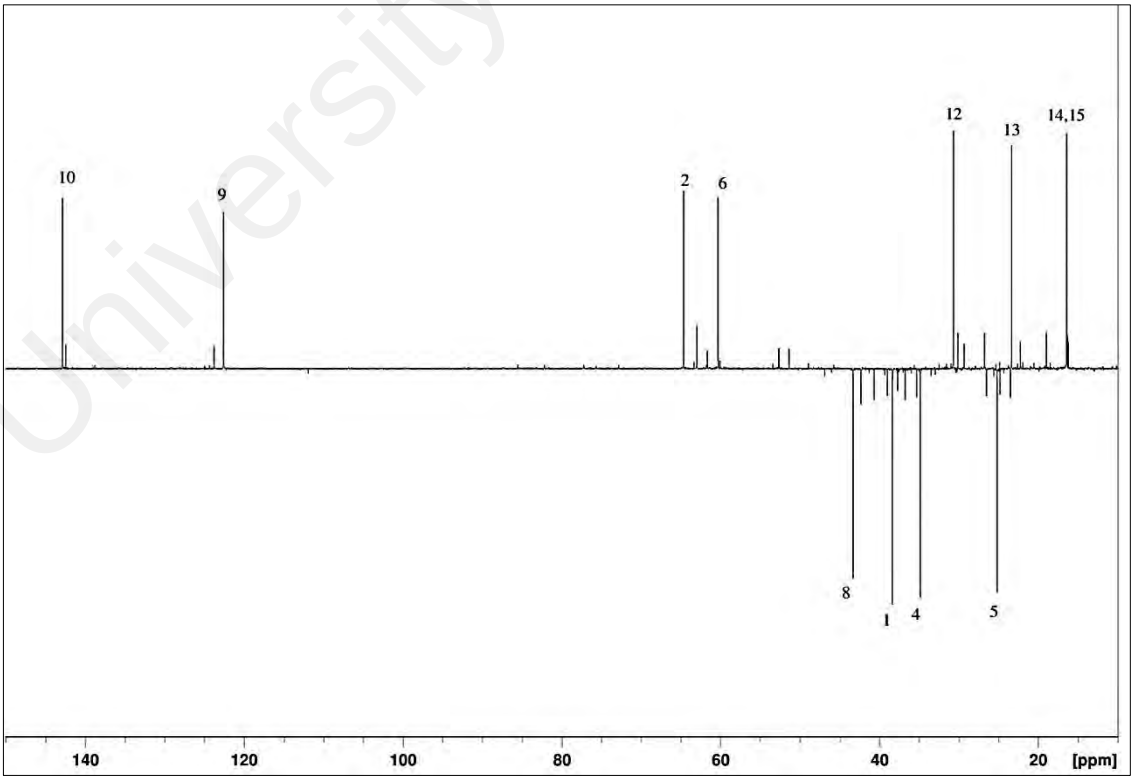


**Figure 3.38**: DEPT-135 spectrum of 2(3),6(7)-diepoxy-9-humulene (**102**)

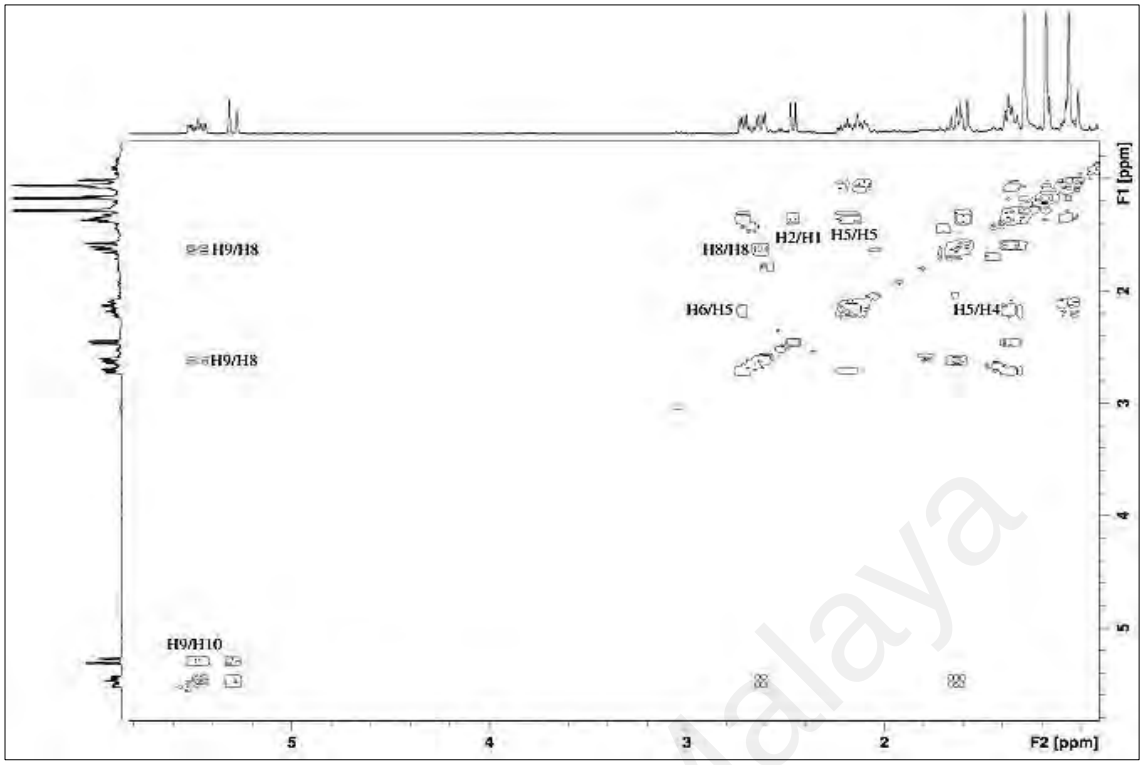


**Figure 3.39**: COSY spectrum of 2(3),6(7)-diepoxy-9-humulene (**102**)

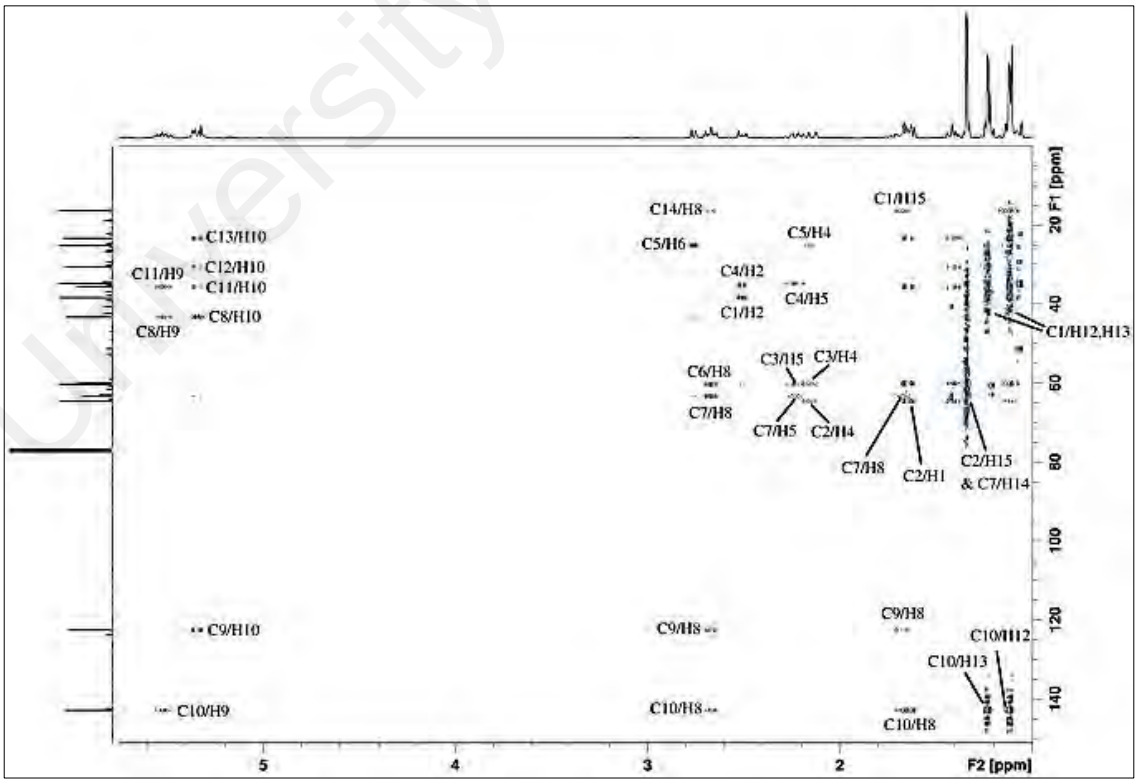


**Figure 3.40**: HMBC spectrum of 2(3),6(7)-diepoxy-9-humulene (**102**)

## 3.7 Compound 103: Stigmasterol

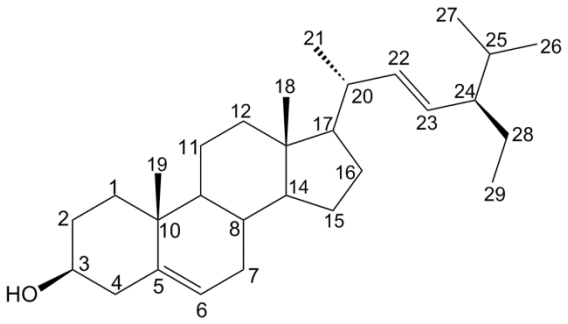


Stigmasterol, **103** was isolated as white amorphous powder. The molecular formula was determined as $C_{29}H_{48}O$ by HR-ESI-MS, which provided a quasi-molecular ion peak $[M+H]^+$ at m/z 413.3783 (calcd. for $C_{29}H_{49}O$, 413.3783), corresponding to six degree of unsaturation. The IR spectrum showed a broad band for hydroxyl (3430 $cm^{-1}$) and olefinic (1653 $cm^{-1}$) functionalities (Gary et al., 2010).

The $^1H$ NMR spectrum (Figure 3.42) showed six methyls; a triplet signal resonated at δ 0.80 (*J* = 6.1 Hz, Me-29), two singlet signal appeared at δ 0.70 (Me-18) and 1.02 (Me-19) together with three doublet signal resonated at δ 0.80 (*J* = 7.4 Hz, Me-27), 0.85 (*J* = 6.3 Hz, Me-26) and 1.02 (*J* = 6.7 Hz, Me-21). An oxymethine signal resonated at δ 3.52 (*ddd*, *J* = 15.8, 11.2, 4.6 Hz, H-3) with three olefinic methine signals resonated at δ 5.35 (*d*, *J* = 5.2 Hz, H-6), 5.02 (*dd*, *J* = 15.1, 8.8 Hz, H-22) and δ 5.02 (*dd*, *J* = 15.1, 8.7 Hz, H-23) were observed.

The $^{13}C$ NMR (Figure 3.43) , DEPT (Figure 3.44) and HSQC experiments of stigmasterol, **103** revealed the presence of twenty nine carbon signal, among which six methyls resonated at δ 12.0 (C-29), 12.2 (C-18), 19.0 (C-27), 19.4 (C-19), 21.1 (C-26) and 21.2 (C-21). A hydroxyl carbon at δ 71.8 (C-3) with three olefinic methine carbon at δ 121.7 (C-6), 129.3 (C-23) and 138.3 (C-22) were identified. An olefinic quaternary carbon signal resonated at δ 140.8 (C-5) were spotted.

Through the COSY experiment (Figures 3.41 and 3.45), the hydroxyl at H-3 (δ 3.52, *ddd*, *J* = 15.8, 11.2, 4.6 Hz) showed interactions with H-2 (δ 1.51, *m* and δ 1.85, *m*) and H-4 (δ 2.29, *dd*, *J* = 13.2, 5.0, 2.0 Hz and δ 2.24, *td*, *J* = 24.1, 13.3, 2.3 Hz). A methine at H-7 showed correlations with methine H-8 (δ 1.47, *m*) and olefinic moieties at H-6 (δ 5.35, *d*, *J* = 5.2 Hz) while another olefinic was observed at the open chain systems from basis correlations between H-23 (δ 5.02, *dd*, *J* = 15.1, 8.8 Hz) with H-22 (δ 5.15, *dd*, *J* = 15.1, 8.7 Hz) and H-24 while H-20 (δ 2.06, *m*) with H-22 (δ 5.15, *dd*, *J* = 15.1, 8.7 Hz).

The HMBC experiment (Figures 3.41 and 3.46) supported that Me-18 (δ 0.70, *s*) and Me-19 (δ 1.02, *s*) were two methyl that fused between rings, were built from basis correlation with C-12 (δ 39.7), C-13 (δ 42.2), C-14 (δ 56.9) and C-5 (δ 140.8), C-9 (δ 50.2) respectively. The formation of geminal methyl between Me-26 (δ 0.85, *d*, *J* = 6.3 Hz) and Me-27 (δ 0.80, *d*, *J* = 7.4 Hz) were deduced from cross correlation between them with C-24 (δ 51.2) and C-25 (δ 31.9). Careful analysis of this experiment suggested that both olefinic moieties were located at C5(6) and C22(23) positions. The double bond was deduced from the correlations of H-6 (δ 5.35, *d*, *J* = 5.2 Hz) with C-4 (δ 42.3), C-7 (δ 31.9) and C-10 (δ 36.5); and C-5 (δ 140.8) with H-4 and H-19, while the position of other double bond was established through the correlation of H-22 (δ 5.15, *dd*, *J* = 15.1, 8.7 Hz) with C-20 (δ 40.5), C-21 (δ 21.2) and C-24 (δ 51.2), while H-23 (δ 5.02, *dd*, *J* = 15.1, 8.8 Hz) with C-20, and C-24.

Complete assignments of all 1D and 2D NMR spectra (Table 3.8) suggested that **103** was stigmasterol (Forgo & Kover, 2004).

**Table 3.8**: $^{1}H$ (600 MHz) and $^{13}C$ (150 MHz) NMR data of stigmasterol (**103**) in $CDCl_3$

| Position | Compound **103** | | (Forgo & Kover, 2004) | |
|---|---|---|---|---|
| | $\delta_H$ (ppm), *J (Hz)* | $\delta_C$ (ppm) | $\delta_H$ (ppm), *J (Hz)* | $\delta_C$ (ppm) |
| 1 | 1.86, *m*<br>1.09, *m* | 37.3 | 1.84, *m*<br>1.08, *m* | 37.6 |
| 2 | 1.85, *m*<br>1.51, *m* | 31.7 | 1.83, *m*<br>1.51, *m* | 31.9 |
| 3 | 3.52, *ddd*<br>(15.8, 11.2, 4.6) | 71.8 | 3.51, *m* | 72.0 |
| 4 | 2.29, *dd* (13.2, 5.0, 2.0)<br>2.24, *td* (24.1, 13.3, 2.3) | 42.3 | 2.30, *m*<br>2.23, *m* | 42.5 |
| 5 | - | 140.8 | - | 140.8 |
| 6 | 5.35, *d* (5.2) | 121.7 | 5.34, *m* | 121.8 |
| 7 | 2.00, *m*<br>1.51, *m* | 31.9 | 1.97, *m*<br>1.50, *m* | 32.1 |
| 8 | 1.47, *m* | 31.9 | 1.46, *m* | 32.2 |
| 9 | 0.94, *dd* (11.5, 5.0) | 50.2 | 0.94, *m* | 50.5 |
| 10 | - | 36.5 | - | 36.5 |
| 11 | 1.41, *m* | 21.1 | 1.50, *m* | 21.2 |
| 12 | 2.01, *m*<br>1.20, *m* | 39.7 | 2.00, *m*<br>1.18, *m* | 40.0 |
| 13 | - | 42.2 | - | 42.2 |
| 14 | 1.02, *m* | 56.9 | 1.01, *m* | 57.1 |
| 15 | 1.58, *m*<br>1.10, *m* | 24.4 | 1.56, *m*<br>1.06, *m* | 24.5 |
| 16 | 1.71, *m*<br>1.27, *m* | 28.9 | 1.72, *m*<br>1.28, *m* | 28.9 |
| 17 | 1.17, *m* | 56.0 | 1.15, *m* | 56.3 |
| 18 | 0.70, *s* | 12.2 | 0.70, *s* | 12.2 |
| 19 | 1.02, *s* | 19.4 | 1.01, *s* | 19.5 |
| 20 | 2.06, *m* | 40.5 | 2.06, *m* | 40.4 |
| 21 | 1.02, *d* (6.7) | 21.2 | 1.03, *d* | 21.4 |
| 22 | 5.15, *dd* (15.1, 8.7) | 138.3 | 5.17. *dd* | 138.3 |
| 23 | 5.02, *dd* (15.1, 8.8) | 129.3 | 5.04, *dd* | 129.7 |
| 24 | 1.54, *m* | 51.2 | 1.54, *m* | 51.5 |
| 25 | 1.54, *m* | 31.9 | 1.55, *m* | 32.2 |
| 26 | 0.85, *d* (6.3) | 21.1 | 0.85, *d* | 21.2 |
| 27 | 0.80, *d* (7.4) | 19.0 | 0.80, *d* | 19.2 |
| 28 | 1.45, *m*<br>1.20, *m* | 25.4 | 1.43, *m*<br>1.18, *m* | 25.4 |
| 29 | 0.80, *t* (6.1) | 12.0 | 0.81, *t* | 12.2 |

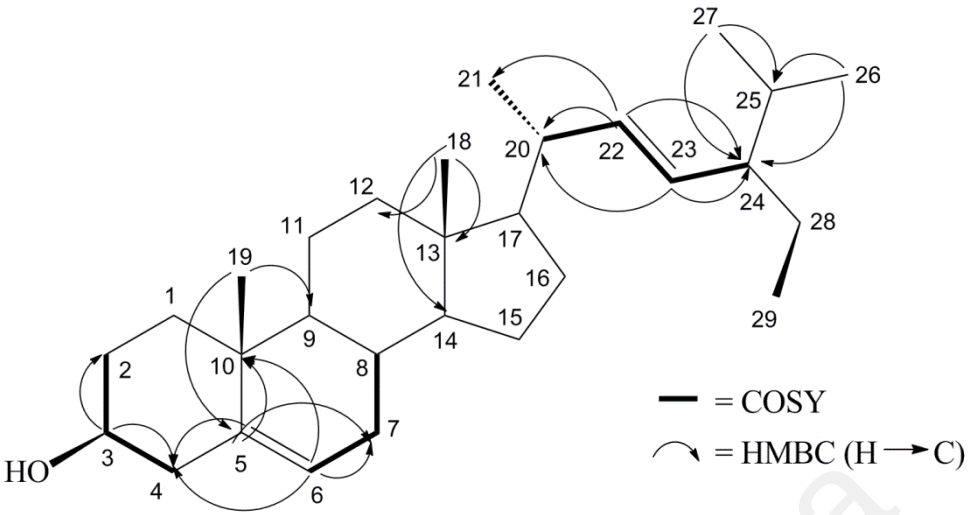


**Figure 3.41**: Selected COSY and HMBC correlations of stigmasterol (**103**)

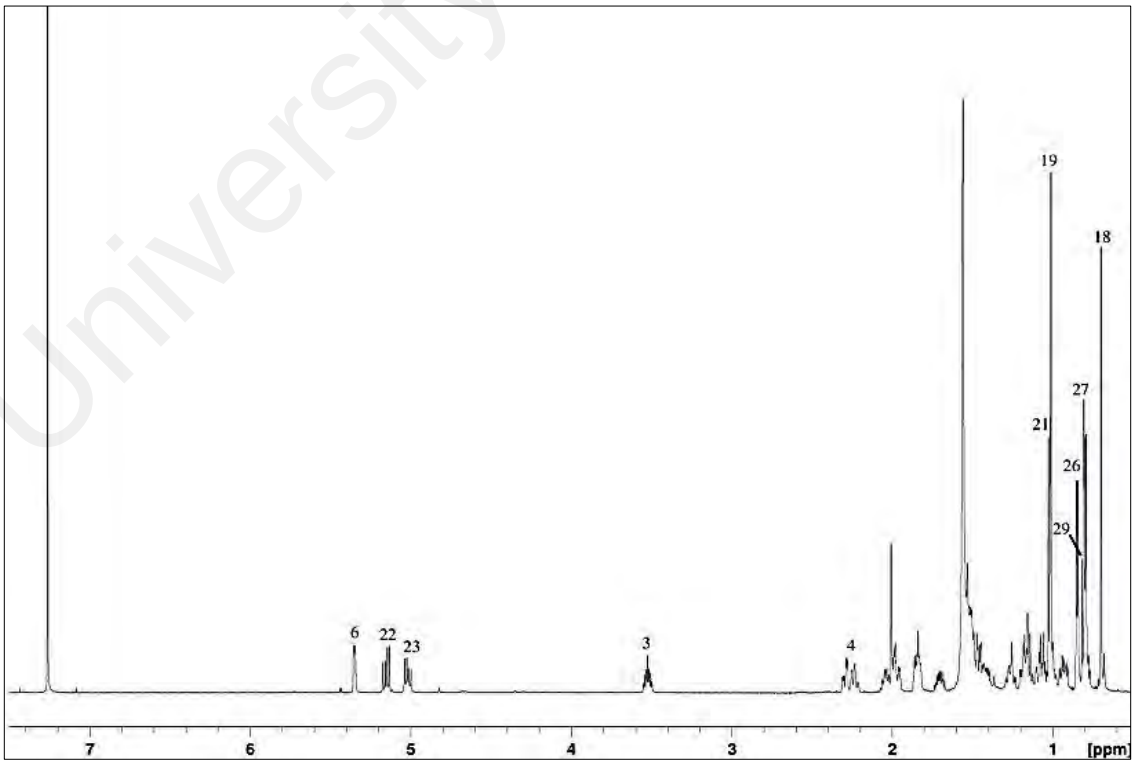


**Figure 3.42**: $^{1}$H (600 MHz) NMR spectrum of stigmasterol (**103**)

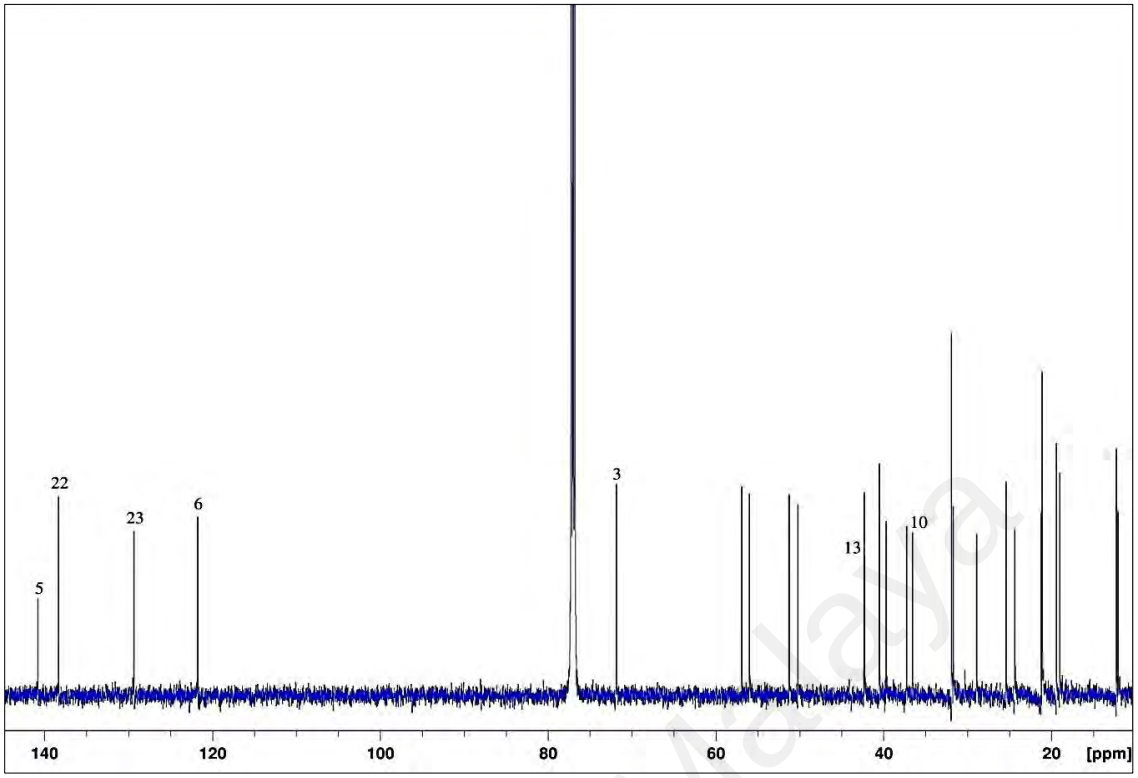


**Figure 3.43**: $^{13}C$ (150 MHz) NMR spectrum of stigmasterol (**103**)

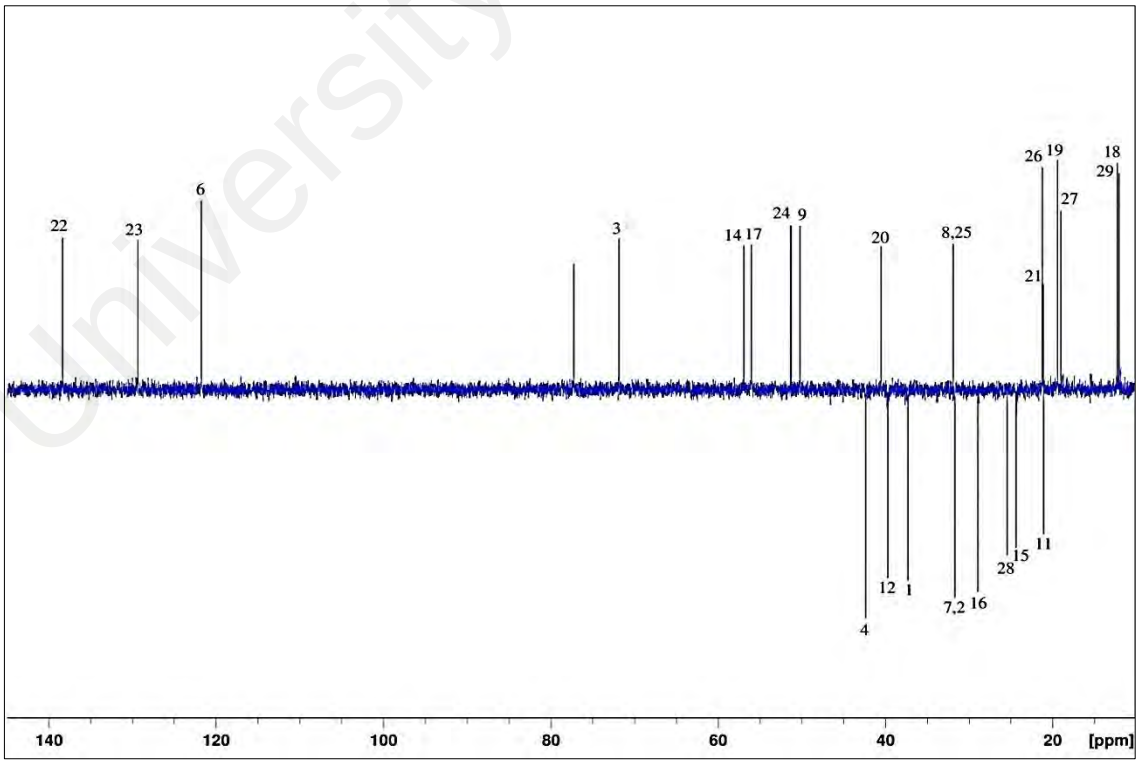


**Figure 3.44**: DEPT-135 spectrum of stigmasterol (**103**)

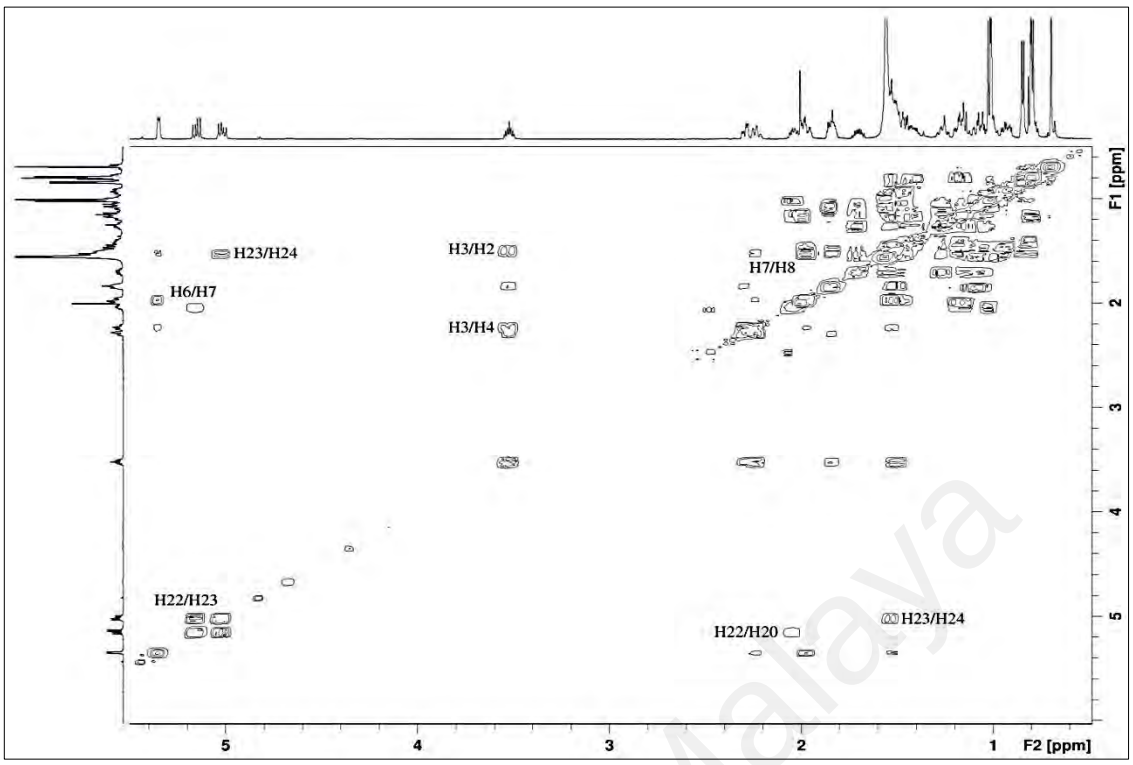


**Figure 3.45**: COSY spectrum of stigmasterol (**103**)

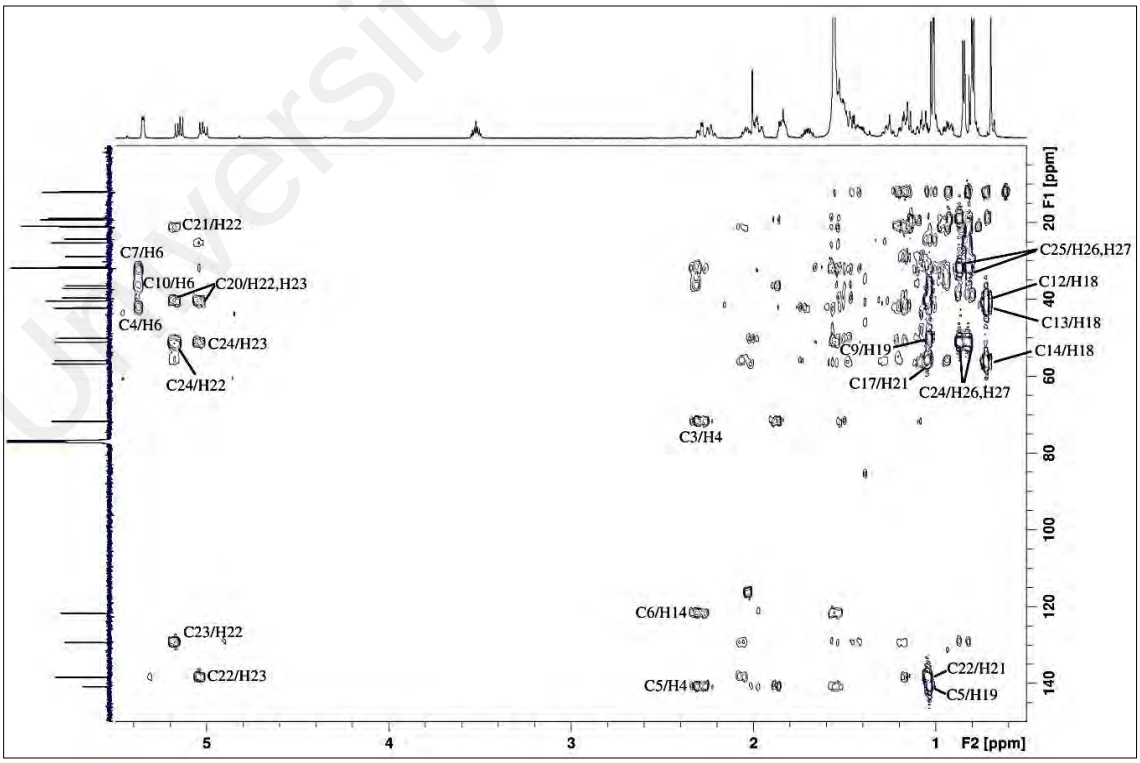


**Figure 3.46**: HMBC spectrum of stigmasterol (**103**)

### 3.8 Compound 104: *β*-sitosterol glycoside

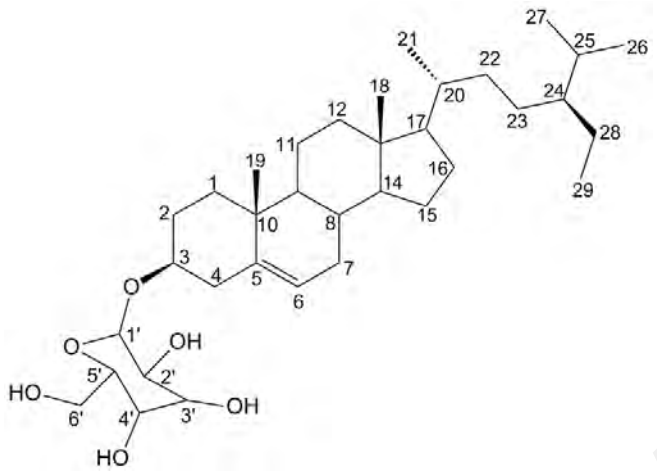


*β*-sitosterol glycoside, **104** was isolated as white amorphous solid and was assigned a molecular formula of $C_{29}H_{49}$ as deduced from its positive LCMS-IT-TOF spectrum ($[M\text{-glucose}]^+$, m/z 397.4; calcd. for $C_{35}H_{60}O_6$, 576.4), consistent with six degrees of unsaturation. The IR spectrum exhibit a strong broad band for hydroxyl (3425 $cm^{-1}$) and medium intensity band for olefinic (1648 $cm^{-1}$) functionalities (Gary et al., 2010).

The $^1$H NMR spectrum (Figure 3.48) indicate the presence of phytosterol which was identified as *β*-sitosterol together with hexose skeleton. It showed six methyls of which two singlet methyls appeared at δ 0.67 (Me-18) and 0.95 (Me-19), three doublet methyls resonated at δ 0.88 (*d*, *J* = 6.4 Hz, Me-26), 0.90 (*d*, *J* = 6.4 Hz, Me-27) and 1.00 (*d*, *J* = 6.4 Hz, Me-21), and one triplet methyl resonated at 0.91 (*t*, *J* = 6.7 Hz, Me-29). An oxymethine and olefinic methine signal were observed resonated at δ 3.97 (*m,* H-3) and δ 5.36 (*dd*, *J* = 4.8, 2.5 Hz, H-6) respectively. The sugar skeleton was identified by an anomeric proton resonated at δ 5.05 (*d*, *J* = 7.7 Hz, H-1'), an indication of a *trans* diaxial configuration of *β*-D-glucose unit (Faizi et al., 2001).

The $^{13}$C NMR (Figure 3.49), DEPT (Figure 3.50) and HSQC experiments of *β*-sitosterol glycoside, **104** revealed the presence of thirty five carbon signal, among which six methyls resonated at δ 11.8 (C-18), 11.9 (C-29), 18.8 (C-21), 19.0 (C-26),

19.2 (C-19) and 19.8 (C-27), one oxymethine at δ 78.4 (C-3) and one olefinic moiety at δ 140.7 (C-5) and 121.7 (C-6) were spotted. An anomeric carbon for the *β*-D-glucose was observed resonated at δ 102.4 (C-1') together with its remaining signals at δ 62.6 (C-6'), 71.5 (C-4'), 75.1 (C-2'), 77.9 (C-3') and 78.2 (C-5').

Through the COSY experiment (Figures 3.47 and 3.51), an oxymethine was confirmed at H-3 (δ 3.97, *m*) position from correlation with an anomeric carbon, H-1' (δ 5.05, *d*, *J* = 7.7 Hz), H-2 and H-4. Another correlation observed were H-2 with H-1, H-6 with H-7 and H-25 with both H-26 and H-27.

The HMBC experiment (Figures 3.47 and 3.52) supported that Me-18 (δ 0.67, *s*) and Me-19 (δ 0.95, *s*) were two methyls that fused between rings, were built from basis correlation with C-12 (δ 39.6), C-13 (δ 42.3), C-17 (δ 56.0) and C-5 (δ 140.7), C-9 (δ 50.1), C-10 (δ 36.7), respectively. The formation of geminal methyl between Me-26 (δ 0.88, *d*, *J* = 6.4 Hz) and Me-27 (δ 0.90, *d*, *J* = 6.4 Hz) were deduced from cross correlation between them with C-24 (δ 45.8) and C-25 (δ 29.3). An olefinic moiety was confirmed at C5(6) positions on interactions between C-5 (δ 140.7) with H-1, H-4 and H-19 while H-6 (δ 5.36, *dd*, *J* = 4.8, 2.5 Hz) with C-8 and C-10. Through depth analysis of this experiment, it was suggested that the glucose structure was bonded to C-3 positions from basis correlations between anomeric carbon, C-1' (δ 102.4) with H-3 (δ 3.97, *m*). Others correlations observed from the sugar moiety were H-2' with C-1', C-3'; H-4' with C-2', C-5' and C-5' with H-6'.

All the combined spectal analysis of 1D and 2D NMR spectra (Table 3.9) suggested that (**104**) was *β*-sitosterol glycoside or trivially named as daucosterol (Paulo et al., 2000).

**Table 3.9**: $^{1}H$ (400 MHz) and $^{13}C$ (100 MHz) NMR data of *β*-sitosterol glycoside (**104**) in $C_5D_5N$

| Position | Compound **104** | | (Paulo et al., 2000) | |
|---|---|---|---|---|
| | $\delta_H$ (ppm), *J* (*Hz*) | $\delta_C$ (ppm) | $\delta_H$ (ppm), *J* (*Hz*) | $\delta_C$ (ppm) |
| 1 | 0.98, *m*<br>1.71, *m* | 37.3 | 0.95, *m*<br>1.70, *m* | 38.4 |
| 2 | 1.77, *m*<br>2.14, *m* | 30.0 | 1.76, *m*<br>2.14, *m* | 31.1 |
| 3 | 3.97, *m* | 78.4 | 3.94, *m* | 79.0 |
| 4 | 2.48, *m*<br>2.75, *m* | 39.1 | 2.48, *dt* (24.1, 3.0, 2.0)<br>2.73, *ddd* (13.0, 4.4, 1.9) | 40.2 |
| 5 | - | 140.7 | - | 141.8 |
| 6 | 5.36, *dd* (4.8, 2.5) | 121.7 | 5.35, *d* (5.1) | 122.8 |
| 7 | 1.55, *m*<br>1.89, *m* | 31.8 | 1.52, *m*<br>1.89, *m* | 33.1 |
| 8 | 1.37, *m* | 32.0 | 1.37, *m* | 32.9 |
| 9 | 0.89, *m* | 50.1 | 0.90, *m* | 51.2 |
| 10 | - | 36.7 | - | 37.8 |
| 11 | 1.43, *m* | 21.1 | 1.06, *m* | 22.2 |
| 12 | 1.13, *m*<br>1.99, *m* | 39.6 | 1.11, *m*<br>1.97, *m* | 40.8 |
| 13 | - | 42.3 | - | 43.4 |
| 14 | 0.91, *m* | 56.6 | 0.91, *m* | 57.7 |
| 15 | 1.30, *m* | 24.3 | 1.03, *m*<br>1.54, *m* | 24.3 |
| 16 | 1.25, *m*<br>1.84, *m* | 28.3 | 1.24, *m*<br>1.83, *m* | 29.4 |
| 17 | 1.10, *m* | 56.0 | 1.08, *m* | 57.1 |
| 18 | 0.67, *s* | 11.8 | 0.65, *s* | 12.9 |
| 19 | 0.95, *s* | 19.2 | 0.93, *s* | 20.3 |
| 20 | 1.37, *m* | 36.2 | 1.40, *m* | 37.3 |
| 21 | 1.00, *d* (6.4) | 18.8 | 0.98, *d* (6.5) | 19.9 |
| 22 | 1.10, *m*<br>1.40, *m* | 34.0 | 1.07, *m*<br>1.39, *m* | 35.1 |
| 23 | 1.26, *m* | 26.2 | 1.24, *m* | 27.2 |
| 24 | 1.01, *m* | 45.8 | 0.95, *m* | 46.9 |
| 25 | 1.69, *m* | 29.3 | 1.68, *m* | 30.3 |
| 26 | 0.88, *d* (6.4) | 19.0 | 0.84, *s* | 20.1 |
| 27 | 0.90, *d* (6.4) | 19.8 | 0.86, *d* (0.5) | 20.9 |
| 28 | 1.05, *m*<br>1.52, *m* | 23.2 | 1.27, *m* | 25.4 |
| 29 | 0.91, *t* (6.7) | 11.9 | 0.88, *d* (2.1) | 13.1 |
| 1' | 5.05, *d* (7.7) | 102.4 | 5.05, *d* (7.7) | 103.4 |
| 2' | 4.08, *dd* (8.2, 8.0) | 75.1 | 4.06, *dd* (8.3, 8.2) | 76.2 |
| 3' | 4.31, *m* | 77.9 | 4.29, *m* | 79.5 |
| 4' | 4.29, *m* | 71.5 | 4.29, *m* | 72.5 |
| 5' | 4.01, *m* | 78.2 | 3.99, *m* | 79.4 |
| 6' | 4.44, *ddd* (11.7, 5.2, 2.0)<br>4.59, *dd* (11.7, 2.0) | 62.6 | 4.40, *dd* (11.8, 5.3)<br>4.56, *dd* (11.8, 2.4) | 63.7 |

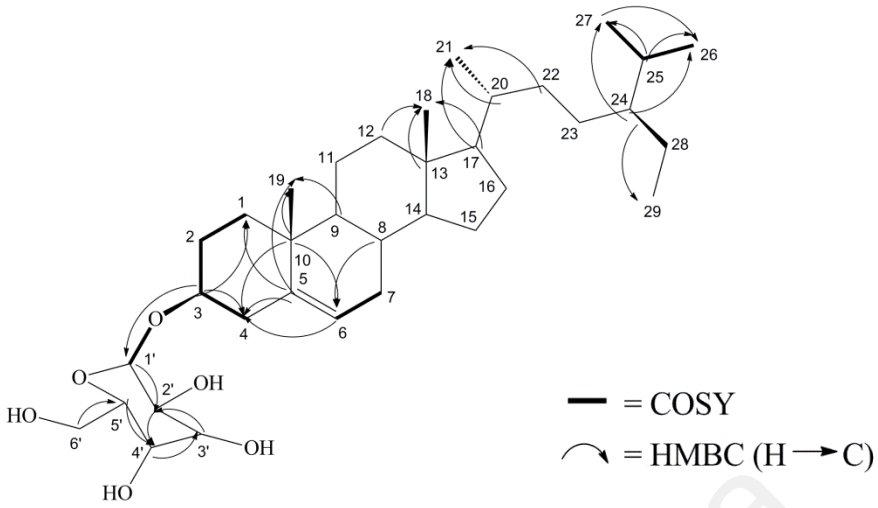


**Figure 3.47**: Selected COSY and HMBC correlations of *β*-sitosterol glycoside (**104**)

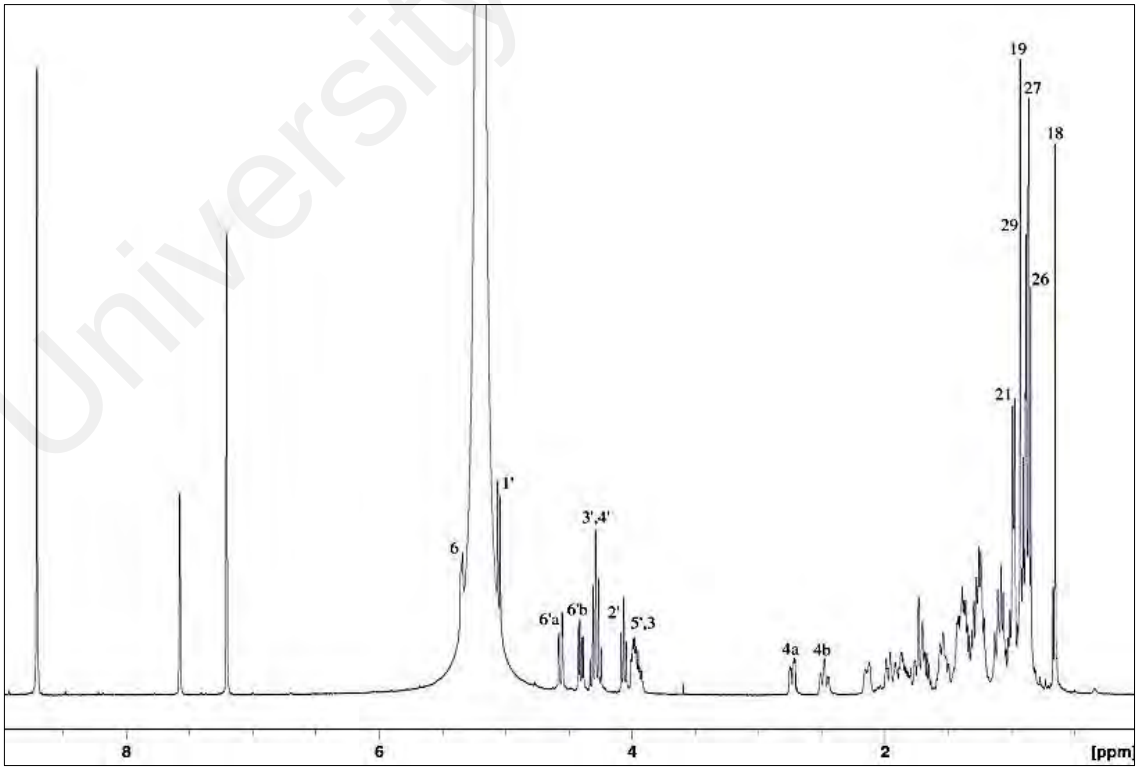


**Figure 3.48** : $^{1}$H (400 MHz) NMR spectrum of *β*-sitosterol glycoside (**104**)

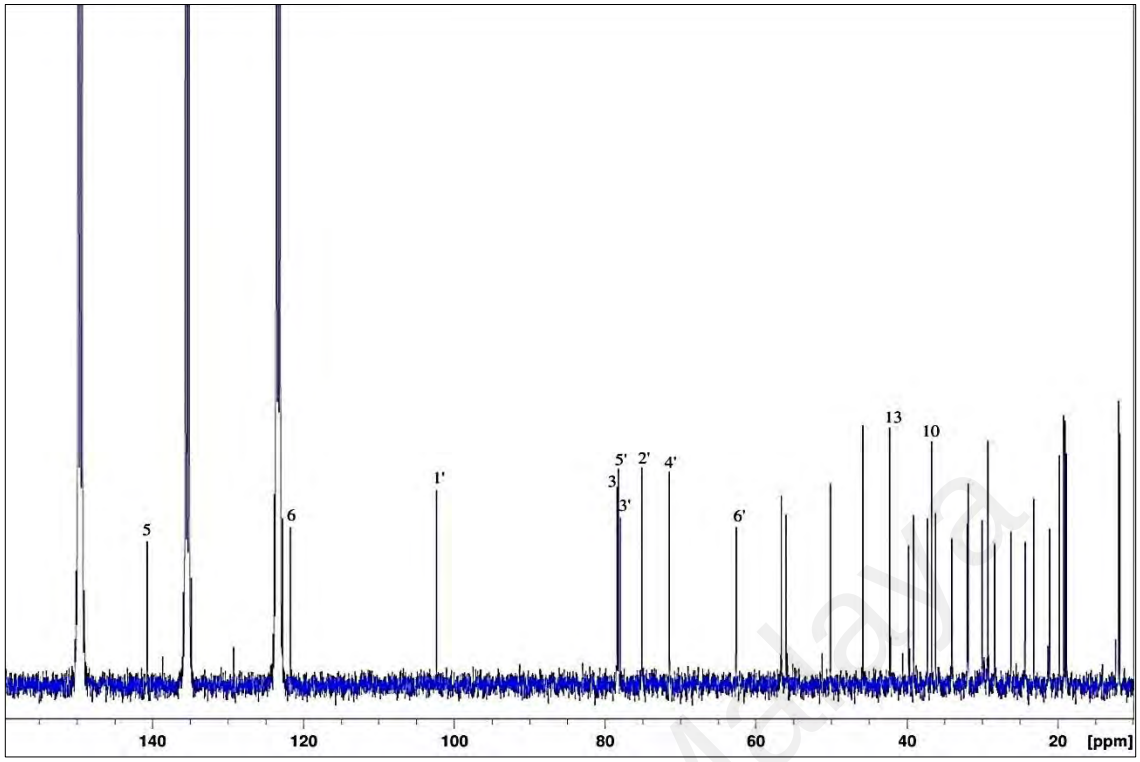


**Figure 3.49**: $^{13}C$ (100 MHz) NMR spectrum of $\beta$-sitosterol glycoside (**104**)

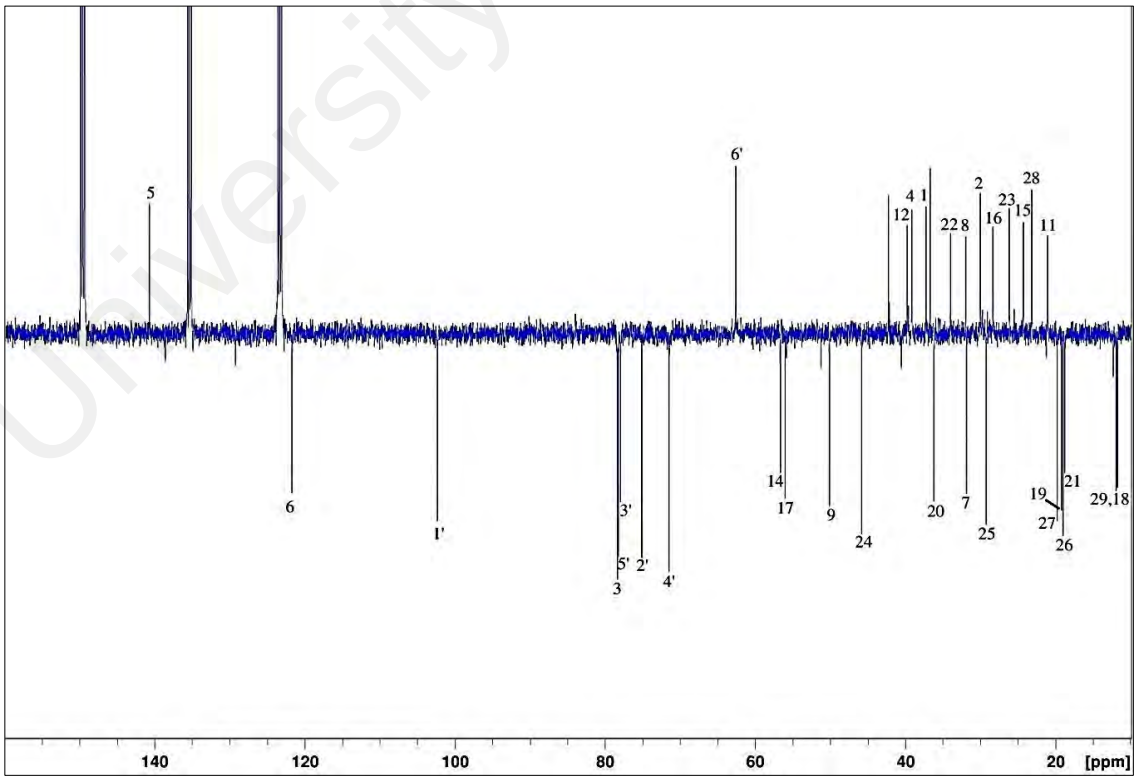


**Figure 3.50**: DEPT-135 spectrum of $\beta$-sitosterol glycoside (**104**)

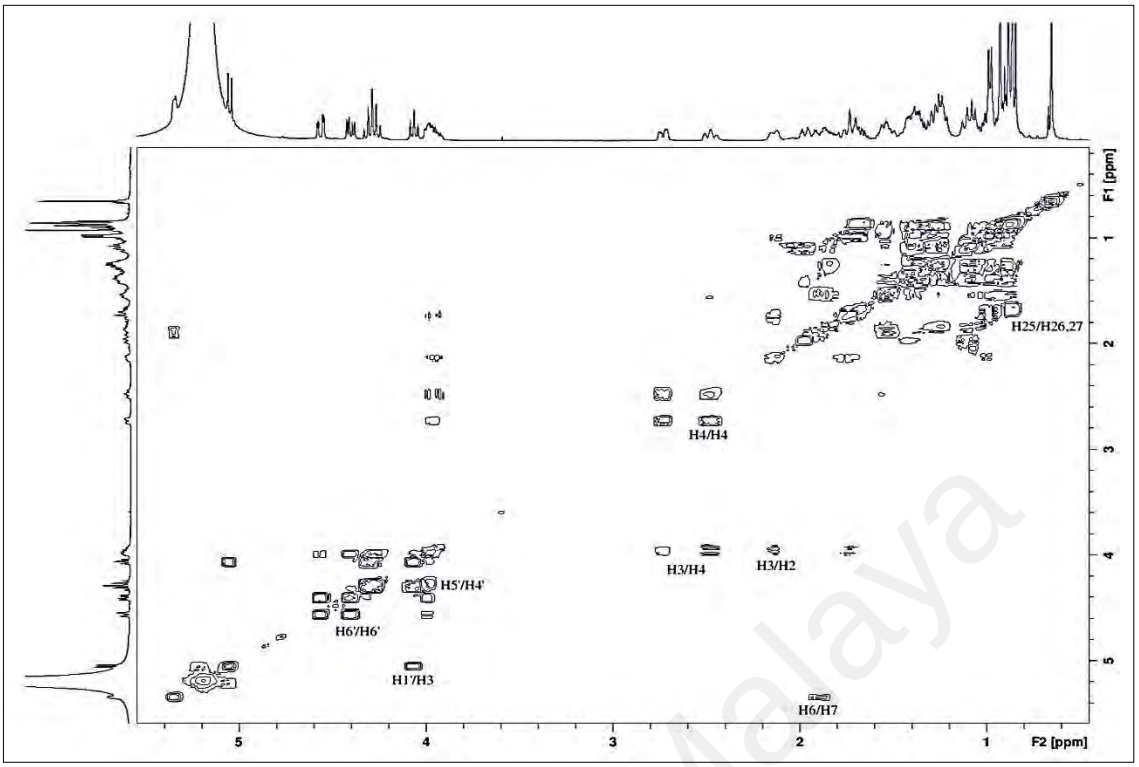


**Figure 3.51**: COSY spectrum of *β*-sitosterol glycoside (**104**)

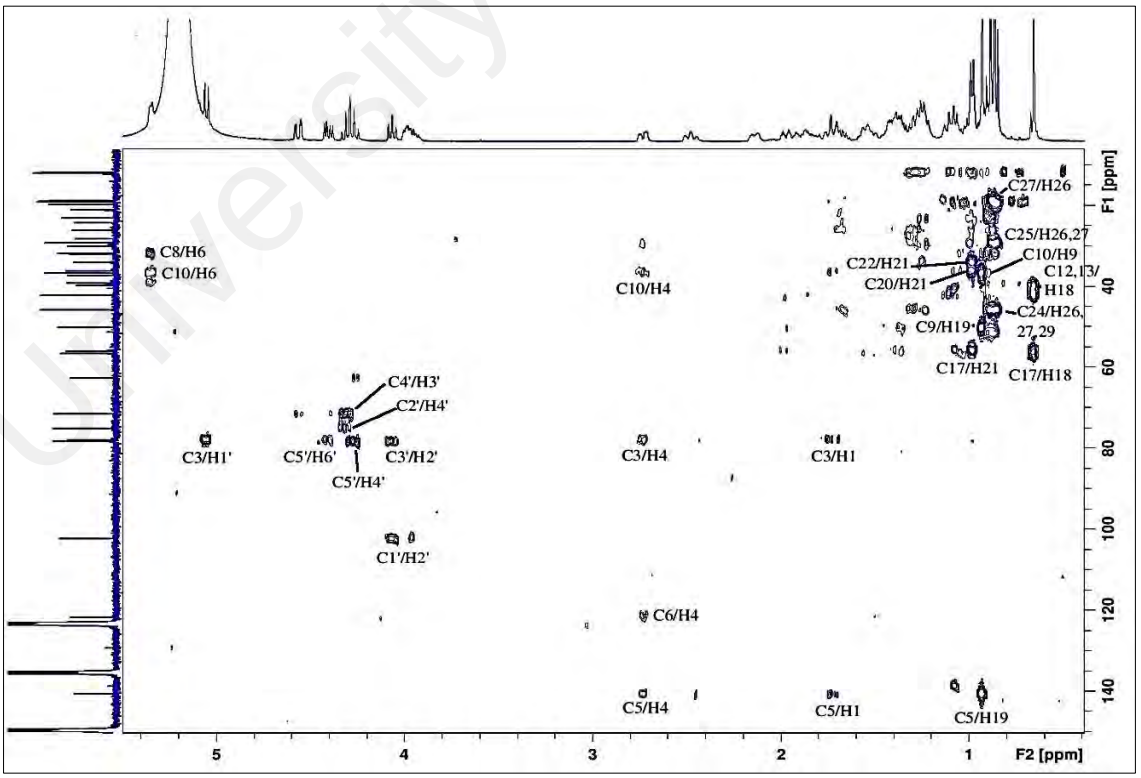


**Figure 3.52**: HMBC spectrum of *β*-sitosterol glycoside (**104**)

## 3.9 Compound 105: 4-hydroxy-3-methoxybenzoic acid

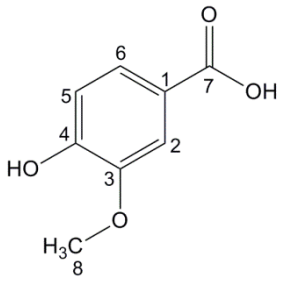


4-hydroxy-3-methoxybenzoic acid, **105** was afforded as white amorphous solid. Its molecular formula was determined as $C_8H_8O_4$ by HR-ESI-MS, which provided a molecular ion peak at m/z 167.09 $[M-H]^-$ (calcd. for $C_8H_9O_4$, 169.0501) corresponding to four degree of unsaturation. The IR spectrum showed a strong absorption band of hydroxyl (3436 $cm^{-1}$), C=C aromatic group (1674 and 1433 $cm^{-1}$) and C-O stretch (1288 $cm^{-1}$) functionalities (Gary et al., 2010).

The $^1H$ NMR spectrum (Figure 3.54) showed benzene signals resonated at δ 6.85 (*d*, *J* = 7.7 Hz, H-5) and δ 7.57 (*br s*, H-2 and H-6). A hydroxyl moiety resonated at δ 4.90 (OH-4, *br s*) together with a downfield shifts of methyl protons of δ 3.91 (Me-8) suggested that it is vicinal to a heteroatom group were also spotted.

The $^{13}C$ NMR (Figure 3.55) together with DEPT and HSQC experiments of 4-hydroxy-3-methoxybenzoic acid, **105** showed the presence of total eight carbon signal; three olefinic methine resonated at δ 112.4 (C-2), 114.4 (C-5) and 123.9 (C-6) while other three olefinic quaternary carbons resonated at δ 121.7 (C-1), 147.3 (C-3) and 151.3 (C-4). Two carbon signals belonged to methoxy carbon, C-8 resonated at δ 55.0 and carbonyl carbon at δ 168.8 (C-7) were identified.

Through the COSY experiment (Figures 3.53 and 3.56), only correlation between H-5 (δ 6.85, *d*, *J* = 7.7 Hz) and H-6 (δ 7.57, *br s*) was observed thus suggesting that **105** would have a trisubstituted benzene systems.

From the analysis of HMBC experiment (Figures 3.53 and 3.57), the presence of a carboxyl moiety was suggested at C-7 (δ 168.8) based on correlation with H-2 (δ 7.57, *br s*) and H-6 (δ 7.57, *br s*) while a hydroxyl at C-4 (δ 151.3) position was deduced through interaction with H-5 (δ 6.85, *d*, *J* = 7.7 Hz) and H-6. A methyl bearing oxygen group was suggested lies at C-3 (δ 147.3) position on interrelationship with H-5 and H-6.

Extensive of all the NMR spectra (Table 3.10) suggested that **105** was 4-hydroxy-3-methoxybenzoic acid, trivially name vanillic acid (Gonzalez-Baro et al., 2008).

**Table 3.10**: $^{1}H$ (400 MHz) and $^{13}C$ NMR (100 MHz) data of 4-hydroxy-3-methoxybenzoic acid (**105**) in $CD_3OD$

| Position | Compound **105** | | (Gonzalez-Baro et al., 2008) | |
|---|---|---|---|---|
| | $\delta_H$ (ppm), *J (Hz)* | $\delta_C$ (ppm) | $\delta_H$ (ppm), *J (Hz)* | $\delta_C$ (ppm) |
| 1 | - | 121.7 | - | 121.6 |
| 2 | 7.57, *br s* | 112.4 | 7.44 | 112.7 |
| 3 | - | 147.3 | - | 147.2 |
| 4 | - | 151.3 | - | 151.1 |
| 5 | 6.85, *d* (7.7) | 114.4 | 6.86 | 115.1 |
| 6 | 7.57, *br s* | 123.9 | 7.44 | 123.5 |
| 7 | - | 168.8 | 12.47 | 167.3 |
| 8 | 3.91, *s* | 55.0 | 3.92 | 55.6 |
| OH-4 | 4.90, br s | - | 9.82 | - |

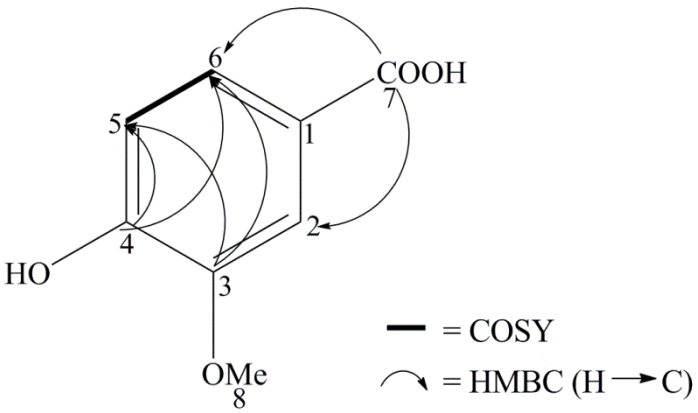


**Figure 3.53**: Selected COSY and HMBC correlations of 4-hydroxy-3-methoxybenzoic acid (**105**)

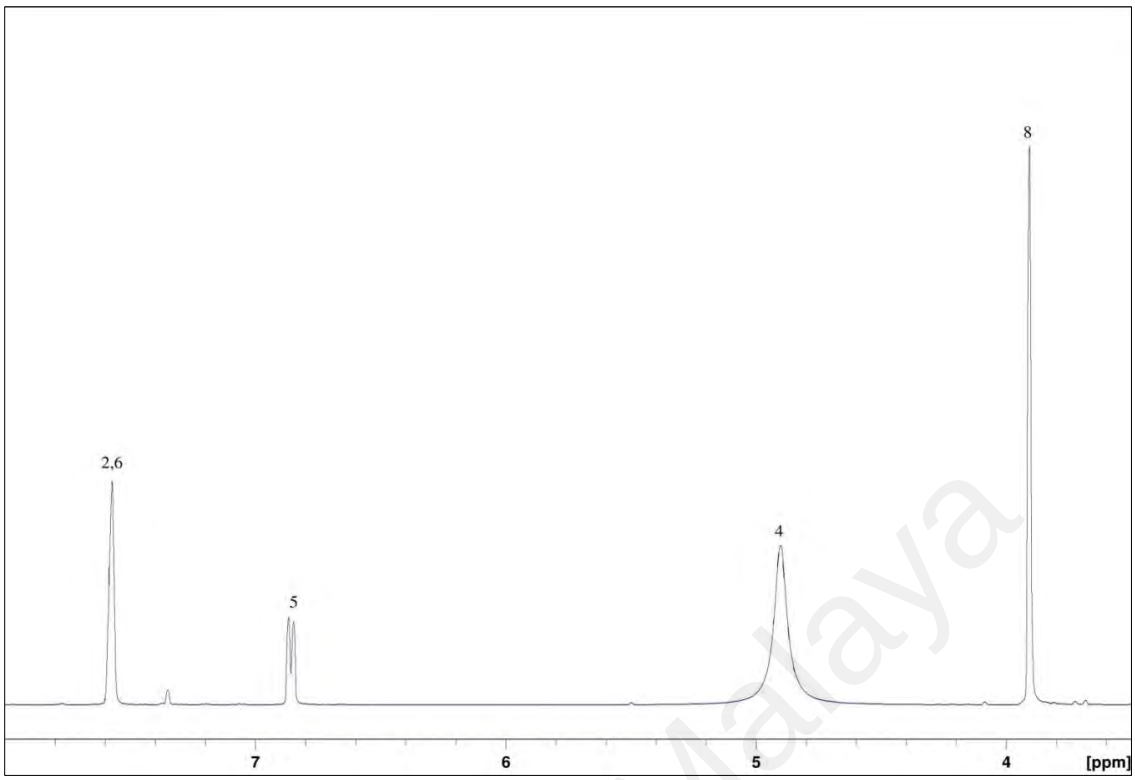


**Figure 3.54**: $^{1}H$ (400 MHz) NMR spectrum of 4-hydroxy-3-methoxybenzoic acid (**105**)

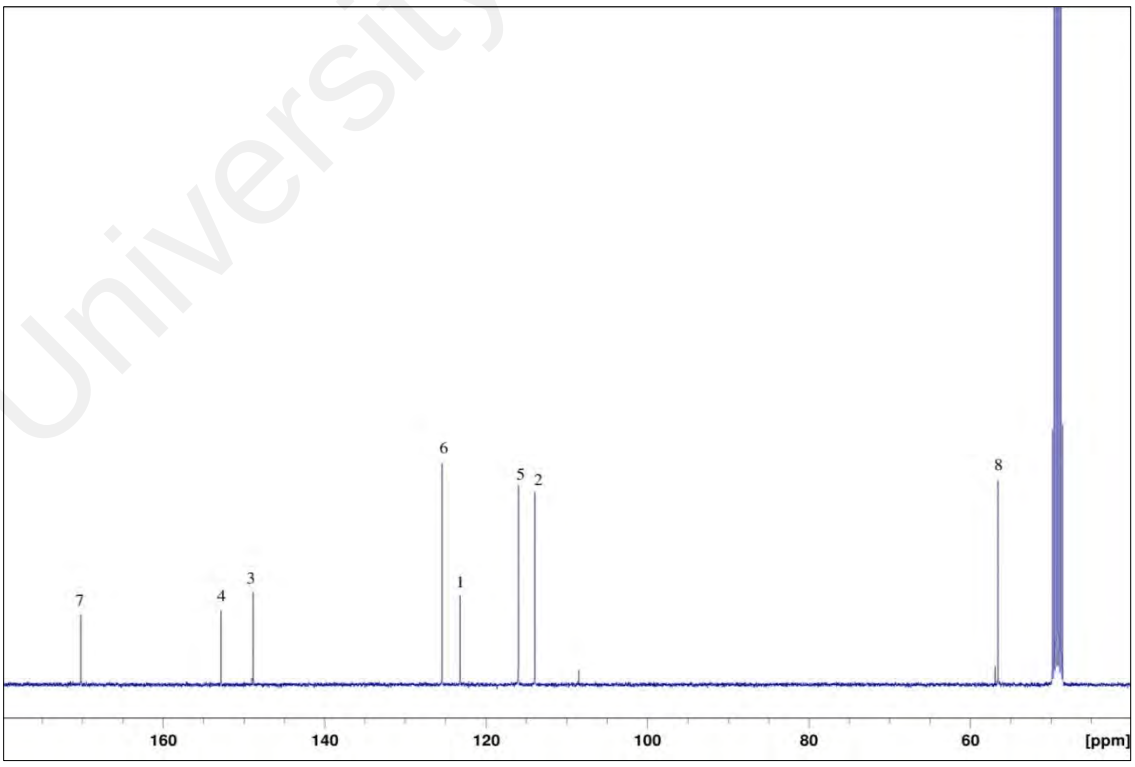


**Figure 3.55**: $^{13}C$ (100 MHz) NMR spectrum of 4-hydroxy-3-methoxybenzoic acid (**105**)

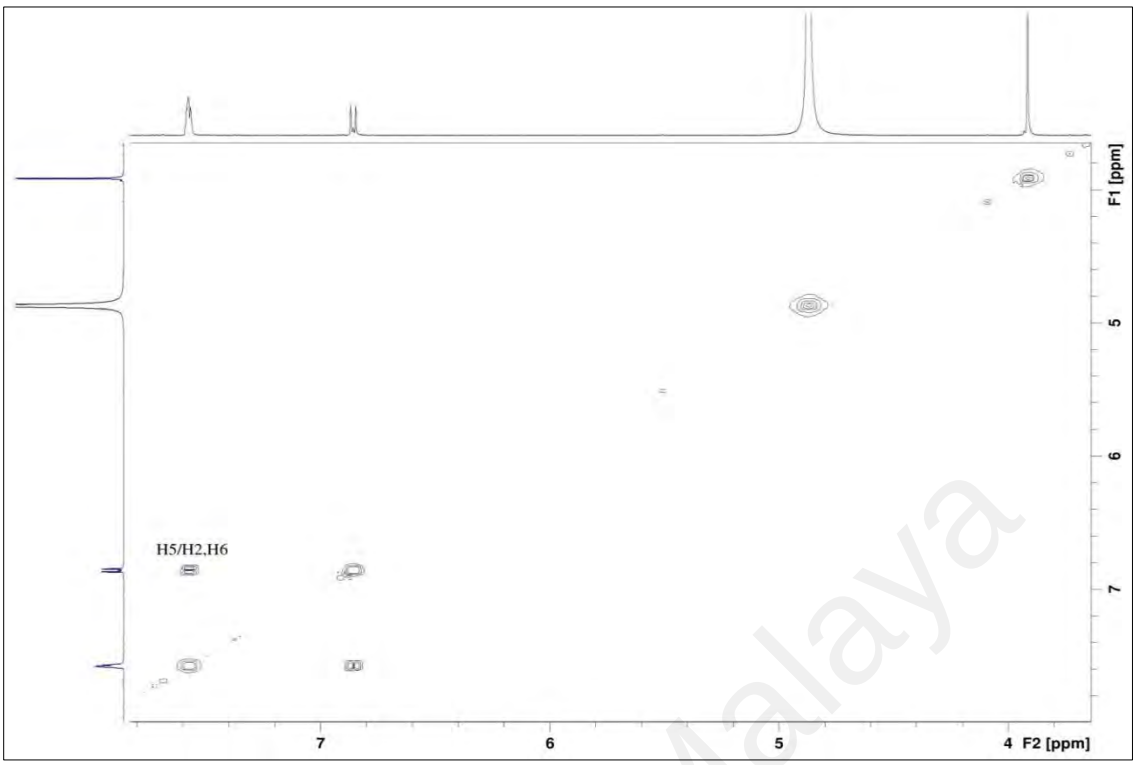


**Figure 3.56**: COSY spectrum of 4-hydroxy-3-methoxybenzoic acid (**105**)

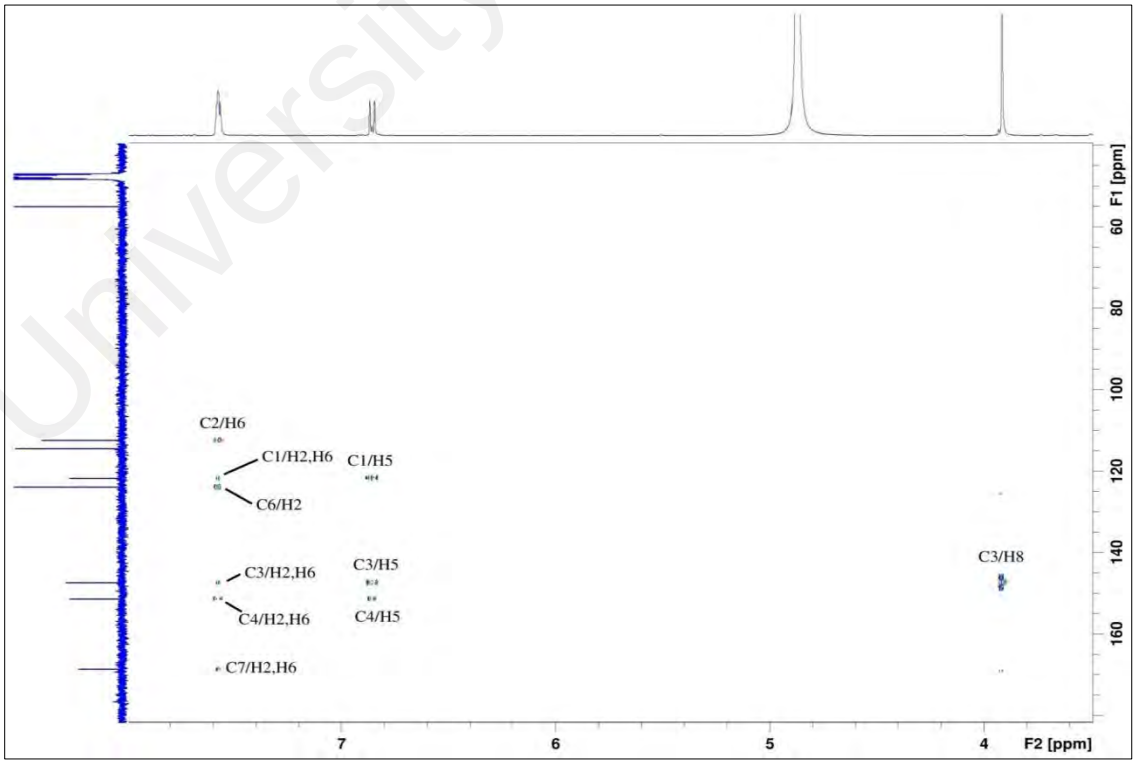


**Figure 3.57**: HMBC spectrum of 4-hydroxy-3-methoxybenzoic acid (**105**)

### 3.10 Compound 106: 4-hydroxy-4,8-dimethyl-1-tetralone

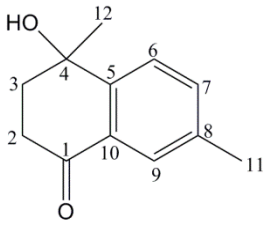


4-hydroxy-4,8-dimethyl-1-tetralone, **106** was isolated as yellowish oil. The HR-ESI-MS revealed a quasi-molecular ion peak $[M+H]^+$ at m/z 191.1132 (calcd. for $C_{12}H_{15}O_2$, 191.1072), thus **106** suggested to possess a molecular formula of $C_{12}H_{14}O_2$ and five degree of unsaturation. The IR spectrum showed a broad band of hydroxyl group (3402 $cm^{-1}$), a strong band at of $sp^2$ C-H stretch (2935 $cm^{-1}$) and a medium band of C=O carbonyl stretch (1702 $cm^{-1}$) (Gary et al., 2010).

The $^1H$ NMR spectrum (Figure 3.59) revealed the presence of three different signals type resonated at δ 7.43 (*dd*, *J* = 8.0, 1.6 Hz, H-7), 7.60 (*d*, 8.0 Hz, H-6) and 7.81 (*s*, H-9), suggesting that the system would be a trisubtituted benzene ring. The unusual downfield shifts of methyl signals at δ 2.38 (*s*, Me-11) was observed. The non-equivalent methylene signals at δ 2.69 (*ddd*, *J* = 9.6, 9.2, 7.2 Hz, H-2a) and 2.87 (*dt*, *J* = 10.8, 5.2 Hz, H-2b) indicating that it is near to an electron withdrawing group.

The $^{13}C$ NMR (Figure 3.60) coupled with DEPT (Figure 3.61) and HSQC experiments of 4-hydroxy-4,8-dimethyl-1-tetralone, **106** spotted the presence of total twelve carbon signals; three olefinic methine resonated at δ 125.2 (C-6), 127.2 (C-9) and 135.2 (C-7) with three olefinic quaternary carbon resonated at δ 130.4 (C-10), 137.8 (C-8) and 146.6 (C-5). Other two carbon signals belonged to a quaternary oxygenated carbon at δ 70.2 (C-4) and a carbonyl carbon resonated at δ 197.5 (C-1) were observed.

Through the COSY experiment (Figure 3.58 and 3.62), it was observed that H-2 (δ 2.69, *ddd*, *J* = 9.6, 9.2, 7.2 Hz and δ 2.87, *dt*, *J* = 10.8, 5.2 Hz) correlated with H-3 (δ

2.27, *m*) while H-6 (δ 7.60, *d*, *J* = 8.0 Hz) correlated with H-7 (δ 7.43, *dd*, *J* = 8.0, 1.6 Hz).

The in depth analysis of HMBC experiment (Figure 3.58 and 3.63) supported that two cyclic systems were joined through correlation between H-6 with C-4 (δ 70.2) and C-10 (δ 130.4), H-9 (δ 7.81, *s*) with C-1 (δ 197.5) and C-5 (δ 146.6), and C-5 with H-7 and H-3 (δ 2.27, *m*). A carbonyl moiety was observed at C-1 (δ 197.5) position from interrelationship with H-2, H-3 and H-9. Careful analysis suggested that both methyls were located at Me-11(12) position from correlation of Me-11 (δ 2.38, *s)* with C-7 (δ 135.2), C-8 (δ 137.8) and C-9 (δ 127.2) while Me-12 (δ 1.63, *s)* appeared as geminal of hydroxyl group through correlation with C-2 (δ 35.9), C-3 (δ 38.4), C-4, and C-5.

Detailed analysis of 1D and 2D NMR spectra (Table 3.11) suggested that **106** was 4-hydroxy-4,8-dimethyl-1-tetralone (Achenbach & Schwinn, 1995).

**Table 3.11**: $^{1}H$ (400 MHz) and $^{13}C$ (100 MHz) NMR data of 4-hydroxy-4,8-dimethyl-1-tetralone (**106**) in $CDCl_3$

| Position | Compound **106** | | (Achenbach & Schwinn, 1995) | |
|---|---|---|---|---|
| | $\delta_H$ (ppm), *J (Hz)* | $\delta_C$ (ppm) | $\delta_H$ (ppm), *J (Hz)* | $\delta_C$ (ppm) |
| 1 | - | 197.5 | - | 197.4 |
| 2 | 2.69, *ddd* (9.6, 9.2, 7.2)<br>2.87, *dt* (10.8, 5.2) | 35.9 | 2.69, *ddd* (18.0, 9.0, 7.0)<br>2.88, *dt* (18.0, 5.5) | 35.8 |
| 3 | 2.27, *m* | 38.4 | 2.28, *m* | 38.3 |
| 4 | 3.64, *br s* | 70.2 | - | 70.0 |
| 5 | - | 146.6 | - | 146.6 |
| 6 | 7.60, *d* (8.0) | 125.2 | 7.60, *d* (8.0) | 127.0 |
| 7 | 7.43, *dd* (8.0, 1.6) | 135.2 | 7.43, *dd* (8.0, 2.0) | 135.1 |
| 8 | - | 137.8 | - | 137.6 |
| 9 | 7.81, *s* | 127.2 | 7.81, *d* (2.0) | 125.0 |
| 10 | - | 130.4 | - | 130.2 |
| 11 | 2.38, *s* | 21.0 | 2.38, *s* | 20.8 |
| 12 | 1.63, *s* | 29.1 | 1.62, *s* | 28.9 |

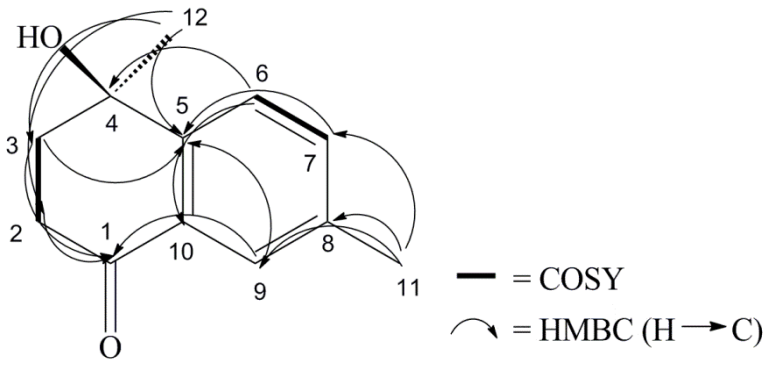


**Figure 3.58**: Selected COSY and HMBC correlations of 4-hydroxy-4,8-dimethyl-1-tetralone (**106**)



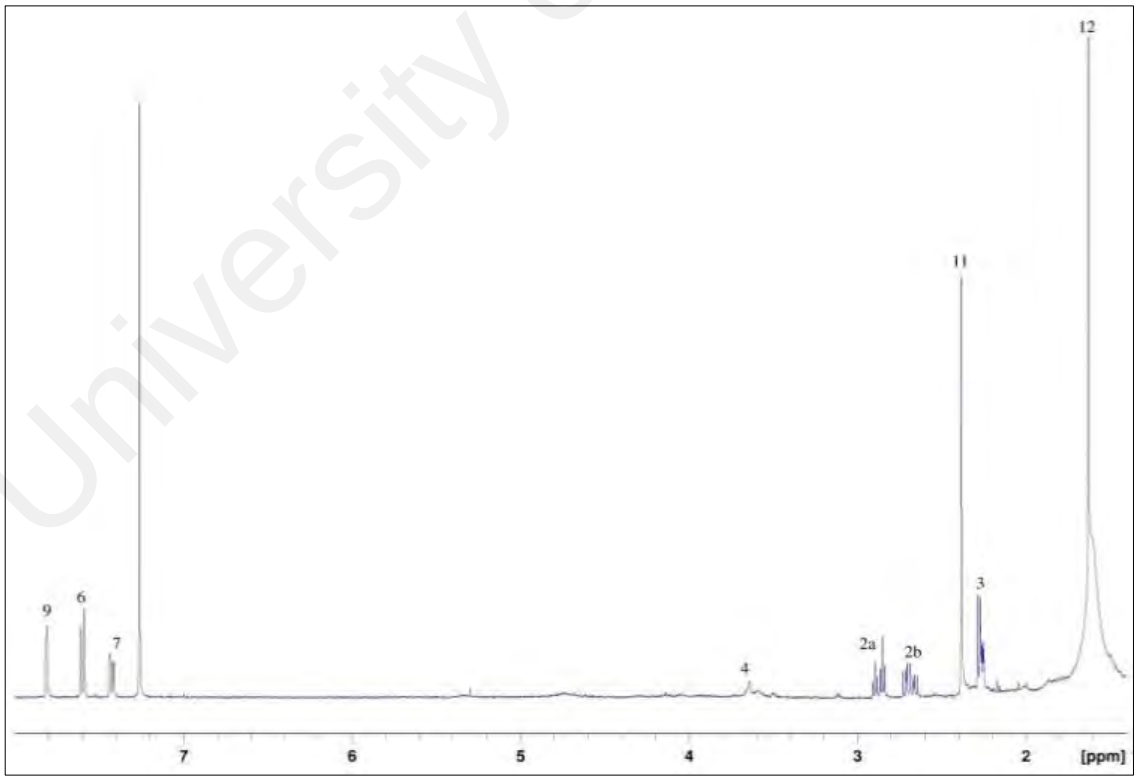


**Figure 3.59**: $^{1}H$ (400 MHz) NMR spectrum of 4-hydroxy-4,8-dimethyl-1-tetralone (**106**)

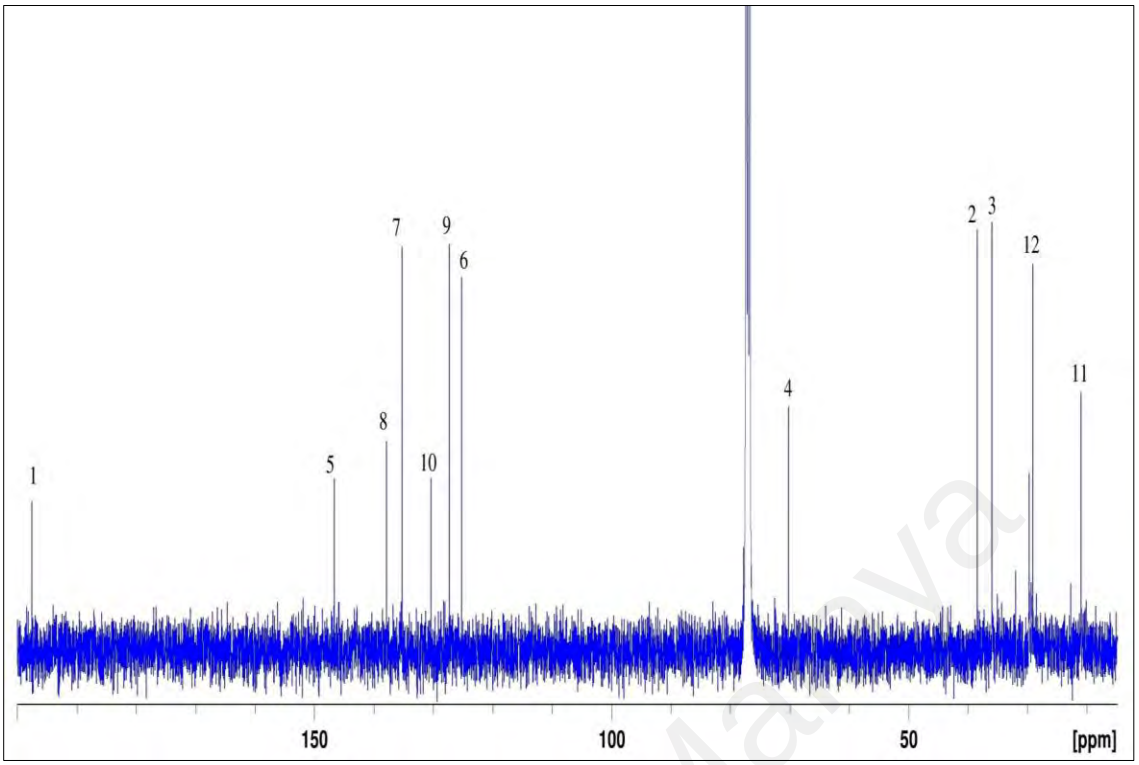


**Figure 3.60**: $^{13}C$ (100 MHz) NMR spectrum of 4-hydroxy-4,8-dimethyl-1-tetralone (**106**)

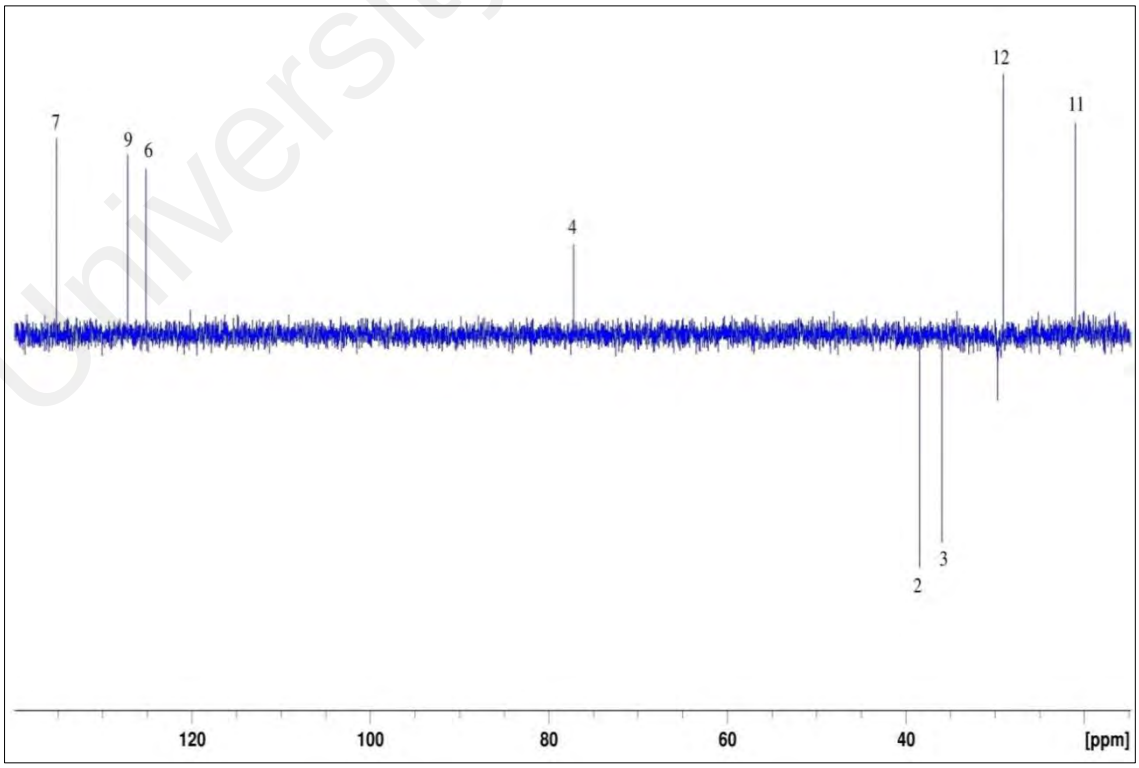


**Figure 3.61**: DEPT-135 spectrum of 4-hydroxy-4,8-dimethyl-1-tetralone (**106**)

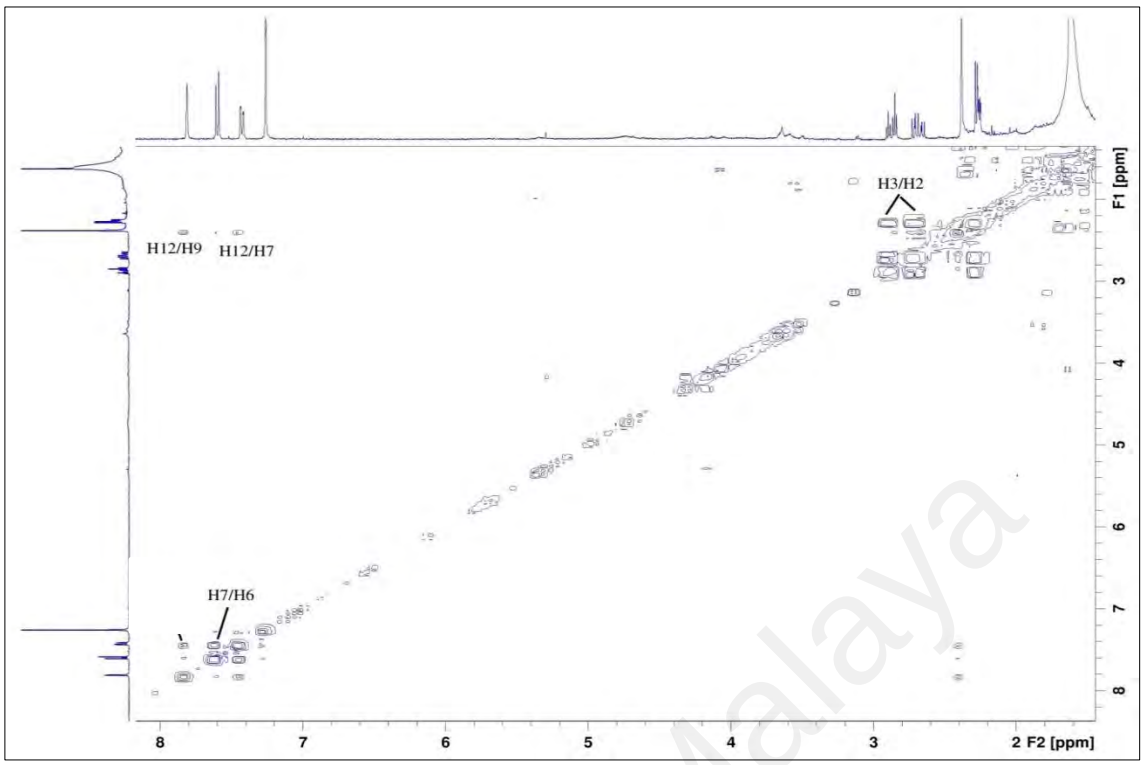


**Figure 3.62**: COSY spectrum of 4-hydroxy-4,8-dimethyl-1-tetralone (**106**)

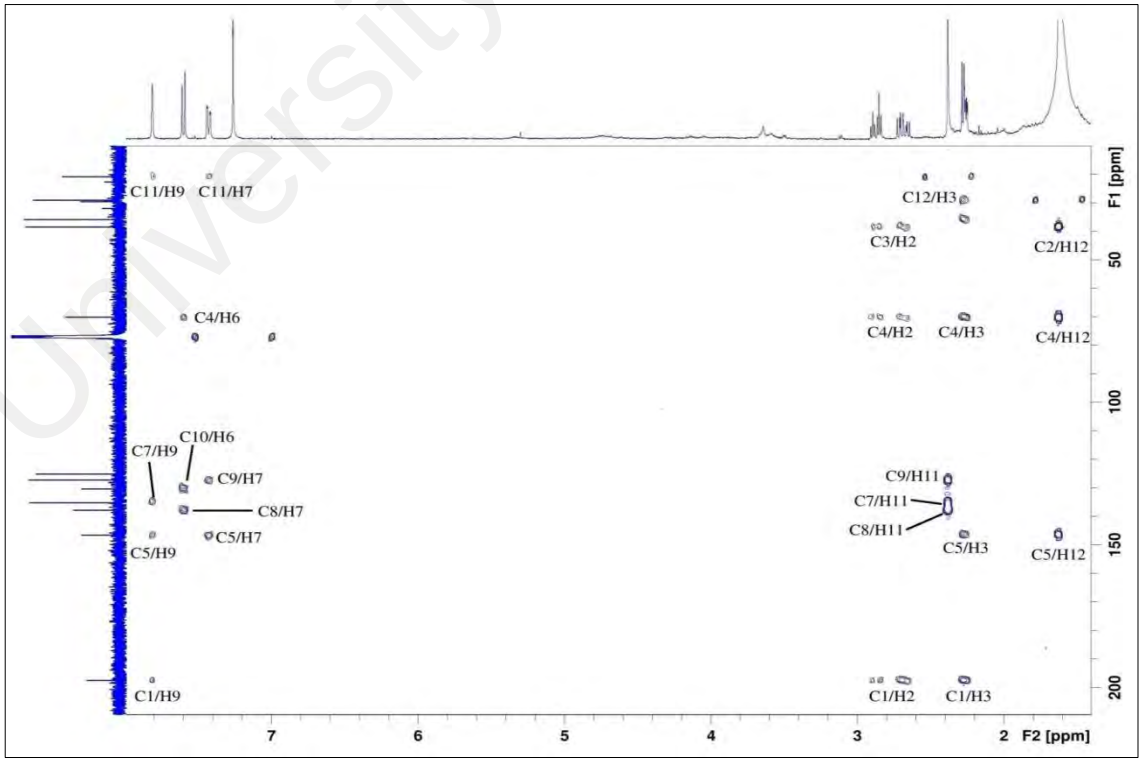


**Figure 3.63**: HMBC spectrum of 4-hydroxy-4,8-dimethyl-1-tetralone (**106**)

### 3.11 Cytotoxic activities

Cancer starts in cells which are the building blocks of the body. Each cells will grow and replaced continuously as its dies. Somehow, this cycle went wrong where new cell grow even when the body does not need them and an old cell does not die as they should. These extra cells can form a tumor.

Cell viability and cytotoxic assays are used to measures the effect of drug/chemicals on the basis of the functions of cells by assessing the cellular damage (Kar & Sivamani, 2015). Cytotoxic activities of compounds **97** and **98** were evaluated against four different cancer cell lines; liver (Hep3b and HepG2), ovary (SK-OV-3), breast (MCF-7), leukemia (Kasumi-1) and the human normal lung fibroblast cell (MRC-5).

Compound **97** showed good cytotoxicity against Kasumi-1 cell line with $IC_{50}$ observed at 2.11 ± 0.48. The compound also exhibited moderate activity towards MCF-7 and weak activity against SK-OV-3 cell lines which $IC_{50}$ observed were 8.85 ± 1.36 and 14.35 ± 0.78 respectively (Table 3.12).

Compound **98** exhibited good cytotoxicity activities against both Hep3b and HepG2 cell lines, with $IC_{50}$ values at 2.28 ± 0.00 and 4.00 ± 0.63 respectively. The compound also showed weak activities towards SK-OV-3 and MCF-7 cancer cell lines with $IC_{50}$ values of 14.95 ± 0.60 and 18.18 ± 1.83 respectively (Table 3.12).

From the SI values, compound **97** was selective towards MCF-7 cancer cell line (SI = 3.08) while compound **98** were selective towards both HepG2 and Hep3b cancer cell line respectively (SI = 5.02 and 8.81).

Due to their high selectivity and abundance; both compounds **97** and **98**, suggested could be a good candidate as lead compounds in inducing apoptosis towards leukemia and liver cancer.

**Table 3.12**: $IC_{50}$ and SI value for selected compounds on various type of cancer cell line in 72h treatment. The data are expressed as mean ± SD from at least 3 independent experiments.

| Cell lines | 3-oxo-lup-20(29)-en-28-oic acid (**97**) | | 3β-hydroxy-5-glutinen-28-oic acid (**98**) | |
|---|---|---|---|---|
| | $IC_{50}$ value (µg/mL) | SI | $IC_{50}$ value (µg/mL) | SI |
| HepG2 | nd | nd | 4.00 ± 0.63 | 5.02 |
| Hep3b | nd | nd | 2.28 ± 0.00 | 8.81 |
| SK-OV-3 | 14.35 ± 0.78 | 1.90 | 14.95 ± 0.60 | 1.34 |
| MCF-7 | 8.85 ± 1.36 | 3.08 | 18.28 ± 1.83 | 1.10 |
| Kasumi-1 | 2.11 ± 0.48 | nd | nd | nd |
| MRC-5 | 27.23 ± 5.04 | 1.00 | 20.09 ± 1.33 | 1.00 |

# CHAPTER 4: CONCLUSION

The chemistry of the Meliaceae family has attracted great interest to many scientists with the isolations of structurally interesting and bioactive limonoids and terpenoids. However, the phytochemical studies on the genus *Walsura* continues to fall behind with other more popular genera such as *Azadirachta, Aglaia, Dysoxylum* and *Chisocheton* over the years. To date, only eight *Walsura* species have been chemically investigated. The phytochemical investigation in this research has proven that the *Walsura* genus was equally important in producing interesting compounds, structurally and biologically.

The phytochemical study on the dichloromethane extract of the barks of *W. pinnata* Hassk species have led to isolation of ten pure compounds including five triterpenoids (**97-101**), one sesquiterpenoid (**102**), two sterols (**103,104**) and two aromatic derivatives (**105, 106**). Oleanane triterpenoid, **100** with conjugated diene structure was previously unreported compound and compounds **99, 101, 102** and **104** were first time reported in this *Walsura* genus. The detailed spectroscopic discussions on each of the isolated compounds were presented in Chapter 3.

Further cytotoxic activities of compound **97** and **98** were measured *in vitro* against four cancer cell lines; liver (Hep3b and HepG2), ovary (SK-OV-3), breast (MCF-7), and leukemia (Kasumi-1). Compound **97** showed good cytotoxicity against leukemia, Kasumi-1 cell line with $IC_{50}$ value observed was 2.11 ± 0.48 µg/mL while compound **98** exhibited good cytotoxicity activities against both liver cancer cell line, Hep3b ($IC_{50}$: 2.28 ± 0.00 µg/mL , SI = 8.81) and HepG2 ($IC_{50}$: 4.00 ± 0.63 µg/Ml, SI = 5.02). The details on the cytotoxic activities were briefly described in Chapter 5.

In this study, the isolation of new compound (**100**) has contributed to the library of natural products and the bioactive triterpenoids, compounds **97** and **98** can be used as lead compounds in the development of anti-cancer therapeutic agents.

# CHAPTER 5: EXPERIMENTAL

## 5.1 Plant materials

The plant materials of *Walsura pinnata* were collected at 243 km, from Gua Musang, Kelantan to Kuala Lipis, Pahang. The sample was identified by Tarelli. O. and Din. M. N. with the voucher specimen KL 4571 and was deposited at the Herbarium of Chemistry Department, Faculty of Science, University of Malaya.

## 5.2 Instrumentations

The 1-D and 2-D NMR were recorded on BRUKER Avance II NMR spectrometers (400 or 600 MHz for $^{1}H$ and 100 or 150 MHz for $^{13}C$). The deuterated NMR solvents used are as in Table 5.1:

**Table 5.1**: NMR shifts of selected deuterated solvents

| **Solvents** | **Chemical formula** | **$^{1}H$ shift(s) in ppm (*multiplicity*)** | **$^{13}C$ shift(s) in ppm (*multiplicity*)** | **Peak for trace of water (ppm)** |
|---|---|---|---|---|
| Chloroform | $CDCl_3$ | 7.26 (*1*) | 77.00 (*3*) | 1.5 |
| Methanol | $CD_3OD$ | 3.30 (*5*) | 49.05 (*7*) | 4.8 |
| Pyridine | $C_5D_5N$ | 7.20 (*1*), 7.56 (*1*), 8.71 (*1*) | 123.44 (*3*) 135.51 (*3*) 179.68 (*3*) | 5.0 |

The ESIMS and LCMS-IT-TOF spectra were obtained on an Agilent 6530 Accurate-Mass Q-TOF ESI LC/MS with ZORBAX Eclipse XDB-C18 Rapid Resolution HT (4.6 mm i.d x 50 mm x 1.8 μm column).

Ultraviolet absorption spectra were obtained using Shimadzu UV-250 Ultraviolet-Visible Spectrometer. Spectroscopic grade of both methanol and acetonitrile were used as solvents with wavelength recorded in range between 200 nm – 400 nm.

The IR spectra were obtained on Perkin-Elmer FT-IR spectrometer RX1 with spectroscopic chloroform as the solvent.

The optical rotations were recorded on a JASCO (Japan) P1020 Automatic Polarimeter Machine equipped with a tungsten lamp with methanol and chloroform as solvents.

### 5.3 Solvents

All the solvents used for extractions and isolations process were of analytical grade and were distilled prior to use. The solvents used were hexane, dichloromethane, ethyl acetate, chloroform, acetone and methanol.

### 5.4 Chromatography

Purification processes were performed using various chromatography techniques in manner of classical or modern techniques.

For the Thin Layer Chromatography (TLC), aluminium supported silica gel Merck 60 $F_{254}$ plates were used for visualized isolated compounds based on spot of TLC. It was then were visualized under the UV light (245 nm and 365 nm) using UVGL-58 model.

Preparative Thin Layer Chromatography (PTLC) silica gel 60 $F_{254}$ glass plate (20 cm x 20 cm) were used for separation of compounds that have higher $R_f$ values. The plates were developed in closed chambers under the influence of gravity. Some plates were developed for once or twice to achieve a more desirable level of separations. The same model of UV light was used for the detection of bands. The bands were scratched and diluted with dichloromethane and methanol before being filtered by Celite and were reduced and concentrated at 40 $^{o}$C.

Column chromatography performed was based on the TLC results; several sizes of silica gel 60 $F_{254}$ were used with different combinations of solvents based on their

polarity index ranging from n-hexane, dichloromethane, ethyl acetate, chloroform and methanol.

## 5.5 Reagents

Vanillin spray reagent was used routinely while modified *p*-anisaldehyde was also used when necessary.

For vanillin reagent, 3.0 g of vanillin was dissolved in 100 mL of absolute ethanol followed by addition of 0.5 mL sulphuric acid. The reagent was sprayed over the dried developed TLC and heated until coloured spots appeared.

For modified *p*-anisaldehyde reagent, 0.5 mL of *p*-anisadehde was mixed with a mixture of 10 mL glacial acetic acid and 85 mL of methanol. About 5 mL of sulphuric acid was added to the mixture. The reagent was sprayed over the dried developed TLC and then heated to 110 $^{o}$C until coloured spots appeared.

## 5.6 Extraction

The extraction processes were carried out using simple maceration method. The barks of *W. pinnata* (1.5 kg) were first defatted with hexane and then soaked with dichloromethane, both for 48 hours. Periodically stirring was applied throughout the duration to enhance the extraction yield. After two days, the liquid extracts were separated from the plant material by straining with filter paper and were reduced and concentered at 40 $^{o}$C using the rotary evaporator. The plant materials again were subjected to the same extraction procedure for twice, each time with fresh solvent. The whole procedure was repeated once again to obtain the methanol extracts. The schematic flow of the extraction procedure were simplified in Figure 5.1

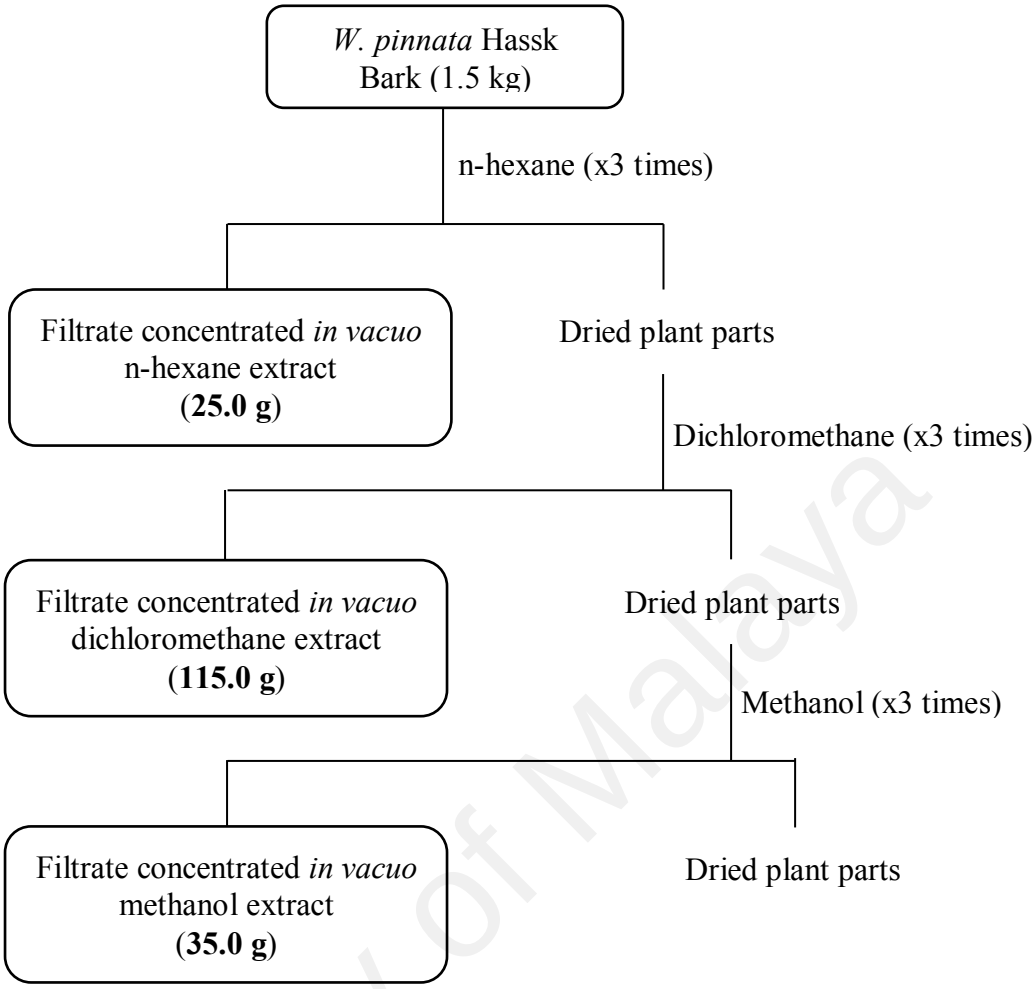


**Figure 5.1**: Extraction flow from the bark of *W. pinnata* Hassk

## 5.7 Isolations and purifications

All separations were carried out under gravity using gradient elution method by combinations of different solvent systems as the mobile phase; hexane: ethyl acetate, dichloromethane: acetone and chloroform: acetone. The eluent were collected in test tubes and be monitored with TLC for purity.

The developed TLCs were viewed under an ultraviolet lamp with dual wavelength; 254 nm and 365 nm, to detect any UV–active compounds. The vanillin and modified *p*-anisaldehyde spray reagent were also used to visualize the position of separated compounds on the developed TLC plate. The reagents was sprayed over the dried develop TLC plate and subjected to heated until the spots were visible.

The test tubes which gave spots with same $R_f$ values on the TLCs were pooled as a fraction. Each fraction was then treated separately to extensive small CC or PTLC while certain fractions were separated using RHPLC until a single spot on the TLC was obtained.

The dichloromethane crude extract (15.00 g) was fractionated by open CC eluting with 90:10 to 10:90 n-hexane-EtOAc to give 11 major fractions (A-K). Fractions C (2.77 g) was separated by CC over silica gel, eluting with 75:25 n-hexane-EtOAc to furnished **98** (150.0 mg) and **97** (320.4 mg). Fraction D (3.57 g) was subjected to CC over silica gel eluting with 90:10 to 10:90 $CH_2Cl_2$:Acetone to yield 12 sub-fractions (D1-D12) and then D5 was further purified by CC over silica gel to obtained **100** (1.2 mg) and **99** (1.1 mg). Fraction E (2.21 g) was subjected to CC over silica gel again eluting with 90:10 to 50:50 $CH_2Cl_2$:Acetone to yield 7 sub-fractions (E1–E7) and then sub-fraction E4 (80.60 mg) was further purified by preparative TLC eluted with a $CH_2Cl_2$:Acetone:MeOH (87:10:3) gradient systems to furnished **101** (2.2 mg) while **102** (30.3 mg) was afforded from sub-fraction E6 (1.30 g) from CC over silica gel eluting with 70:30 $CH_2Cl_2$:Acetone. Fraction F (0.56 g) was further subjected to Sephadex column using an isocratic eluent systems (85:15 $CH_2Cl_2$:MeOH) to give **103** (4.3 mg) and **105** (2.3 mg). Finally, Fraction I (1.55 g) was purified by open CC eluting with gradient eluent 80:20 to 60:40 n-hexane:EtOAc to afforded 5 subsfractions (I1 – I5). Subfraction I2 (0.4 g) and I5 (0.5 g) was further subjected to CC over silica gel using 80:20 and 60:40 n-hexane:EtOAc to give **106** (1.6 mg) and **104** (5.0 mg) respectively. The schematic flow of the isolation of all the compounds were simplified in Figure 5.2

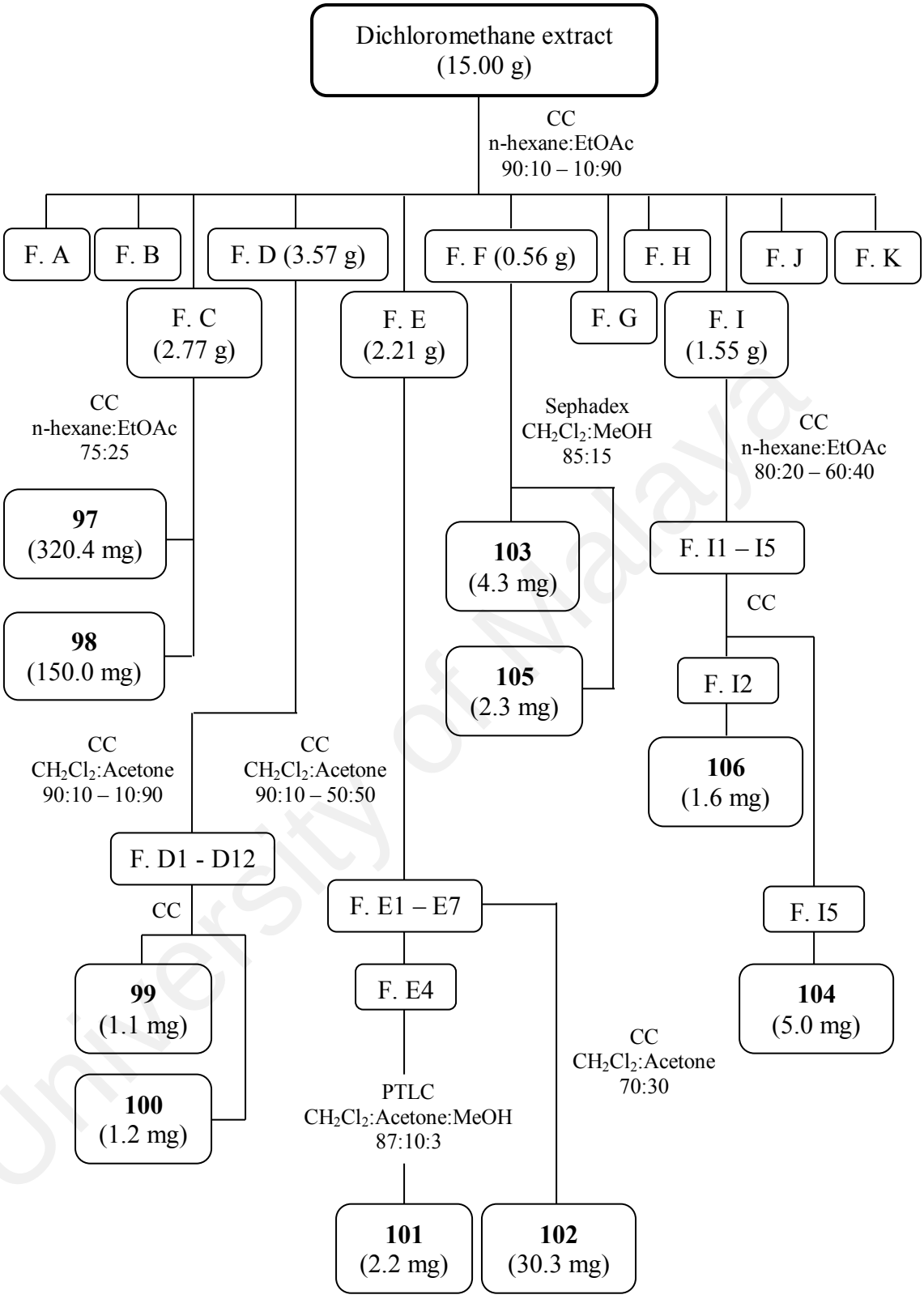


**Figure 5.2**: Compounds isolated from the dichloromethane extract of *W. pinnata*'s bark

## 5.8 Cytotoxic screening on SK-OV-3 and MCF-7 cell line

Compounds **97** and **98** were subjected to Neutral Red Cytotoxic Assay in order to determine its cytotoxic activity on the human breast MCF-7 adenocarcinoma, human ovarian SK-OV-3 adenocarcinoma and human normal lung fibroblast MRC-5 cell.

### 5.8.1 Chemicals

Roswell Park Memorial Institute (RPMI) 1640 medium, Dulbecco's Modified Eagle Medium (DMEM), and Minimum Essential Media (MEM) medium were purchased from Sigma. Fetal bovine serum was obtained from PAA Lab., Austria. Accutase in DPBS, 0.5 mM EDTA was purchased from iCT, CA. HEPES (4-(2-hydroxyethyl)-1-piperazineethanesulfonic acid) was purchased from Molekula, UK while Neutral Red was purchased from ICN, Ohio. All other chemicals and solvents used were of the highest purity grade available were purchased from BDH AnalaR, UK and Sigma-Aldrich, USA. Cell culture plastic ware was obtained from Nunc (Denmark).

### 5.8.2 Cell lines

Human breast MCF-7 adenocarcinoma, human ovarian SK-OV-3 adenocarcinoma and human normal lung fibroblast MRC-5 cell were purchased from American Type Culture Collection (ATCC, USA). MCF-7 cells was cultured in RPMI 1640 media, SK-OV-3 in DMEM media while MRC-5 in MEM media supplemented with 10% (v/v) fetal bovine serum as a complete growth media. Cells were maintained in 25 $cm^2$ flask with 10 mL of media and were incubated at 37 $^oC$ in an incubator with 5% $CO_2$ in a humidified atmosphere (Shel Lab.). The culture was sub-cultured every 2 or 3 days and routinely checked under an inverted microscope (Leica DMI 3000B) for any contamination.

### 5.8.3 Neutral Red Cytotoxic Assay

The neutral red cytotoxic assay is based on the initial protocol described by (Borenfreund & Puerner, 1985). Cells were detached from the flask with 1.0 mL solution of accutase in phosphate buffer solution (PBS) with pH value 7.4. The cell pellet was obtained by centrifugation at 1000 rpm for 5 min and the density of the viable cells was counted by 0.4% of tryphan blue exclusion using a haemocytometer (Hirschman®Technology). Cells were then plated in 96-well microtiter plate (Orange Scientific), at a concentration of 30,000 cells/mL and then incubated in a $CO_2$ incubator at 37 $^{o}$C for 3 hour to allow the cells to adhere before addition of the test agents. After 3 hour, the compounds tested were then added to the wells at six different concentrations of 1, 10, 25, 50, 75 and 100 µg/mL. Incubation with the extracts were carried out for 72 hour. Negative control comprised of cells not treated with any extract. Cisplatin was used as a positive control in the experiments.

At the end of the incubation period, the medium was replaced with a medium containing 50 µg/mL neutral red. The plates were incubated for another 3 hour to allow for uptake of the vital dye into the lysosomes of viable and uninjured cells. After the incubation period, the medium was removed and cells were washed with the Neutral Red washing solution. The dye was eluted from the cells by incubation with 200 µL of neutral red resorb solution for 30 min. at room temperature with rapid agitation on a microtiter plate shaker (Lt Biomax 500). The optical density (OD) was measured at 540 nm using microplate reader (Emax, Molecular Devices). Three replicates plates were used to determine the cytotoxic activity of the isolated compounds and its extracts.

The percentage inhibition of each of the test samples was calculated according to the following equation: % of inhibition = $(OD_{control} - OD_{sample}) / (OD_{control}) \times 100\%$. The $IC_{50}$ is the concentration of extract/compounds that causes 50% inhibition or cell

death and obtained by plotting the percentage of inhibition against respective concentrations used in the assay using MsExcel. According to the US National Cancer Institute Plant Screening Program, a crude extract is generally considered to have active cytotoxic activity if the $IC_{50}$ value in carcinoma cells, following incubation between 48 and 72 hour, is equal or less than 20 µg/mL, while it is equal or less than 4 µg/mL for pure compounds (Boik, 2001).

The selectivity index (SI) was also calculated from the ratio of $IC_{50}$ against MRC-5 and tumor cell lines. The SI values indicate the selectivity of the sample towards the cancer cells tested. Sample with SI value greater than 3.0 were considered to have high selectivity and considered less toxic towards normal cell line (Mahavorasirikul et al., 2010b).

### 5.9 Cytotoxic screening on Hep-G2 and Hep-3b cell line

Compound **98** was subjected to MTT assay in order to determine theirs cytotoxic activity on the both human tumor liver cell line, HepG2 and Hep3b.

#### 5.9.1 Chemicals

DMEM was purchased from Lonza, USA while Eagle Minimum Essential Medium (EMEM) medium and sodium pyruvate were purchased from Sigma. Fetal bovine serum was obtained from Cambrex, USA. MTT (3-(4,5-dimethylthiazol-2-yl)-2,5-diphenyltetrazolium bromide) powder was purchased from Calbiochem, USA and diluted in 1× PBS (Lonza, USA). Trypsin was obtained from Lonza, USA and dilute in 1× PBS with 0.25% (v/v) EDTA (ethylenediaminetertaacetic acid) (Gibco, USA). Trypan blue solution were purchased from Merck, Germany and further diluted in 1× PBS.

### 5.9.2 Cell lines

Tumor liver cell line, HepG2 was obtained from Faculty of Medicine University Malaya and Hep3b was purchased from ATCC (HB-8064). HepG2 was cultured in DMEM while Hep3b cultured in EMEM culture media with sodium pyruvate and all culture media supplemented with 10% (v/v) fetal bovine serum as a complete growth media. Cells were maintained in 25 $cm^2$ flask with 4 mL of complete media and were incubated at 37 $^{o}$C in an incubator with 5% $CO_2$ in a 95.0% humidified atmosphere. The cell cultures were sub-cultured every 2 or 3 days and routinely checked under a fluorescence microscope for any unusual growth or contamination.

### 5.9.3 Viability assay: MTT assay

The cytotoxic effects of compound **98** on both liver cancer cell lines which was readily dissolved in DMSO with stock concentration of 20mM were determined using MTT dyes which measuring reducing of yellow solution tetrazole into purple crystals formazan by cells. Briefly cell lines were washed with 1× PBS. The spent of 1× PBS then carefully aspirated and cells were detached using 0.25% (v/v) trypsin solution after incubated at 37$^{o}$C for 8 minutes. Trypsin were neutralized by adding culture medium containing 10% FBS with ratio of 1:3. The cell pellets obtained by centrifuged for 5 min under 1.5 × $10^3$ rpm. Spent medium then discarded and re-suspend with fresh media supplemented with 10% FBS to make a single cells suspension.

Determination of viable cell count was done using trypan blue exclusion methods. Approximately 20 µL of cell suspension was dilute in 20 µL of 0.08% (v/v) of trypan blue solution and mixed well before incubate for 3 minutes. The solution was then transferred to a haemocytometer counting chamber. Using an inverted microscope (Labscope, Taiwan) at 100× magnification, the number of unstained viable cells was

obtained from four different quadrant with square grid represent 0.1 $mm^3$ or $10^{-4}$ mL volume. The number of viable cells count was determined using following formula:

$$Cell\ concentration\ \left(\frac{cell}{mL}\right) = \left(\frac{Average\ no\ of\ cell\ counted}{Volume\ counted\ (mL)}\ X\ Dilution\ factor\right)$$

Cells suspension then dilute in fresh medium supplemented with 10% FBS to give the desire density of cells of 1.0 x $10^5$ cells/mL. A total of 1.0 x $10^4$ cells/well were plated in triplicates in 100 µL per well in a 96 flat bottom well plate and incubated in 37°C with 5.0% of $CO_2$ for overnight to allow cells to adherence to the well surface. Commencement of compound **98** treatment was done for various concentrations (0, 10, 20, 40, 60, 80 and 100 µM). Wells containing media only used as negative control while cells treated with DMSO act as solvent control to ensure that DMSO does not induce significant cytotoxic effects to the cells. Serial dilution of cell culture were made by plating the cells by descending concentration (10000, 5000, 2500, and 1250 cells/well) to construct a standard curve for quantification purposes. After completion of incubation treatment for 72 hour, 20 µL of MTT solution (5 mg/mL) was added to the each wells and followed by incubation in dark condition at 37°C for 1.5 hour. The spent media with MTT were aspirated and purple formazan crystal was dissolved by adding 200 µL of DMSO and mix well until purple formazan crystal completely dissolves. Absorbance values of each wells was measured at 570 nm wavelength with a 650 nm reference wavelength. All measurements were conducted using the Tecan Sunrise microtiter plate reader (Tecan Switzerland) and quantified using Magellan Ver. 6.3 (Tecan, Switzerland).

The selectivity index (SI) was also calculated from the ratio of $IC_{50}$ against MRC-5 and tumor cell lines. The SI values indicate the selectivity of the sample towards the cancer cells tested. Sample with SI value greater than 3.0 were considered

to have high selectivity and considered less toxic towards normal cell line (Mahavorasirikul et al., 2010a).

### 5.10 Cytotoxic screening on Kasumi-1 cell line

Compound **97** was subjected to MTS assay in order to determine theirs cytotoxic activity on the human acute myeloblastic leukemia cell line (Kasumi-1).

#### 5.10.1 Chemicals

Kasumi-1 was obtained from the Riken (Ibaraki, Japan). Cell culture media Roswell Park Memorial Institute-1640 (RPMI-1640), Iscove's Modified Dulbecco's Medium (IMDM), Hanks Balanced Salt Solution (HBSS), phosphate buffer saline (PBS), fetal bovine serum (FBS), L-glutamine and positive control (cytarabine and idarubicin) were obtained from Wako Pure Chemicals Industries Ltd (Osaka, Japan).

#### 5.10.2 Cell line

Kasumi-1 cells was maintained in RPMI-1640 medium supplemented with 10% heat-inactivated FBS, 2 mM L-glutamine in a cell incubator (inCuSafe, Sanyo Electric, Osaka, Japan) at 37 ºC with a humidified atmosphere of 5% $CO_2$.

#### 5.10.3 Viability assay: MTS assay

The cytotoxicity of compound **97** which was readily dissolved in DMSO (Wako Pure Chemicals Industries Ltd, Osaka, Japan) as a stock solution of 400 mM was evaluated against Kasumi-1 cell line. The cells were plated at a density of 2 x $10^4$ cells per well in 96-well plates and treated continuously with compound **97** (0.390 – 100 µM) for 24, 48 or 72 hours. At the end of the treatment, 20 µL of MTS reagent was added. The plates were incubated for 4 hours in the cell incubator and absorbance was read using a microplate reader (MultiSkan FC, ThermoScientific, MA, USA) at 490 nm, with 690 nm as the background wavelength. The percent viable cell was calculated with respect to DMSO control and 50% inhibitory concentration ($IC_{50}$) was determined by

dose-response curve fitting using Prism 5.02 software (GraphPad Software Inc., CA. USA).

## 5.11 Physical Data of the Isolated Compounds

**3-oxo-lup-20(29)-en-28-oic acid, 97**

Physical appearance : White amorphous powder

Mass (m/z) : 455.3581 $[M+H]^+$

$[\alpha]_D^{25}$ : +13.4 (c = 0.01, MeOH)

Molecular formula : $C_{30}H_{46}O_3$

IR $\nu_{max}$ ($cm^{-1}$) : 3440, 2942, 1701

NMR : Table 3.2, Figures 3.1 - 3.7

**3*β*-hydroxy-5-glutinen-28-oic acid, 98**

Physical appearance : White crystal

Mass (m/z) : 456.3603 $[M-H]^-$

$[\alpha]_D^{25}$ : +53.0 (c = 0.01, MeOH)

Molecular formula : $C_{30}H_{48}O_3$

IR $\nu_{max}$ ($cm^{-1}$) : 3396, 2933, 1695, 1180

NMR : Table 3.3, Figures 3.8 - 3.13

**3-oxo-olean-11-en-28,13*β*-olide, 99**

Physical appearance : White amorphous solid

Mass (m/z) : 453.3434 $[M+H]^+$

Molecular formula : $C_{30}H_{44}O_3$

IR $\nu_{max}$ ($cm^{-1}$) : 1765, 1705, 1640

NMR : Table 3.4, Figures 3.14 - 3.19

**3-oxo-olean-9(11),12-dien-28-oic, 100**

Physical appearance : White amorphous powder

Mass (m/z) : 453.3434 $[M+H]^+$

$[\alpha]_D^{25}$ : +71.0 (c = 0.4, $CHCl_3$)

Molecular formula : $C_{30}H_{44}0_3$

IR $\nu_{max}$ ($cm^{-1}$) : 3436, 2941, 1701

UV/Vis $\lambda_{max}$ (MeOH) nm (log $\varepsilon$) : 210 (4.44), 275 (3.95).

NMR : Table 3.5, Figures 3.20 - 3.27

**3-oxo-20(24)-epoxy-12*β*,25-dihydroxydammarane, 101**

Physical appearance : Colourless needle

Mass (m/z) : 474.3709 $[M+H]^+$

Molecular formula : $C_{30}H_{50}O_4$

IR $\nu_{max}$ ($cm^{-1}$) : 3433, 2953, 1706

NMR : Table 3.6, Figures 3.28 - 3.34

**2(3),6(7)-diepoxy-9-humulene, 102**

Physical appearance : White amorphous powder

Mass (m/z) : 233.1755 $[M+H]^+$

Molecular formula : $C_{15}H_{22}O_2$

IR $\nu_{max}$ ($cm^{-1}$) : 2957, 976

NMR : Table 3.7, Figures 3.35 - 3.40

**Stigmasterol, 103**

Physical appearance : White amorphous powder

Mass (m/z) : 413.3783 $[M+H]^+$

Molecular formula : $C_{29}H_{48}O$

IR $\nu_{max}$ ($cm^{-1}$) : 3430, 1653

NMR : Table 3.8, Figures 3.41 - 3.46

***β*-sitosterol glycolside, 104**

Physical appearance : White amorphous solid

Mass (m/z) : m/z 397.4 $[M\text{-glucose}]^+$

Molecular formula : $C_{29}H_{49}$

IR $\nu_{max}$ ($cm^{-1}$) : 3425, 1648

NMR : Table 3.9, Figures 3.47 - 3.52

**4-hydroxy-3-methoxybenzoic acid, 105**

Physical appearance : White amorphous solid

Mass (m/z) : 167.09 $[M\text{-}H]^-$

Molecular formula : $C_8H_8O_4$

IR $\nu_{max}$ ($cm^{-1}$) : 3436, 1674, 1433, 1288

NMR : Table 3.10, Figures 3.53 - 3.57

**4-hydroxy-4,8-dimethyl-1-tetralone, 106**

Physical appearance : Yellowish oil

Mass (m/z) : 191.1132 $[M+H]^+$

Molecular formula : $C_{12}H_{14}O_2$

IR $\nu_{max}$ ($cm^{-1}$) : 3402, 2935, 1702

NMR : Table 3.11, Figures 3.58 - 3.63

## REFERENCES


Achenbach, H., & Schwinn, A. (1995). Aporphinoid alkaloids and terpenoids from *Piptostigma fugax*. *Phytochemistry, 38*(4), 1037-1048.

Ageta, H., Arai, Y., Suzuki, H., Kiyotani, T., & Kitabayashi, M. (1995). NMR spectra of triterpenoids. III. Oleanenes and migrated oleanenes. *Chemistry and Pharmaceutical Bulletin, 43*(2), 198-203.

Aramadhaka, L. R., Prorock, A., Dragulev, B., Bao, Y., & Fox, J. W. (2013). Connectivity maps for biosimilar drug discovery in venoms: The case of Gila Monster Venom and the anti-diabetes drug Byetta. *Toxicon, 69*, 160-167.

Atta-ur, R., Zareen, S., Choudhary, M. I., Ngounou, F. N., Yasin, A., & Parvez, M. (2002). Terminalin A, a novel triterpenoid from *Terminalia glaucescens*. *Tetrahedron Letters, 43*(35), 6233-6236.

Balakrishna, K., Rao, R. B., Patra, A., & Ali, S. U. (1995). Constituents of *Walsura piscidia*. *Fitoterapia, 66*(6), 548.

Balakrishna, K., Sukumar, E., & Connolly, J. D. (2003). Piscidenone and Piscidinol G, two new protolimonoids from *Walsura piscidia*. *Natural Product Sciences, 9*(4), 304-306.

Boik, J. (2001). *Natural compounds in cancer therapy* (S. Farnell Ed.). Minnesota, USA: Oregon Medical Press.

Borenfreund, E., & Puerner, J. A. (1985). Toxicity determined in vitro by morphological alterations and neutral red absorption. *Toxicology Letters, 24*(2-3), 119-124.

Bowsher, C., Steer, M., & Tobin, A. (2008). *Plant Biochemistry* (E. Owen Ed. 1st ed.). USA: Garland Science, Taylor & Francis Group.

Breitmaier, E. (2006). *Terpenes: Flavors, Fragrances, Pharmaca, Pheromones* (J. W. Sons Ed. Vol. 1st): John Wiley & Sons.

Bringmann, G., Irmer, A., Feineis, D., Gulder, T. A. M., & Fiedler, H.-P. (2009). Convergence in the biosynthesis of acetogenic natural products from plants, fungi, and bacteria. *Phytochemistry, 70*(15-16), 1776-1786.

Castellanos, L., Correa, R. S., Martinez, E., & Calderon, J. S. (2002). Oleanane triterpenoids from *Cedrela montana* (Meliaceae). *Zeitschrift für Naturforschung C, 57*, 575-578.

Chatterjee, A., Kundu, A. B., Chakrabortty, T., & Chandrasekharan, S. (1968). Structure of walsurenol, a pentacyclic triterpene alcohol from *Walsura tubulata*. *Chemical Communications, 7*(7), 418-419.

Chaturvedula, V. S. P., Schilling, J. K., Johnson, R. K., & Kingston, D. G. I. (2003). New cytotoxic lupane triterpenoids from the twigs of *Coussarea paniculata*. *Journal of Natural Products, 66*(3), 419-422.

Corner, E. J. H. (1940). *Wayside Trees of Malaya* (2nd edition ed. Vol. 1). Singapore: Government Printing Office.

Cragg, G. M., & Newman, D. J. (2005). Plants as a source of anti-cancer agents. *Journal of Ethnopharmacology, 100*(1–2), 72-79.

Das, M. C., & Mahato, S. B. (1983). Triterpenoids. *Phytochemistry, 22*(5), 1071-1095.

Division, B. a. F. M. (2014). *Fifth National Report to the Convention on Biological Diversity*. Malaysia: Ministry of Natural Resources and Environment.

Elfita, E., Muharni, M., Latief, M., Darwati, D., Widiyantoro, A., Supriyatna, S., Bahti, H. H., Dachriyanus, D., Cos, P., Maes, L., Foubert, K., Apers, S., & Pieters, L. (2009). Antiplasmodial and other constituents from four Indonesian Garcinia spp. *Phytochemistry, 70*(7), 907-912.

Faizi, S., Ali, M., Saleem, R., Irfanullah, & Bibi, S. (2001). Complete $^{1}H$ and $^{13}C$ NMR assignments of stigma-5-en-3-*O*-*β*-glucoside and its acetyl derivative. *Magnetic Resonance Chemistry, 39*(7), 399-405.

Forgo, P., & Kover, K. E. (2004). Gradient enhanced selective experiments in the $^{1}H$ NMR chemical shift assignment of the skeleton and side-chain resonances of stigmasterol, a phytosterol derivative. *Steroids, 69*(1), 43-50.

Fumimoto, R., Sakai, E., Yamaguchi, Y., Sakamoto, H., Fukuma, Y., Nishishita, K., Okamoto, K., & Tsukuba, T. (2012). The coffee diterpene kahweol prevents osteoclastogenesis via impairment of NFATc1 expression and blocking of Erk phosphorylation. *Journal of Pharmacological Science, 118*(4), 479-486.

Gary, M. L., Donald, L. P., George, S. K., & James, R. V. (2010). *Spectroscopy* (B. C. C. Learning Ed. Fourth ed.). Belmont, USA: Mary Finch.

Gauthier, C., Legault, J., & Pichette, A. (2009). Recent progress in the synthesis of naturally occurring triterpenoid saponins. *Mini Review of Organic Chemistry, 6*(4), 321-344.

Giang, P. M., Son, P. T., Jin, H. Z., Lee, J. H., & Lee, J. J. (2009). Comparative study on inhibitory activity of zerumbone and zerumbone 2,3-epoxide on NF-κB activation and NO production. *Scientia Pharmaceutica, 77*(3), 589-595.

Goldstein, A., Aronow, L., & Kalman, S. M. (1970). Principles of Drug Action. The Basis of Pharmacology. *Journal of Medicinal Chemistry, 13*(2), 337-337.

Gonzalez-Baro, A. C., Parajon-Costa, B. S., Franca, C. A., & Pis-Diez, R. (2008). Theoretical and spectroscopic study of vanillic acid. *Journal of Molecular Structures, 889*(1-3), 204-210.

Govindachari, T. R., Kumari, G. N. K., & Suresh, G. (1995). Triterpenoids from *Walsura piscidia*. *Phytochemistry, 39*(1), 167-170.

Han, M.-L., Shen, Y., Leng, Y., Zhang, H., & Yue, J.-M. (2014). New rearranged limonoids from *Walsura cochinchinensis*. *RSC Advances, 4*(37), 19150.

Han, M.-L., Shen, Y., Wang, G.-C., Leng, Y., Zhang, H., & Yue, J.-M. (2013). 11beta-HSD1 inhibitors from *Walsura cochinchinensis*. *Journal of Natural Products, 76*(7), 1319-1327.

Han, M.-L., Zhang, H., Yang, S.-P., & Yue, J.-M. (2012). Walsucochinoids A and B: new rearranged limonoids from *Walsura cochinchinensis*. *Organic Letters, 14*(2), 486-489.

Heymann, H., Tezuka, Y., Kikuchi, T., & Supriyatna, S. (1994). Constituents of *Sindora sumatrana* Miq. I. Isolation and NMR spectral analysis of sesquiterpenes from the dried pods. *Chemical and Pharmaceutical Bulletin, 42*(1), 138-146.

Hou, L., Tang, G.-H., Zhang, Y., Hao, X.-J., Zhao, Q., & He, H.-P. (2013). A new carotane sesquiterpene from *Walsura robusta*. *Zhongguo Tianran Yaowu, 11*(1), 84-86.

Ji, K.-L., Li, X.-N., Liao, S.-G., Hu, H.-B., Li, R., & Xu, Y.-K. (2016). Cytotoxic limonoids from the leaves of *Walsura robusta*. *Phytochemistry Letters, 15*, 53-56.

Ji, K. L., Zhang, P., Hu, H. B., Hua, S., Liao, S. G., & Xu, Y. K. (2014). Limonoids from the leaves and twigs of *Walsura yunnanensis*. *Journal of Natural Products, 77*(8), 1764-1769.

Jiang, L. (2013). Three tetranortriterpenoids from *Walsura yunnanensis*. *Chemistry of Natural Compounds, 48*(6), 1013-1016.

Kar, B., & Sivamani, S. (2015). Apoptosis: basic concepts, mechanisms and clinical implications. *International Journal of Pharmaceutical Science Research, 6*(3), 940-950.

Kinghorn, A. D., & Powell, R. G. (2004). Special Issue for Monroe Wall and Mansukh Wani. *Journal of Natural Products, 67*(2), 127-128.

Kuroyanagi, M., Shiotsu, M., Ebihara, T., Kawai, H., Ueno, A., & Fukushima, S. (1986). Chemical studies on *Viburnum awabuki* K. Koch. *Chemical and Pharmaceutical Bulletin, 34*(*10*), 4012-4017.

Lehane, B. (1977). *The Power of Plants* (First Edition ed.). New York: Mcgraw-Hill.

Luo, X.-D., Wu, D.-G., Cai, X.-H., & Kennelly, E. J. (2006). New antioxidant phenolic glycosides from *Walsura yunnanensis*. *Chemistry and Biodiversity, 3*(2), 224-230.

Luo, X.-D., Wu, S.-H., Ma, Y.-B., & Wu, D.-G. (2000). Tetranortriterpenoids from *Walsura yunnanensis*. *Journal of Natural Products, 63*(7), 947-951.

Luo, X.-D., Wu, S.-H., Ma, Y.-B., & Wu, D.-G. (2001). Chemical constituent from *Walsura yunnanensis*. *Yunnan Zhiwu Yanjiu, 23*(4), 515-520.

Mahavorasirikul, W., Viyanant, V., Chaijaroenkul, W., Itharat, A., & Na-Bangchang, K. (2010a). Cytotoxic activity of Thai medicinal plants against human

cholangiocarcinoma, laryngeal and hepatocarcinoma cells in vitro. *BMC Complementary and Alternative Medicine, 10*, 55.

Mahavorasirikul, W., Viyanant, V., Chaijaroenkul, W., Itharat, A., & Na-Bangchang, K. (2010b). Cytotoxic activity of Thai medicinal plants against human cholangiocarcinoma, laryngeal and hepatocarcinoma cells in vitro. *BMC Complementary and Alternative Medicine, 10*, 55-62.

Mahmod, I. I., Abdul Malek, E., Morita, H., Santhanaraju, C., & Ismail, I. S. (2013). Terpenes of *Walsura chrysogyne* (Meliaceae). *Letters in Organic Chemistry, 10*(8), 584-589.

Mini, J. J., & Gajendran, N. (2015). In vitro α-glucosidase inhibition and antioxidant activity of *Walsura trifoliata* (A. Juss.) harms. *Indian Journal of Science and Technology, 8*(Suppl.7), 16-23.

Mohamad, K., Hirasawa, Y., Lim, C. S., Awang, K., Hadi, A. H. A., Takeya, K., & Morita, H. (2008). Ceramicine A and Walsogyne A, novel limonoids from two species of Meliaceae. *Tetrahedron Letters, 49*(27), 4276-4278.

Mohamad, K., Yusoff, M., Awang, K., Ahmad, K., & Ng, S. W. (2009). Pinnatane A from the bark of *Walsura pinnata* Hassk. *Acta Crystallographica Section E, 65*(6), o1317.

Nugroho, A. E., Okuda, M., Yamamoto, Y., Hirasawa, Y., Wong, C.-P., Kaneda, T., Shirota, O., Hadi, A. H. A., & Morita, H. (2013). Walsogynes B–G, limonoids from *Walsura chrysogyne*. *Tetrahedron, 69*(20), 4139-4145.

Paulo, A., Jimeno, M. L., Gomes, E. T., & Houghton, P. J. (2000). Steroidal alkaloids from *Cryptolepis obtusa*. *Phytochemistry, 53*(3), 417-422.

Pearce, H. L., & Miller, M. A. (2005). The evolution of cancer research and drug discovery at Lilly Research Laboratories. *Advances in Enzyme Regulation, 45*, 229-255.

Pennington, T. D., & Styles, B. T. (1975). A generic monograph of the Meliaceae. *Blumea, 22*, 419-450.

Phillips, D. R., Rasbery, J. M., Bartel, B., & Matsuda, S. P. T. (2006). Biosynthetic diversity in plant triterpene cyclization. *Current Opinion on Plant Biology, 9*(3), 305-314.

Phontree, K., Sichaem, J., Khumkratok, S., Siripong, P., & Tip-pyang, S. (2014). Trichostemonoate, a new anticancer tirucallane from the stem bark of *Walsura trichostemon*. *Natural Product Communications, 9*(9), 1253-1254.

Purushothaman, K. K., Duraiswamy, K., Connolly, J. D., & Rycroft, D. S. (1985). Triterpenoids from *Walsura piscidia*. *Phytochemistry, 24*(10), 2349-2354.

Rao, M. S. A., Suresh, G., Ashok Yadav, P., Rajendra Prasad, K., Lakshma Nayak, V., Ramakrishna, S., Rao, C. V., & Babu, K. S. (2012). Novel apo-tirucallane triterpenoids from *Walsura trifoliata*. *Tetrahedron Letters, 53*(46), 6241-6244.

Rao, M. S. A., Suresh, G., Ashok Yadav, P., Rajendra Prasad, K., Usha Rani, P., Venkata Rao, C., & Suresh Babu, K. (2015). Piscidinols H–L, apotirucallane triterpenes from the leaves of *Walsura trifoliata* and their insecticidal activity. *Tetrahedron, 71*(9), 1431-1437.

Ridley, H. N. (1952). *The Flora of the Malay Peninsula* (D. P. O. Dr. F. S. P. Ng Ed. Second edition ed. Vol. IV). London: L. Reeve & CO., LTD.

Ruzicka, L. (1953). Isoprene rule and the biogenesis of terpenic compounds. *Experientia, 9*, 357-367.

Sichaem, J., Aree, T., Khumkratok, S., Jong-aramruang, J., & Tip-pyang, S. (2012). A new cytotoxic apotirucallane from the roots of *Walsura trichostemon*. *Phytochemistry Letters, 5*(3), 665-667.

Sichaem, J., Khumkratok, S., Siripong, P., Tip-pyang, S. (2014). New cytotoxic apotirucallanes from the leaves of *Walsura trichostemon*. *Journal of Natural Medicine, 68*(2), 436-441.

Sichaem, J., Siripong, P., Tip-pyang, S., & Phaopongthai, J. (2014). A new cytotoxic tirucallane from the twigs of *Walsura trichostemon*. *Natural Product Communications, 9*(3), 367-368.

Stanforth, S. P. (2006). *Natural Product Chemistry at a Glance* (R. P. P. Ltd Ed.): Blackwell Publishing Ltd.

Thimmappa, R., Geisler, K., Louveau, T., O'Maille, P., & Osbourn, A. (2014). Triterpene biosynthesis in plants. *Annual Review on Plant Biology, 65*, 225-257.

Uddin, M. H., Otsuka, M., Muroi, T., Ono, A., Hanif, N., Matsuda, S., Higa, T., & Tanaka, J. (2009). Deoxymanoalides from the nudibranch *Chromodoris willani*. *Chemistry and Pharmaceutical Bulletin, 57*(8), 885-887.

Valverde, S., Escudero, J., Lopez, J. C., & Rabanal, R. M. (1985). Two terpenoids from *Salvia bicolor*. *Phytochemistry, 24*(1), 111-113.

von Oppen-Bezalel, L., & Shaish, A. (2009). Application of the Colorless Carotenoids, Phytoene, and Phytofluene in Cosmetics, Wellness, Nutrition, and Therapeutics *The Alga Dunaliella* (pp. 423-444). New York: Science Publishers.

Wang, G.-C., Yu, J.-H., Shen, Y., Leng, Y., Zhang, H., & Yue, J.-M. (2016). Limonoids and triterpenoids as 11β-HSD1 inhibitors from *Walsura robusta*. *Journal of Natural Products, 79*(4), 899-906.

Xu, R., Fazio, G. C., & Matsuda, S. P. T. (2004). On the origins of triterpenoid skeletal diversity. *Phytochemistry, 65*(3), 261-291.

Ye, R., Hu, D., Zhang, Y., Huang, Y., Sun, X., Wang, J., Chen, X., Zhou, H., Zhang, D., Mungthin, M., & Pan, W. (2016). Distinctive origin of artemisinin-resistant *Plasmodium falciparum* on the China-Myanmar border. *Scientific Reports, 6*, 20100.

Yin, S., Wang, X.-N., Fan, C.-Q., Liao, S.-G., & Yue, J.-M. (2007). The First Limonoid Peroxide in the Meliaceae Family: Walsuronoid A from *Walsura robusta*. *Organic Letters, 9*(12), 2353-2356.

Yokomaku, A., Misao, K., Omoto, T., & Hirano, N. (2010). JP2010090317A.

Zhang, N., Li, N., Sun, Y.-N., Li, J.-L., Xing, S.-S., Tuo, Z.-D., & Cui, L. (2014). Diacylglycerol compounds from barks of *Betula platyphylla* with inhibitory activity against acyltransferase. *Chinese Herbal Medicine, 6*(2), 164-167.

Zhang, Y., Islam, M. A., & McAlpine, S. R. (2015). Synthesis of the Natural Product Marthiapeptide A. *Organic Letters, 17*(21), 5149-5151.

Zhou, Z.-W., Yin, S., Zhang, H.-Y., Fu, Y., Yang, S.-P., Wang, X.-N., Wu, Y., Tang, X.-C., & Yue, J.-M. (2008). Walsucochins A and B with an unprecedented skeleton isolated from *Walsura cochinchinensis*. *Organic Letters, 10*(3), 465-468.

## LIST OF PUBLICATION AND PAPER PRESENTED

### A. Publication

Leong, K. H., Mahdzir, M. A., Md. Din, M. F., Awang, K., Tanaka, Y., Kulkeaw, K., Ishitani, T., & Sugiyama, D. (2017). Induction of intrinsic apoptosis in leukaemia stem cells and in vivo zebrafish model by betulonic acid isolated from *Walsura pinnata* Hassk (Meliaceae). *Phytomedicine, 26*, 11-21.

### B. Paper Presented

Title: Chemical Constituents from *Walsura pinnata* Hassk

Oral Presentation

The 3rd International Postgraduate Conference on Science and Mathematics (IPCSM) 2015. October 10-11, 2015, Sultan Idris Education University, Perak, Malaysia

Phytomedicine 26 (2017) 11–21

Contents lists available at ScienceDirect

Phytomedicine

journal homepage: www.elsevier.com/locate/phymed

# Induction of intrinsic apoptosis in leukaemia stem cells and *in vivo* zebrafish model by betulonic acid isolated from *Walsura pinnata* Hassk (Meliaceae)

Kok Hoong Leong[a,b,*], Mohamad Azrul Mahdzir[c], Mohd Fadzli Md Din[c], Khalijah Awang[b,c], Yuka Tanaka[d], Kasem Kulkeaw[e], Tohru Ishitani[f], Daisuke Sugiyama[g,h]

[a] Department of Pharmacy, Faculty of Medicine, University of Malaya, 50603 Kuala Lumpur, Malaysia
[b] Centre of Natural Products and Drug Discovery (CENAR), University of Malaya, 50603 Kuala Lumpur, Malaysia
[c] Department of Chemistry, Faculty of Science, University of Malaya, 50603 Kuala Lumpur, Malaysia
[d] Department of Cell Biology, Faculty of Medicine, Fukuoka University, Fukuoka, 812-8582, Japan
[e] Department of Research and Development of Next Generation Medicine, Faculty of Medical Sciences, Kyushu University, Fukuoka, 812-8582, Japan
[f] Division of Cell Regulation Systems, Department of Immunobiology and Neuroscience, Medical Institute of Bioregulation, Kyushu University, Fukuoka, 812-8582, Japan
[g] Department of Clinical Study, Center for Advanced Medical Innovation, Kyushu University, Fukuoka, 812-8582, Japan
[h] Center for Clinical and Translational Research, Kyushu University, Fukuoka, 812-84582, Japan

ARTICLE INFO

*Article history:*
Received 16 June 2016
Revised 13 December 2016
Accepted 21 December 2016

*Keywords:*
Leukaemia stem cells
Betulonic acid
Meliaceae
Apoptosis
Zebrafish

ABSTRACT

*Background:* Leukaemia stem cells (LSC) have been associated with disease relapse and chemotherapy resistance. Betulonic acid (BA), a pentacyclic lupane-type triterpenoid, was reported to exhibit cytotoxicity toward various cancer cells and to be capable of inducing intrinsic apoptosis in solid tumours. However, the *in vitro* and *in vivo* apoptotic effects of BA against LSC remain unknown.
*Hypothesis/Purpose:* We aimed to determine whether BA isolated from bark of *Walsura pinnata* Hassk (Meliaceae) has pro-apoptotic effects on LSC in *in vitro* and *in vivo* models.
*Study design/Methods:* The population of high purity LSC was isolated from the Kasumi-1 cell line using magnetic sorting and characterised by flow cytometry. Cell viability was assessed using the MTS assay to examine dose- and time-dependent effects. The colony formation assay was performed in MethoCult® H4435 enriched media. Apoptosis was analysed using Annexin-V and propidium iodide staining, mitochondrial transmembrane potential was studied using JC-1 staining, and expression of apoptosis related genes (*BAX*, *Bcl-2* and *survivin*) was evaluated by real time-polymerase chain reaction (RT-PCR). Caspase 3/7 and 9 activities were monitored through Promega Caspase-Glo® over a period of 24 h. The *in vivo* antileukaemia activity was evaluated using LSC xenotransplanted zebrafish, observed for DNA fragmentation from apoptosis by TUNEL assay.
*Results:* BA maintained its potency against the LSC population in comparison to parental Kasumi-1 cells (fold differences $\leq 1.94$) over various treatment time points and significantly inhibited the formation of colonies by LSC. Apoptosis was triggered by BA through the upregulation of *BAX* and suppression of *Bcl-2* and *survivin* genes with the loss of mitochondrial transmembrane potential, leading to the activation of caspase 9 followed by downstream caspase 3/7. BA was able to suppressed leukaemia formation and induced apoptosis in LSC xenotransplanted zebrafish.
*Conclusions:* The results demonstrate that BA inhibited the proliferative and colonogenic properties of LSC. BA induced apoptosis in LSC through the mitochondria pathway and was effective in the *in vivo* zebrafish model. Therefore, BA could be a lead compound for further development into a chemotherapy agent against LSC.



*Abbreviations:* ALDH, aldehyde dehydrogenase; AML, acute myelogenous leukaemia; BA, betulonic acid; DMSO, dimethyl sulfoxide; DNA, deoxyribonucleic acid; FBS, foetal bovine serum; HBSS, Hanks Balanced Salt Solution; $IC_{50}$, 50% inhibitory concentration; IMDM, Iscove's Modified Dulbecco's Medium; JC-1, 1st J-aggregate-forming cationic dye; LSC, leukaemia stem cells; MACS, magnetic-activated cell sorting; MTS, (3-(4,5-dimethylthiazol-2-yl)-5-(3-carboxymethoxyphenyl)-2-(4-sulfophenyl)-2H-tetrazolium); NMR, nuclear magnetic resonance; PI, propidium iodide; RPMI-1640, Roswell Park Memorial Institute-1640; RT-PCR, reverse transcription polymerase chain reaction; RNA, ribonucleic acid; RQ, relative quantity; TUNEL, terminal deoxynucleotidyl transferase dUTP nick end labelling; TLC, thin layer chromatography.

* Corresponding author.
*E-mail address:* leongkh@um.edu.my (K.H. Leong).

http://dx.doi.org/10.1016/j.phymed.2016.12.018
0944-7113/